AIE active piperazine appended naphthalimide-BODIPYs: Photophysical properties and applications in live cell lysosomal tracking

Bhupendra Kumar Dwivedi,[a] Roop Shikha Singh,[a] Afsar Ali,[a] Vinay Sharma,[b] Shaikh M Mobin,[b] and Daya Shankar Pandey*[a]

[a]Department of Chemistry, Institute of Science, Banaras Hindu University, Varanasi–221 005 (UP), India

[b]School of Basic Sciences, Discipline of Chemistry, Indian Institute of Technology Indore, Indore–453 552 (MP), India

Contents

General information - ^{1}H, ^{11}B, ^{13}C and ^{19}F spectra have been acquired on a JEOL AL 500/300 FT-NMR spectrometer using tetramethylsilane $Si(CH_3)_4$ as an internal reference. Electrospray ionization mass spectrometric (ESI-MS) measurements have been made on a Bruker Daltonics Amazon SL ion trap mass spectrometer (micrOTOF-Q II 10348). Electronic absorption and fluorescence spectra have been acquired on Shimadzu UV-1800 and Perkin-Elmer *LS* 55 spectrometers respectivelly. Absolute fluorescence quantum yields of the solid samples were measured using a calibrated Horiba JOBIN YVON integrating sphere instrument. SEM images were obtained on a JEOL JSM 840A Scanning Electron Microscope. TEM image were acquired on EM-410 LS Transmission Electron Microscope. Crystal data for **NPB1** and **NPB3** were collected on a Bruker APEX II diffractometer at room temperature with Mo Kα radiation (λ = 0.71073 Å). Data for **NPB4** was collected on a dual source super nova CCD system from Agilent Technologies (Oxford Diffraction) at room temperature with Cu Kα radiation (λ = 1.54184 Å). The structures were solved by direct methods (SHELXS 97) and refined by full-matrix least squares on F^2 (SHELX 97).[1] Non-hydrogen atoms were refined with anisotropic thermal parameters. Hydrogen atoms were geometrically fixed and refined using a riding model. Computer program PLATON was used for analyzing interaction and stacking distances.[2] The CCDC deposition Nos. 1577071 (**NPB1**), 1577072 (**NPB3**) and 1577073 (**NPB4**), contain supplementary crystallographic data for this paper. An Olympus confocal laser scanning microscope was used for cellular imaging studies while BD LSRFortessa was employed for flow cytometry. MTT plates were read on a BioTek microplate reader.

Theoretical studies. Quantum chemical calculations have been performed at B3LYP Density Functional Theory (DFT) level using B3LYP/6-31G** for **NPB1–NPB4**.[3] The geometry optimization and frequency calculations have been performed using Gaussian 09 suits of program.[4]

Experimental details

Reagents. The solvents were dried and distilled prior to use following standard literature procedures.[5] Acenaphthene, methyl amine, ethyl amine, hexyl amine, octyl amine, piperazine, 4-fluorobenzaldehyde, pyrrole, trifluoroacetic acid, 2,3-dichloro-5,6-dicyano-1,4-benzoquinone (DDQ), triethylamine and boron trifluoride diethyl etherate were procured from Sigma Aldrich, India and used as received without further purifications.

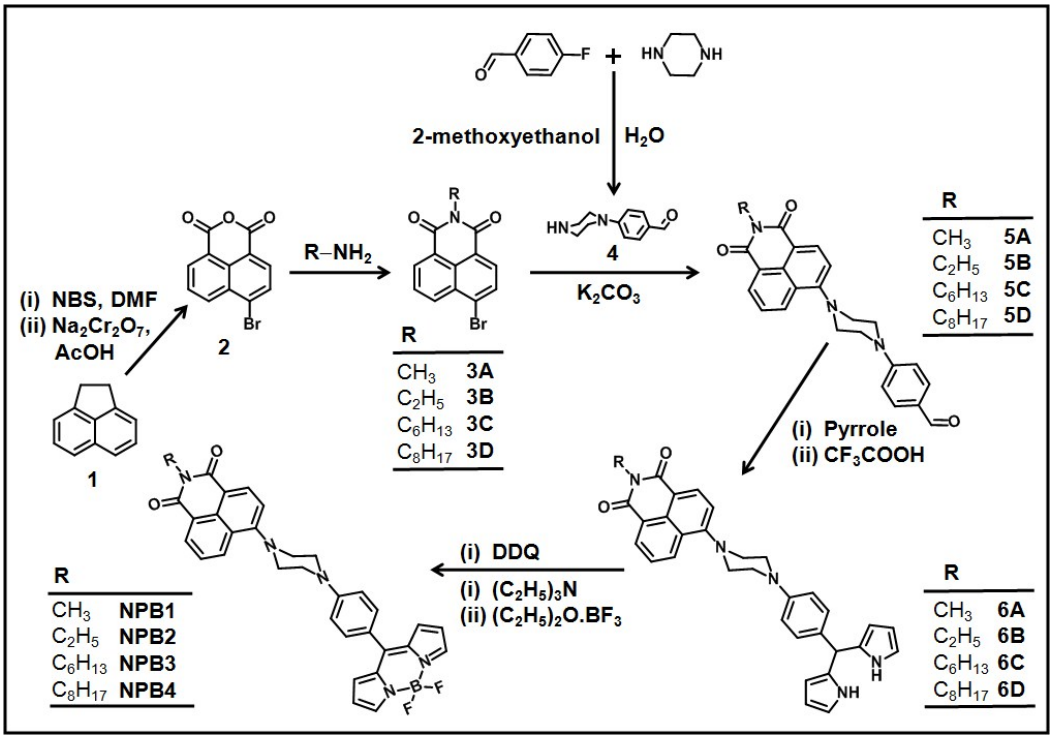

Scheme 1 Synthetic route to **NPB1**–**NPB4**.

6-Bromo-benzo[de]isochromene-1,3-dione (2) was synthesized following the reported method.[6]

6-Bromo-2-methyl-1H-benzo[de]isoquinoline-1,3(2H)-dione (3A) was synthesized following the reported method.[7]

6-Bromo-2-ethyl-1H-benzo[de]isoquinoline-1,3(2H)-dione (3B) was synthesized following the reported method.[8]

6-Bromo-2-hexyl-1H-benzo[de]isoquinoline-1,3(2H)-dione (3C) was synthesized following the reported method.[9]

6-Bromo-2-octyl-1H-benzo[de]isoquinoline-1,3(2H)-dione (3D) was synthesized following the reported method.[7]

4-(Piperazin-1-yl)benzaldehyde (4) was synthesized following the reported method.[10,11]

Synthesis of 4-(4-(2-methyl-1,3-dioxo-2,3-dihydro-1H-benzo-[de]isoquinolin-6-yl)piperazin-1-yl)benzaldehyde (5A): Compound **4** (0.228 g, 1.2 mmol), and K_2CO_3 (0.663 g, 4.8 mmol) were dissolved in DMF (20 ml). After stirring for 30 min, 4-bromo-N-methylnaphthalimide **3A** (0.290 g, 1 mmol) was added it and subsequently the reaction mixture was refluxed for 24 h. After completion of reaction, potassium carbonate was removed by filtration and solvent evaporated under reduced pressure. The residue thus obtained was extracted using EtOAc (100 ml) and organic layer washed with H_2O followed by saturated NaCl solution. The organic layer was dried over anhydrous sodium sulphate and solvent was removed under reduced pressure to afford crude product which was further purified using column chromatography (Silica gel, DCM/hexane as eluent). **5A** was isolated as a light yellow colored solid. Yield: 0.333 g, 83.4%. ^{1}H NMR (500 MHz, $CDCl_3$): δ = 3.42 (t, 4H, piperazine-H), 3.54 (s, 3H, methyl-H), 3.70 (t, 4H, piperazine-H), 7.02 (d, 2H, phenyl-H), 7.26 (s, 1H, naphthalene-H), 7.73 (d, 1H, naphthalene-H), 7.81 (d, 2H, phenyl-H), 8.46 (d, 1H, naphthalene-H), 8.54 (d, 1H, naphthalene-H), 8.61(d, 1H, naphthalene-H), 9.82(s, 1H, aldehyde-H); ^{13}C NMR (125 MHz, $CDCl_3$) δ = 27.10, 48.44, 52.76, 113.55, 114.11, 114.59, 115.25, 117.42, 123.33, 126.10, 126.30, 127.00, 127.91, 129.78, 130.01, 131.27, 131.31, 131.95, 132.50, 134.05, 155.31, 155.47, 164.26, 164.71, 190.59 ppm; IR (KBr pellet): 2925, 2829, 2727, 1695, 1649, 1598, 1514, 1450, 1398, 1360, 1310, 1284, 1227, 1170, 1054, 1038, 1009, 976, 925, 817, 783, 759, 660, 681, 644, 622, 511 cm^{-1}.

Synthesis of 4-(4-(2-ethyl-1,3-dioxo-2,3-dihydro-1H-benzo[de]isoquinolin-6-yl)piperazin-1-yl)benzaldehyde (5B): It was prepared following the above procedure for **5A** using 4-bromo-N-ethylnaphthalimide (**3B**) (0.304 g, 1.0 mmol) in place of **3A**. It was isolated as a light yellow coloured solid. Yield: 0.335 g, 81%. ^{1}H NMR (500 MHz, $CDCl_3$) δ = 1.33 (t, 3H, methyl-H), 3.43 (t, 4H, piperazine-H), 3.72 (s, 4H, piperazine-H), 4.24 (d, 2H, methylene-H), 7.04 (d, 2H, phenyl-H), 7.27 (t, 1H, naphthalene-H), 7.74 (s, 1H, naphthalene-H), 7.83 (d, 2H, phenyl-H), 8.47(d, 1H, naphthalene-H), 8.55 (d, 1H, naphthalene-H), 8.62 (d, 1H, naphthalene-H), 9.84 (s, 1H, aldehyde-H); ^{13}C NMR (75 MHz, $CDCl_3$) δ = 13.38, 30.90, 35.37, 47.57, 52.70, 114.04, 115.19, 117.63, 123.49, 126.01, 126.25, 127.89, 129.79, 131.17, 131.86, 132.33, 154.89, 155.12, 163.72, 164.16, 190.47 ppm; IR (KBr pellet): 2923, 2817, 2737, 1688, 1648, 1594, 1516, 1451, 1387, 1345, 1225, 1170, 1086, 1064, 1038, 995, 941, 914, 882, 868, 787, 761, 716, 644, 622, 519 cm^{-1}.

Synthesis of 4-(4-(2-hexyl-1,3-dioxo-2,3-dihydro-1H-benzo[de]isoquinolin-6-yl)piperazin-1-yl)benzaldehyde (5C): It was also prepared following the same method as adopted for **5A** except that 4-bromo-N-hexylnaphthalimide (0.388 g, 1.0 mmol) **3C** was used as a reagent in place of **3A**. This compound also separated as a light yellow colored solid. Yield: 0.372 g, 79.2%. ^{1}H NMR (500 MHz, $CDCl_3$) δ = 0.88 (t, 3H, methyl-H), 1.33–1.44 (m, 6H, methylene-H), 1.72 (t, 2H, methylene-H), 3.43 (t, 4H, piperazine-H), 3.72 (t, 4H, piperazine-H), 4.16 (t, 2H, methylene-H), 7.04 (d, 2H, phenyl-H), 7.27 (t, 1H, naphthalene-H), 7.74 (m, 1H, naphthalene-H), 7.82 (d, 2H, phenyl-H), 8.46 (d, 1H, naphthalene-H), 8.54 (d, 1H, naphthalene-H), 8.61 (d, 1H, naphthalene-H), 9.84 (s, 1H, aldehyde-H); ^{13}C NMR (125 MHz, $CDCl_3$) δ = 14.03, 22.53, 26.77, 28.07, 31.53, 40.35, 47.50, 52.64, 113.64, 113.98, 115.13, 117.53, 123.40, 125.99, 126.17, 127.80, 129.75, 131.16, 131.84, 132.33, 154.86, 155.08, 163.87, 164.31, 190.47 ppm; IR (KBr pellet): 2925, 2927, 2837, 1694, 1653, 1596, 1514, 1451, 1527, 1389, 1353, 1274, 1225, 1173, 1088, 1001, 922, 810, 783, 756, 676, 667 657, 641, 622 cm^{-1}.

Synthesis of 4-(4-(2-octyl-1,3-dioxo-2,3-dihydro-1H-benzo[de]isoquinolin-6-yl)piperazin-1-yl)benzaldehyde (5D): It was prepared following the mthod employed for **5A** using 4-bromo-N-octylnaphthalimide **3D** (0.388 g, 1.0 mmol) in place of **3A**. It was isolated as a light yellow colored solid. Yield: 0.433 g, 87%. ^{1}H NMR (500 MHz, $CDCl_3$) δ = 0.87 (t, 3H, methyl), 1.27–1.42 (m, 10H, methylene-H), 1.72 (t, 2H; methylene-H), 3.40 (d, 4H, piperazine-H), 3.72 (d, 4H, piperazine-H), 4.16 (t, 2H, methylene-H), 7.04 (d, 2H, phenyl-H), 7.27 (d, 1H, naphthalene-H), 7.75 (m, 1H, naphthalene), 7.82 (d, 2H, phenyl-H), 8.46 (d, 1H, naphthalene-H), 8.54 (d, 1H, naphthalene-H), 8.61 (d, 1H, naphthalene-H), 9.84 (s, 1H, aldehyde-H); ^{13}C NMR (125 MHz, $CDCl_3$) δ = 14.06, 22.60, 27.14, 28.14, 29.32, 31.79, 40.38, 47.52, 52.66, 113.64, 113.99, 115.14, 117.55, 123.42, 126.00, 126.19, 127.81, 129.76, 131.19, 131.86, 132.35, 154.88, 155.09, 163.89, 164.33, 190.50 ppm; IR (KBr pellet): 2925, 2852, 2720, 1698, 1656, 1600, 1516, 1451, 1388, 1358, 1226, 1174, 1102, 926, 818, 787, 759, 512 cm^{-1}.

Synthesis of 6-(4-(4-(di(1H-pyrrol-2-yl)-methyl)-phenyl)-piperazin-1-yl)-2-methyl-1H-benzo [de]isoquinoline-1,3-(2H)-dione (6A): To a stirring solution of compound **5A** (1.598 g, 4.0 mmol) in pyrrole (10.0 ml) catalytic amounts of trifluoroacetic acid (3 drops) was added and the reaction mixture stirred overnight at room temperature. After completion of the reaction (monitored by TLC) ensuing solution was concentrated to dryness under reduced pressure and

the rude product thus obtained was purified by column chromatography (SiO_2; ethylacetate/hexane). The yellow colored band was collected and concentrated to afford the desired product. Yield: 1.609 g, 78%. ^{1}H NMR (500 MHz, $CDCl_3$) δ = 3.43–3.49 (t, 8H, piperazine-H), 3.56 (s, 3H, methyl-H), 5.45 (s, 1H, methine-H), 5.94 (s, 2H, pyrrole-H), 6.17 (d, 2H, pyrrole-H), 6.71 (d, 2H, pyrrole-H), 6.98 (d, 2H, phenyl-H), 7.17 (d, 2H, phenyl-H), 7.26 (t, 1H, naphthalene-H), 7.72 (s, 1H, naphthalene-H), 7.97 (br, 2H, pyrrole N-H), 8.47 (d, 1H, naphthalene-H), 8.55 (d, 1H, naphthalene-H), 8.61 (d, 1H, naphthalene-H); ^{13}C NMR (125 MHz, $CDCl_3$) δ = 27.02, 29.79, 43.24, 49.62, 53.18, 107.10, 108.50, 115.17, 116.53, 117.08, 117.18, 123.30, 125.94, 126.32, 129.32, 129.86, 130.28, 131.28, 132.64, 132.95, 133.94, 150.00, 155.82, 164.40, 164.87 ppm; IR (KBr pellet): 3362, 3097, 2954, 2923, 2828, 1693, 1654, 1589, 1513, 1452, 1413, 1397, 1363, 1287, 1230, 1084, 1038, 784, 758, 720 cm^{-1}; ESI-MS: m/z calcd for $C_{32}H_{29}N_5O_2$ $[M-H]^+$: 514.2; found: 514.2.

Synthesis of 6-(4-(4-(di(1H-pyrrol-2-yl)methyl)-phenyl)-piperazin-1-yl)-2-ethyl-1H-benzo [de]isoquinoline-1,3-(2H)-dione (6B): This compound was prepared following the above procedure for **6A** using **5B** (1.654 g, 4.0 mmol) in place of **5A**. Yield: 1.589 g, 75%. ^{1}H NMR (500 MHz, $CDCl_3$) δ = 1.33 (t, 3H, methyl-H), 3.42 (d, 4H, piperazine-H), 3.48 (d, 4H, piperazine-H), 4.24 (d, 2H, methylene-H), 5.45 (s, 1H, methine-H), 5.94 (s, 2H, pyrrole), 6.17 (d, 2H, pyrrole), 6.71 (d, 2H, pyrrole-H), 6.98 (d, 2H, phenyl-H), 7.17 (d, 2H, phenyl-H), 7.26 (t, 1H, naphthalene-H), 7.72 (t, 1H, naphthalene-H), 7.96 (br, 2H, pyrrole N-H), 8.52 (d, 1H, naphthalene-H), 8.60 (d, 1H; naphthalene-H), 8.61 (t, 1H; naphthalene-H); ^{13}C NMR (125 MHz, $CDCl_3$) δ = 13.48, 35.44, 43.25, 49.62, 53.17, 107.11, 108.52, 115.15, 116.53, 117.16, 117.31, 123.51, 125.92, 126.33, 129.31, 129.96, 130.15, 131.20, 132.53, 132.94, 133.92, 150.01, 155.72, 163.91, 164.36 ppm; IR (KBr pellet): 3355, 3096, 2972, 2926, 2828, 1691, 1648, 1607, 1588, 1512, 1451, 1431, 1386, 1344, 1233, 1200, 1135, 1078, 1061, 993, 941, 783, 720 cm^{-1}; ESI-MS: m/z calcd for $C_{33}H_{31}N_5O_2$ $[M+H]^+$: 530.3; found: 530.3.

Synthesis of 6-(4-(4-(di(1H-pyrrol-2-yl)methyl)phenyl)-piperazin-1-yl)-2-hexyl-1H-benzo [de]isoquinoline-1,3-(2H)-dione (6C): This compound was prepared by following the above procedure for **6A** using compound **5C** (1.991 g, 4.0 mmol) in place of **5A**. Yield: 1.734 g, 74%. ^{1}H NMR (500 MHz, $CDCl_3$) δ = 0.88 (t, 3H; methyl-H), 1.25–1.42 (m, 6H, methylene-H), 1.73 (t, 2H; methylene-H), 3.42–3.48 (m, 8H, piperazine-H), 4.16 (t, 2H, methylene-H), 5.44 (s, 1H,

methine-H), 5.93 (s, 2H, pyrrole-H), 6.16 (m, 2H, pyrrole-H), 6.70 (t, 2H, pyrrole-H), 6.96 (d, 2H, phenyl-H), 7.16(d, 2H, phenyl-H), 7.26(d, 1H, naphthalene-H), 7.70 (t, 1H, naphthalene-H), 7.98 (br, 2H, pyrrole N-H), 8.45 (d, 1H, naphthalene-H), 8.52 (d, 1H, naphthalene-H), 8.59 (d, 1H, naphhalene); ^{13}C NMR (125 MHz, $CDCl_3$) δ = 14.20, 22.66, 26.91, 28.20, 29.75, 31.67, 40.47, 43.24, 49.61, 53.16, 107.11, 108.50, 115.16, 116.52, 117.18, 117.27, 123.47, 125.93, 126.31, 129.31, 129.94, 130.14, 131.23, 132.57, 132.96, 133.94, 150.00, 155.69, 164.09, 164.54 ppm; IR (KBr pellet): 3354, 3091, 2961, 2927, 2854, 1692, 1647, 1609, 1588, 1511, 1451, 1427, 1351, 1359, 1230, 1178, 1140, 1091, 1025, 925, 925, 884, 832, 781, 753, 715, 583, 540 cm^{-1}; HRMS (ESI): m/z calcd for $C_{37}H_{39}N_5O_2$ $[M+H]^+$: 586.3182; found: 586.3177.

Synthesis of 6-(4-(4-(di(1H-pyrrol-2-yl)methyl)-phenyl)-piperazin-1-yl)-2-methyl-1H-benzo [de]-isoquinoline-1,3-(2H)-dione (6D): It was prepared following the above procedure for **6A** using compound **5D** (1991 mg, 4.0 mmol) in place of **5A**. Yield: 1.817 g, 74%. ^{1}H NMR ($CDCl_3$, δ = 0.87 (t, 3H, methyl-H), 1.25–1.43 (m, 10H, methylene-H), 1.71 (m, 2H, methylene-H), 3.41-3.48 (m, 8H, piperazine-H), 4.15 (t, 2H, methylene-H), 5.44 (s, 1H, methine-H), 5.93 (s, 2H, pyrrole-H), 6.17 (m, 2H, pyrrole-H), 6.71 (d, 2H, pyrrole-H), 6.96 (d, 2H, phenyl-H), 7.17 (d, 2H, phenyl-H), 7.25(t, 1H, naphthalene-H), 7.71 (t, 1H, naphthalene-H), 8.00 (br, 2H, pyrrole N-H), 8.45 (d, 1H, naphthalene-H), 8.53 (d, 1H, naphthalene-H), 8.59 (d, 1H, naphthalene); ^{13}C NMR (125 MHz, $CDCl_3$) δ = 14.07, 22.61, 27.15, 28.15, 29.21, 29.34, 31.80, 40.37, 43.13, 49.50, 53.05, 106.99, 108.37, 115.04, 116.40, 117.08, 117.14, 123.34, 125.82, 126.18, 129.21, 129.82, 130.03, 131.13, 132.46, 132.86, 133.85, 149.88, 155.59, 163.98, 164.43 ppm; IR (KBr pellet): 3367, 3099, 2955, 2925, 2854, 1694, 1652, 1612, 1588, 1513, 1452, 1428, 1389, 1358, 1233, 1093, 1027, 928, 885, 837, 785, 760, 716, 586, 540 cm^{-1}; HRMS (ESI): m/z calcd for $C_{39}H_{43}N_5O_2$ $[M-H]^+$: 612.3339; found: 612.3333.

Synthesis of NPB1: To a stirring solution of DDQ (0.545 g, 2.4 mmol) in benzene (20 ml) **6A** (1.031 mg, 2.0 mmol) dissolved in dichloromethane was added dropwise over an hour. The reaction mixture was stirred for an additional 3 h. After completion of the reaction the contents of the flask was evaporated to dryness under reduced pressure. After dissolution of the crude product in DCM, triethylamine (0.75 mL) and $BF_3.Et_2O$ (3.0 mL) were successively added to it and the reaction mixture stirred for 30 min at room temperature. The progress of reaction was monitored by TLC and after completion the reaction mixture was filtered and the filtrate washed

thrice with water, extracted with dichloromethane and concentrated to dryness under reduced pressure. Crude product thus obtained was charged on a flash column (SiO_2; CH_2Cl_2/hexane). The dark orange-red band was collected and concentrated to dryness to afford the desired product. Yield: 0.505 g, 45%. Anal. Calcd for $C_{32}H_{26}BF_2N_5O_2$: C, 68.46; H, 4.67; N, 12.48. Found: C, 68.32; H, 4.69; N, 12.48. ^{1}H NMR (500 MHz, $CDCl_3$) δ = 3.48 (t, 4H, piperazine-H), 3.57 (s, 3H, methyl-H), 3.70 (t, 4H, piperazine-H), 6.57 (t, 2H, pyrrolic-H), 7.04 (d, 2H, pyrrole-H), 7.12 (d, 2H; phenyl-H), 7.30 (t, 1H, naphthalene-H), 7.61 (d, 2H, phenyl-H), 7.76 (t, 1H, naphthalene-H), 7.92 (s, 2H, pyrrole-H), 8.50 (d, 1H, naphthalene-H), 8.57 (d, 1H, naphthalene-H), 8.63 (d, 1H, naphthalene-H); ^{13}C NMR (125 MHz, $CDCl_3$) δ = 27.05, 48.17, 52.92, 114.76, 115.30, 117.48, 118.15, 123.39, 124.95, 126.13, 126.36, 129.85, 131.15, 131.36, 132.55, 132.76, 134.76, 142.92, 147.72, 153.00, 155.41, 164.33, 164.78 ppm; ^{11}B NMR (160.4 MHz, $CDCl_3$) δ= –0.642 ppm (t); ^{19}F NMR (470.6 MHz, $CDCl_3$) δ= –144.99 ppm (q); IR (KBr pellet): 2924, 2852, 1698, 1656, 1598, 1579, 1553, 1528, 1452, 1469, 1389, 1204, 1122, 1080, 877, 911, 828, 777, 713 cm^{-1}; HRMS (ESI): m/z calcd for $C_{32}H_{26}BF_2N_5O_2$ $[M+Na]^+$: 584.2045; found: 584.2041.

Synthesis of NPB2: It was prepared following the above procedure for **NPB1** using **6B** (1.059 g, 2 mmol) in place of **6A**. Yield: 0.150 g, 13%. Anal. Calcd for $C_{33}H_{28}BF_2N_5O_2$: C, 68.88; H, 4.90; N, 12.17. Found: C, 68.10; H, 4.92; N, 12.17. ^{1}H NMR (500 MHz, $CDCl_3$) δ = 1.34 (t, 3H, methyl-H), 3.47 (d, 4H, piperazine-H), 3.71 (d, 4H, piperazine-H), 4.25 (m, 2H, methylene-H), 6.57 (m, 2H, pyrrole-H), 7.04 (d, 2H, pyrrole-H), 7.12 (d, 2H, phenyl-H), 7.30 (t, 1H, naphthalene-H), 7.61 (d, 2H, phenyl-H), 7.76 (d, 1H, naphthalene-H), 7.92 (s, 2H, pyrrole-H), 8.49 (d, 1H, naphthalene-H), 8.57 (d, 1H, naphthalene-H), 8.63 (d, 1H, naphthalene-H); ^{13}C NMR (125 MHz, $CDCl_3$) δ = 13.49, 35.49, 48.17, 52.91, 114.75, 115.27, 117.68, 118.14, 123.58, 124.93, 126.11, 126.36, 129.95, 131.15, 131.29, 132.47, 132.76, 134.77, 142.91, 147.73, 153.00, 155.33, 163.87, 164.30 ppm; ^{11}B NMR (160.4 MHz, $CDCl_3$) δ = –0.642 ppm (t); ^{19}F NMR (470.6 MHz, $CDCl_3$) δ= –144.99 ppm (q); IR (KBr pellet): 2925, 2853, 1691, 1654, 1593, 1531, 1472, 1387, 1349, 1263, 1236, 1202, 1120, 1079, 977, 910, 780, 748 cm^{-1}; ESI-MS: m/z calcd for $C_{33}H_{28}BF_2N_5O_2$ $[M+Na]^+$: 598.2; found: 598.2.

Synthesis of NPB3: It was prepared following the above procedure for **NPB1** using **6C** (1.228 g, 2 mmol) in place of **6A**. Yield: 0.215 g, 17%. Anal. Calcd for $C_{37}H_{36}BF_2N_5O_2$: C, 70.37; H, 5.75; N, 11.09. Found: C, 69.05; H, 5.76; N, 11.23. ^{1}H NMR (500 MHz, $CDCl_3$) δ = 0.89 (t, 3H,

methyl), 1.35–1.44 (m, 6H, methylene-H), 1.73 (t, 2H, methylene-H), 3.47 (m, 4H, piperazine-H), 3.70 (d, 4H, piperazine-H), 4.17 (t, 2H, methylene-H), 6.57 (m, 2H, pyrrole-H), 7.04 (d, 2H, pyrrole-H), 7.12 (d, 2H, phenyl-H), 7.30(t, 1H, naphthalene-H), 7.60 (d, 2H, phenyl-H), 7.76 (d, 1H, naphthalene-H), 7.91 (s, 2H, pyrrole-H), 8.49 (d, 1H, naphthalene-H), 8.56 (d, 1H, naphthalene-H), 8.62 (d, 1H, naphthalene-H); ^{13}C NMR (125 MHz, $CDCl_3$) δ = 14.16, 22.66, 26.91, 28.20, 31.67, 40.51, 47.04, 48.17, 52.91, 114.75, 115.28, 117.65, 118.13, 123.55, 124.91, 126.12, 126.35, 129.94, 131.16, 131.32, 132.50, 132.77, 134.75, 142.89, 147.73, 153.01, 155.31, 164.04, 164.48 ppm; ^{11}B NMR (160.4 MHz, $CDCl_3$) δ = –0.652 ppm (t); ^{19}F NMR (470.6 MHz, $CDCl_3$) δ = –144.97 ppm (q); IR (KBr pellet): 2968, 2927, 2837, 1694, 1653, 1592, 1588, 1560, 1533, 1512, 1470, 1411, 1389, 1353, 1263, 1219, 1200, 1115, 1077, 1053, 976, 908, 831, 777, 758, 739, 706, 674 cm^{-1}; HRMS (ESI): m/z calcd for $C_{37}H_{36}BF_2N_5O_2$ $[M+Na]^+$: 654.2828; found: 654.2829.

Synthesis of NPB4: It was prepared following the above procedure for **NPB1** using **6D** (1.228 g, 2.0 mmol) in place of **6A**. Yield: 0.304 g, 23%. Anal. Calcd for $C_{39}H_{40}BF_2N_5O_2$: C, 71.02; H, 6.11; N, 10.62. Found: C, 70.45; H, 6.14; N, 10.62. ^{1}H NMR (500 MHz, $CDCl_3$) δ = 0.87 (t, 3H; methyl-H), 1.26–1.43 (m, 10H; methylene-H), 1.73 (s, 2H; methylene-H), 3.47 (d, 4H, piperazine-H), 3.70 (s, 4H, piperazine-H), 4.17 (t, 2H, methylene-H), 6.57 (t, 2H, pyrrole-H), 7.04 (d, 2H, pyrrole-H), 7.12 (d, 2H, phenyl-H), 7.31 (d, 1H, naphthalene-H), 7.61 (d, 2H, phenyl-H), 7.75 (s, 1H, naphthalene-H), 7.92 (s, 2H, pyrrole-H), 8.49 (d, 1H, naphthalene-H), 8.56 (d, 1H, naphthalene-H), 8.62 (d, 1H, naphthalene-H); ^{13}C NMR (125 MHz, $CDCl_3$) δ = 13.45, 22.00, 26.53, 27.54, 28.59, 28.72, 31.19, 39.79, 47.44, 52.18, 114.02, 114.55, 116.94, 117.41, 122.85, 124.19, 125.39, 125.61, 129.18, 130.42, 130.58, 131.76, 132.03, 134.03, 142.18, 146.99, 152.27, 154.56, 163.30, 163.75 ppm; ^{11}B NMR (160.4 MHz, $CDCl_3$) δ = –0.652 ppm (t); ^{19}F NMR (470.6 MHz, $CDCl_3$) δ = –144.99 ppm (q); IR (KBr pellet): 2925, 2854, 1746, 1695, 1656, 1599, 1533, 1513, 1469, 1388, 1355, 1263, 1234, 1201, 1120, 1078, 1047, 979, 912, 783, 744 cm^{-1}; ESI-MS: m/z calcd for $C_{39}H_{40}BF_2N_5O_2$ $[M+Na]^+$: 682.3; found: 682.3.

Preparation of buffer solutions: Various standard buffer solutions were prepared by using 50 mM of potassium chloride (pH 1–2), potassium hydrogen phthalate (pH 3–5), potassium dihydrogen phosphate (pH 6–8) and pH measured using pH-meter. In a typical experiment, a mixture of 1:1 buffer and acetonitrile was treated with the probe (**NPB1**–**NPB4**) solution (50 μM). Then the pH adjusted by adding 0.1M of NaOH or 0.1 M HCl solution.

Cytotoxicity Assessment: To explore the applicability of **NPB1**–**NPB4** as bioimaging agents their toxicity has been scruitinized against live cells. Cytotoxicity of **NPB1**–**NPB4** has been investigated on Human cervical cancer cell line (HeLa) using the standard MTT assays.[12] In this regard, HeLa cells were cultured in a T25 flask using minimum essential media (MEM – Himedia) containing 10% fetal bovine serum and 1% penicillin streptomycin and then seeded in a 96 well plate and incubated for 24 h at 37°C, 5% under CO_2 humidified environment. The cells were treated with **NPB1**–**NPB4** in a concentration range of 10–50μM for a period of 16 h and and 48h separately. After treatment the media containing **NPB1**–**NPB4** was replaced with phenol red free MEM media containing 0.5 mg/mL 3-(4,5-dimethylthiazole-2-yl)-2,5-diphenyl tetrazolium bromide (MTT) and incubated for 4 h. Subsequently, MTT containing media was replaced with 100 μL DMSO in each well and after 10 min incubation the plate was read under a Biotek plate-reader at 540 nm. The experiment was performed in triplicate and cell viability calculated using absorbance at 540 nm.

% cell viability = [Mean O.D. of the treated cell / Mean O.D. of the control] * 100

Bioimaging and Lysosome tracking studies: To investigate cellular uptake of **NPB1**–**NPB4** and its applicability in bioimaging, HeLa cells seeded in 27 mm confocal dishes were treated with 10 μM of these compounds and incubated for 30 min Subsequently, the cells were washed thrice with 1X PBS. Intracellular fluorescence was studied by confocal laser scanning microscope using an excitation laser (λ, 488 nm) and emission recorded in the range 500–550 nm. For Lysotracking studies, HeLa cells were first stained with 50 nM Lysotracker red and incubated for 15 min and washed with 1X PBS thrice and imaged under confocal laser scanning microscope and emission was recorded in red channel. Further, 10 μM of **NPB1**–**NPB4** was added without changing the disc position on the microscope and emission was recorded in green channel. The image processing and Pearson's co-localization coefficient was calculated using Olympus FluoView10-ASW 4.2 Viewer software. In order to further investigate the generality of cell staining by **NPB1**–**NPB4**, flow cytometry was performed using BD LSRFortessa. HeLa cells were seeded in a 6 well plate and treated with 10 μM of **NPB1**–**NPB4** for 30 min keeping one unstained control. Further, the cells were tripsinized and re-suspended in a 1X PBS and subjected to flow cytometry.

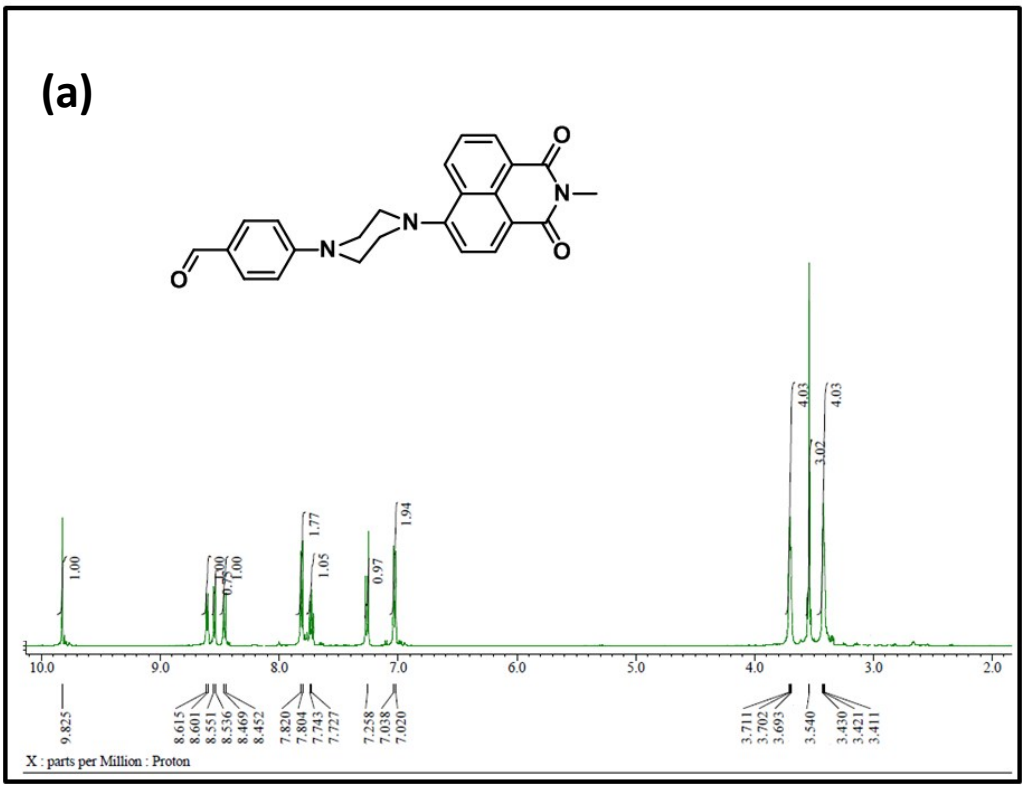

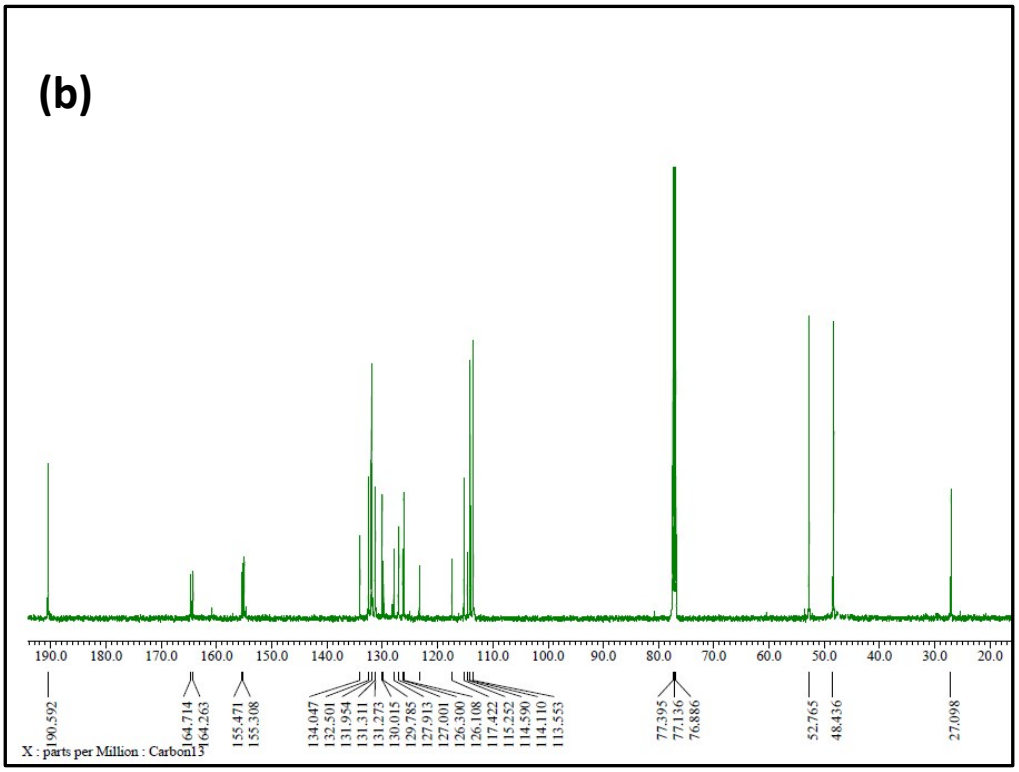

Fig. S1 ^{1}H (a) and ^{13}C (b) NMR spectra of **5A** in $CDCl_3$.

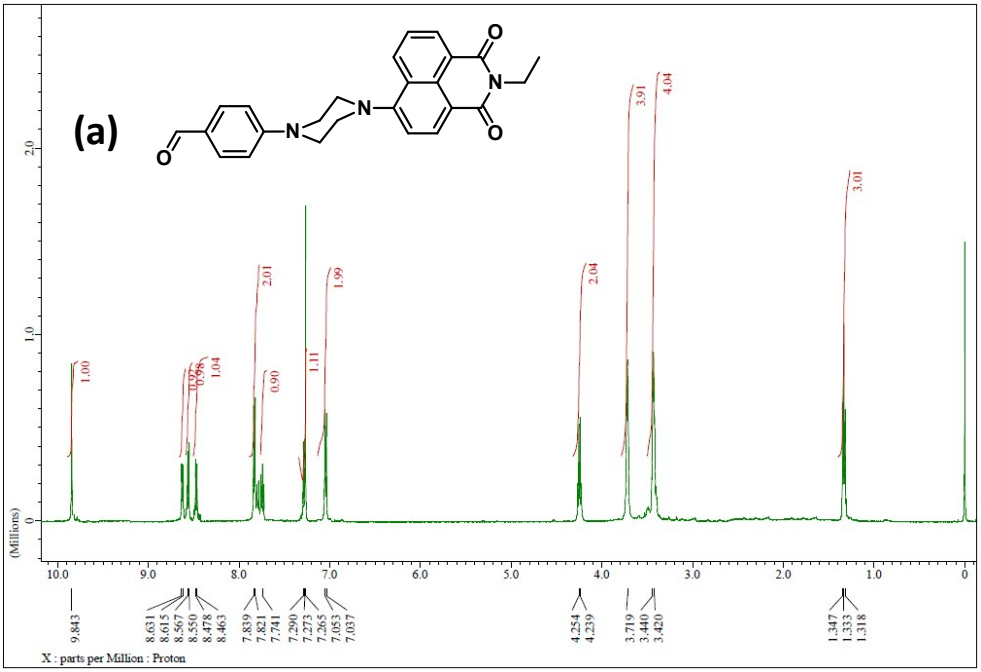

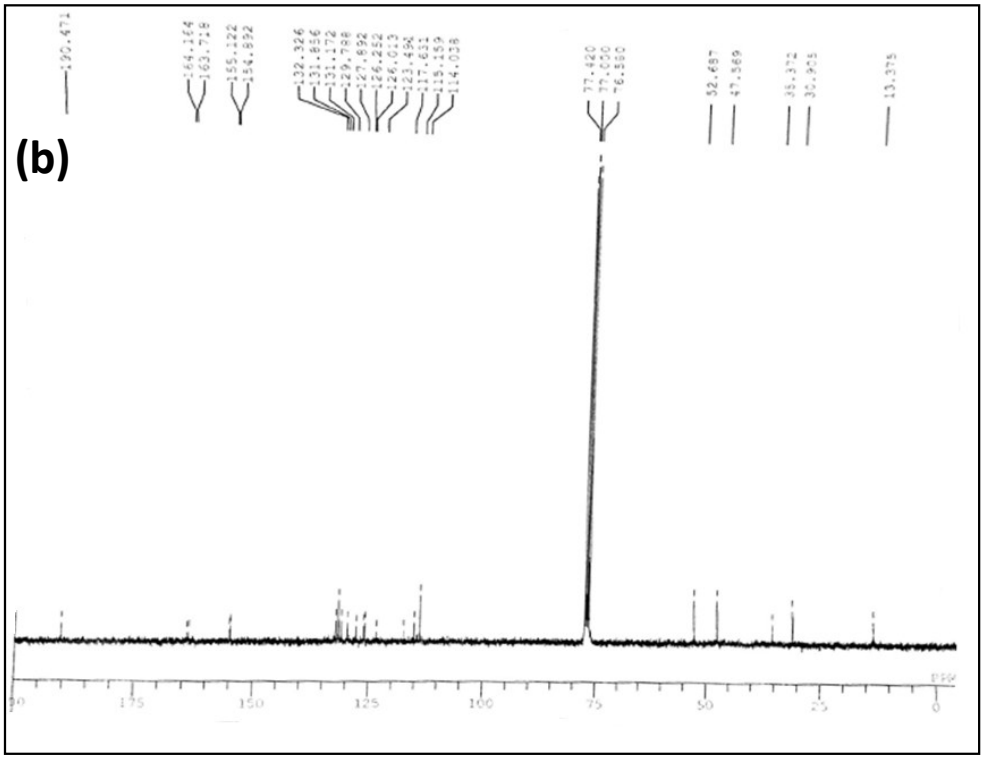

Fig. S2 ^{1}H (a) and ^{13}C (b) NMR spectra of **5B** in $CDCl_3$.

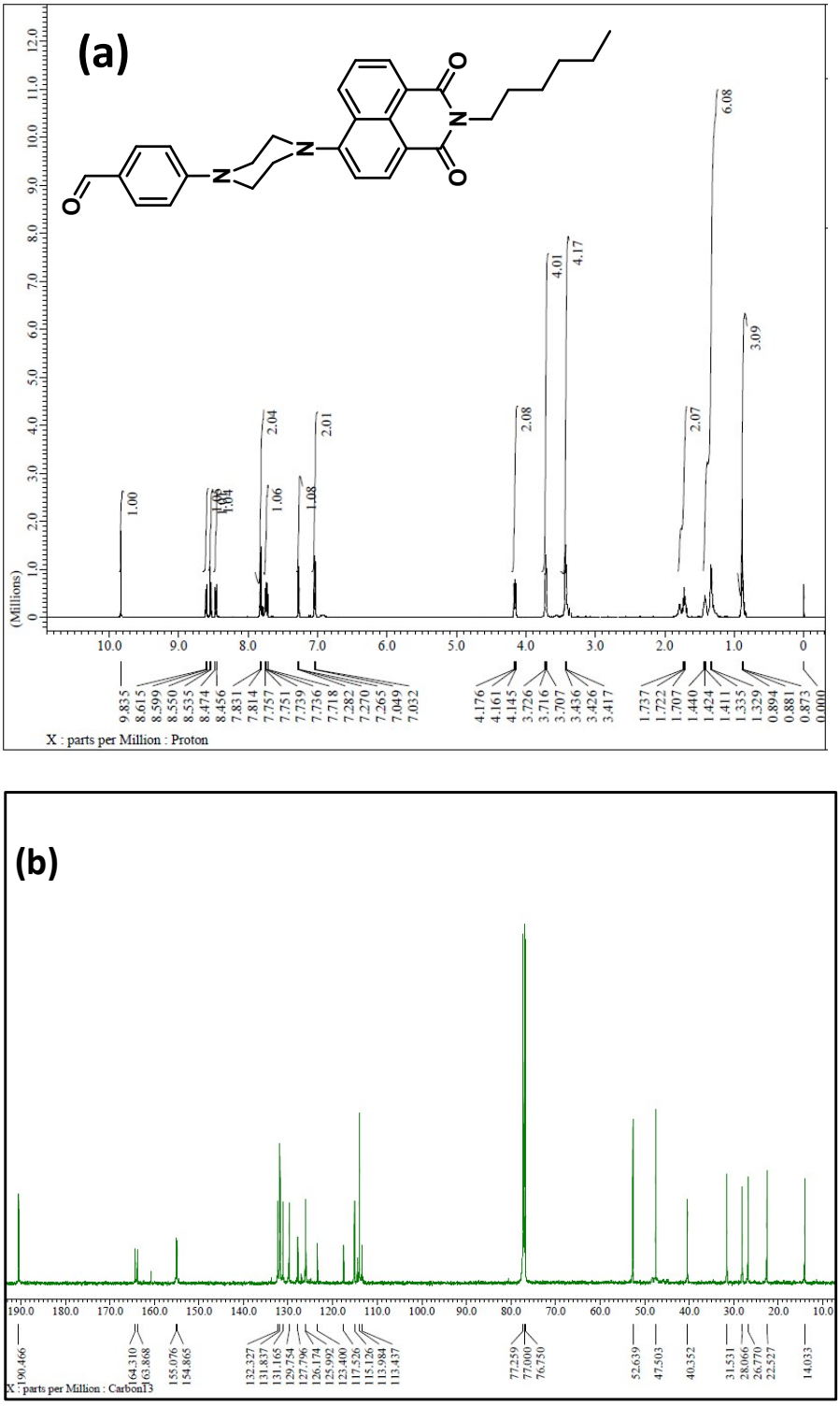

Fig. S3 ^{1}H (a) and ^{13}C (b) NMR spectra of **5C** in $CDCl_3$.

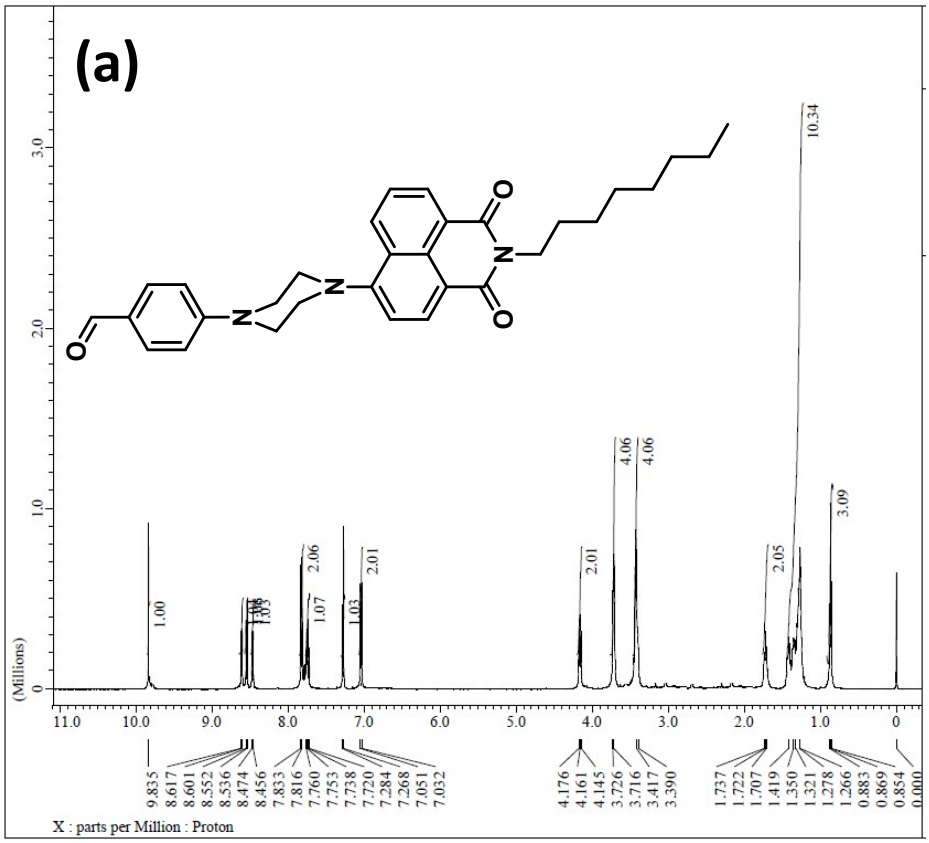

Fig. S4 ^{1}H (a) and ^{13}C (b) NMR spectra of **5D** in $CDCl_3$

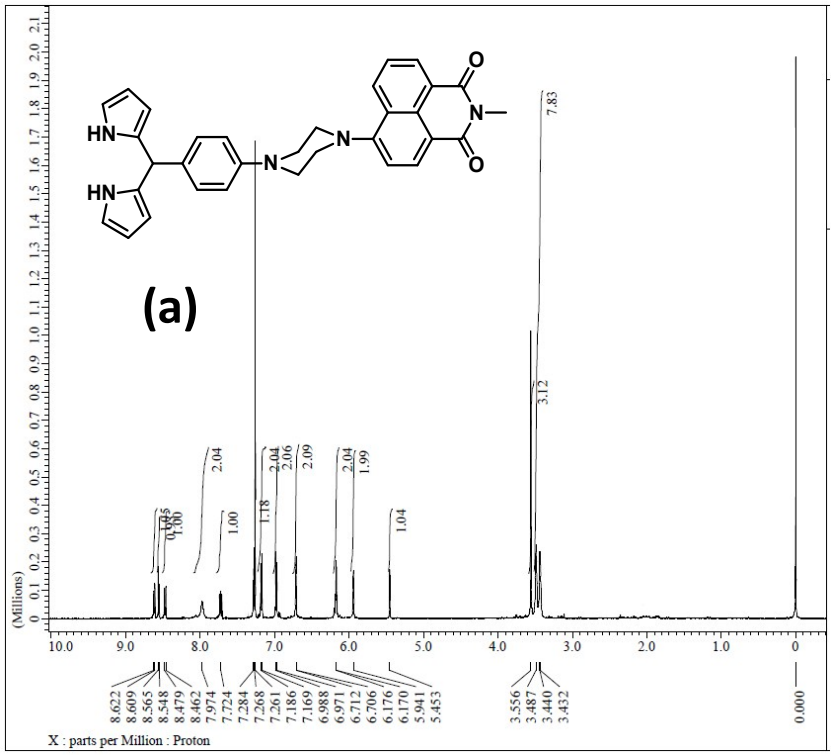

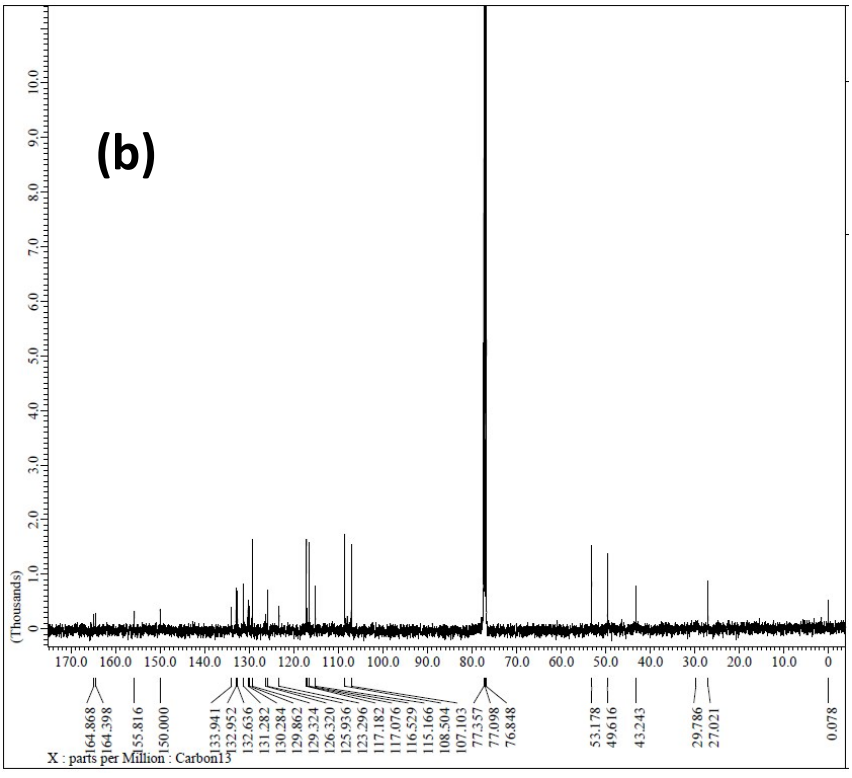

Fig. S5 ^{1}H (a) and ^{13}C (b) NMR spectra of **6A** in $CDCl_3$.

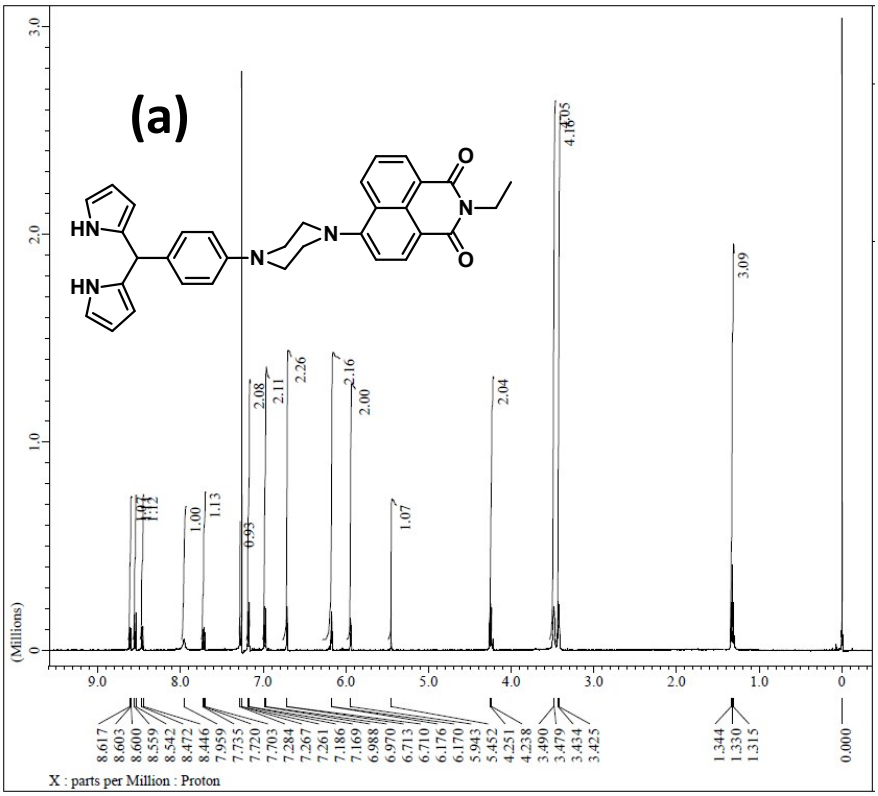

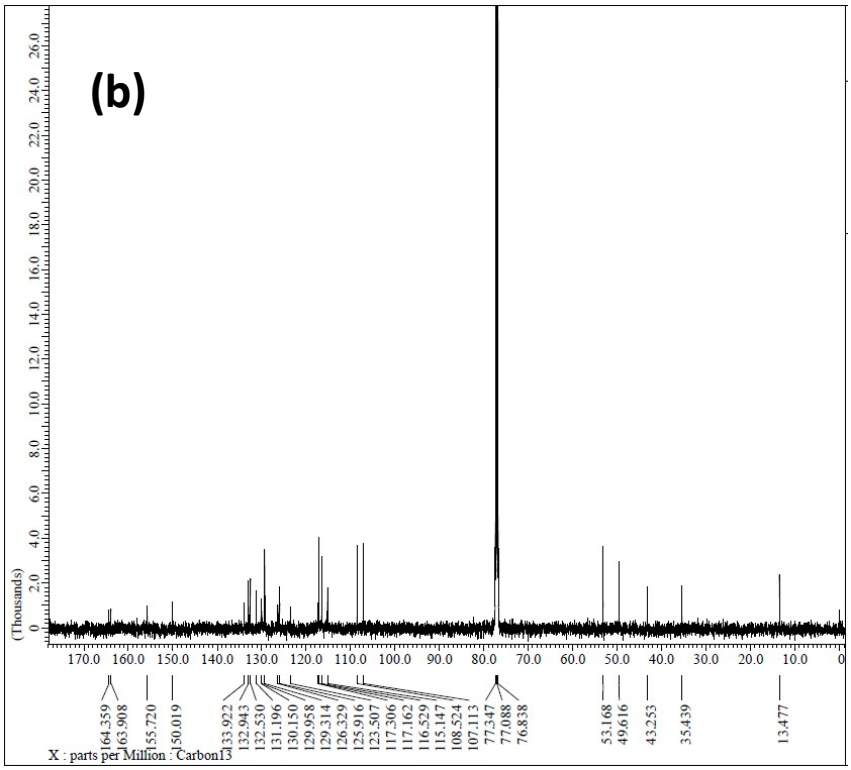

Fig. S6 ^{1}H (a) and ^{13}C (b) NMR spectra of **6B** in $CDCl_3$.

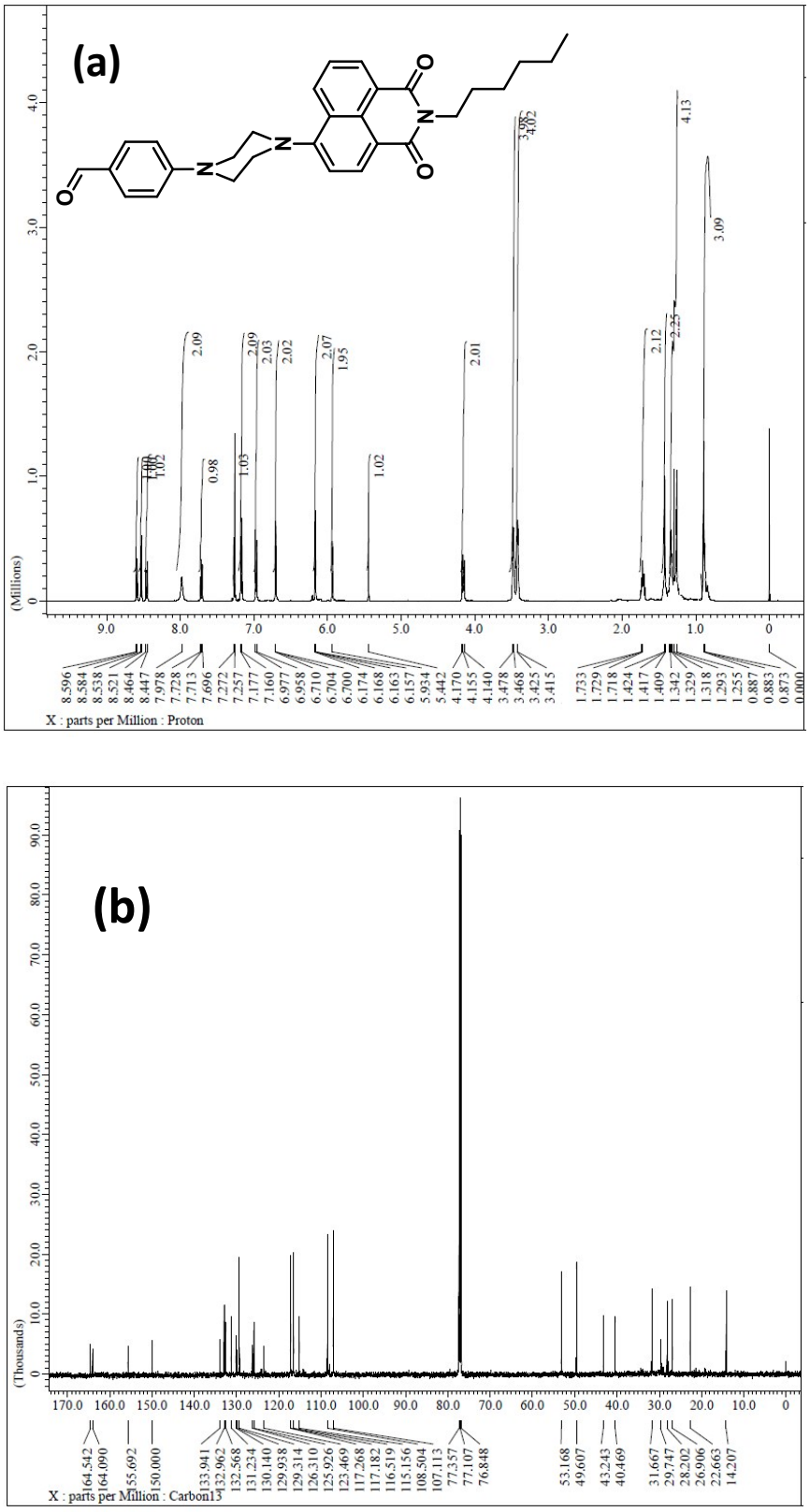

Fig. S7 ^{1}H (a) and ^{13}C (b) NMR spectra of **6C** in $CDCl_3$.

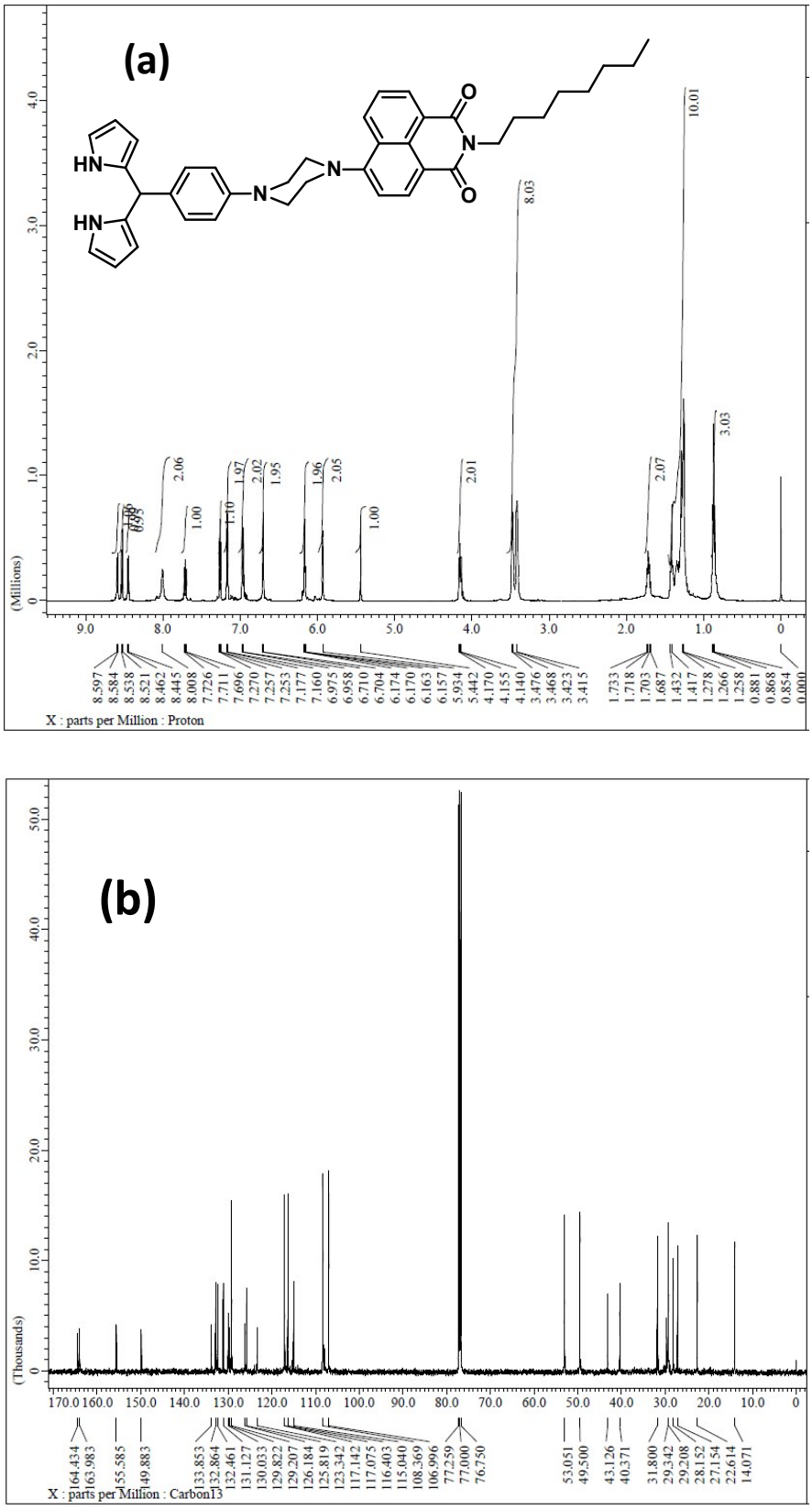

Fig. S8 ^{1}H (a) and ^{13}C (b) NMR spectra of **6D** in $CDCl_3$.

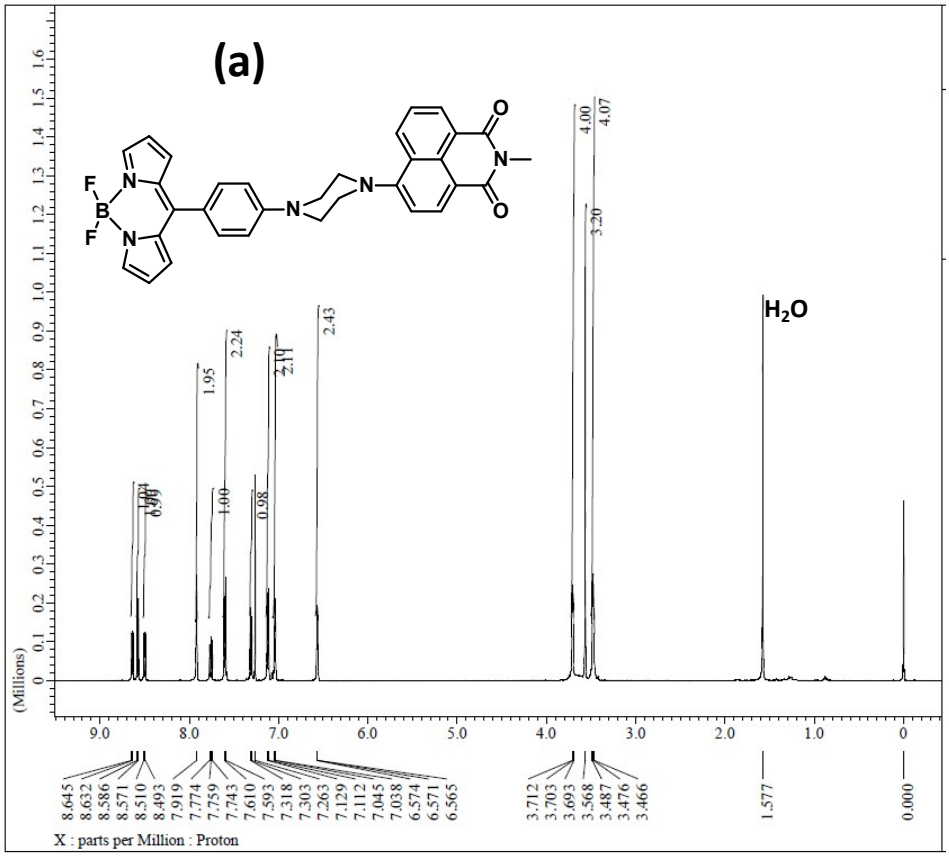

Fig. S9 ^{1}H (a) and ^{13}C (b) NMR spectra of **NPB1** in $CDCl_3$.

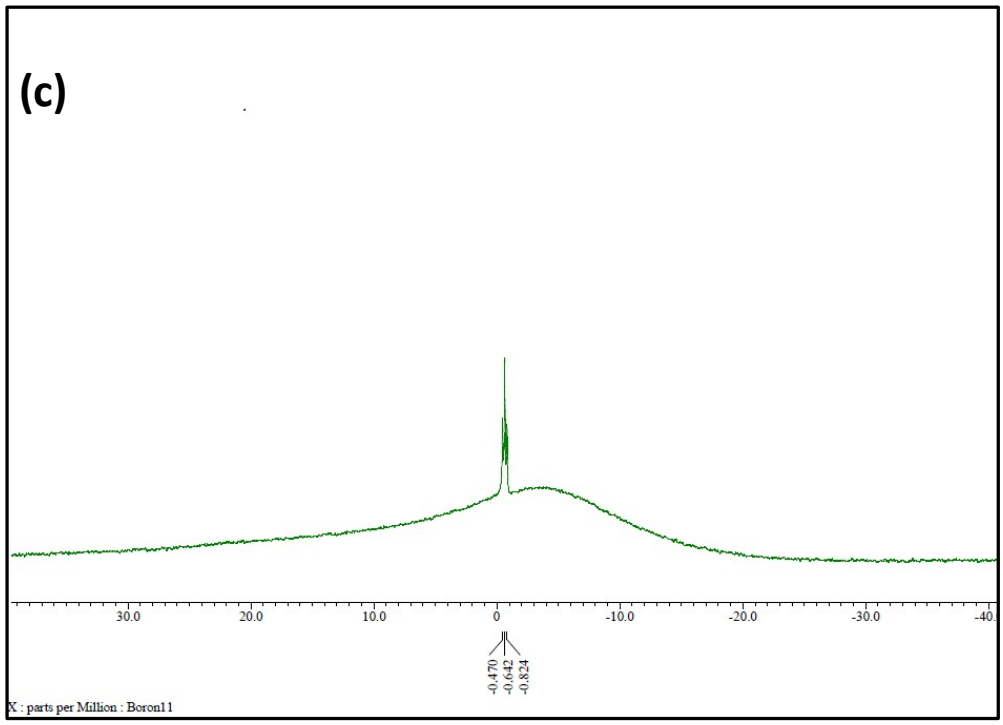

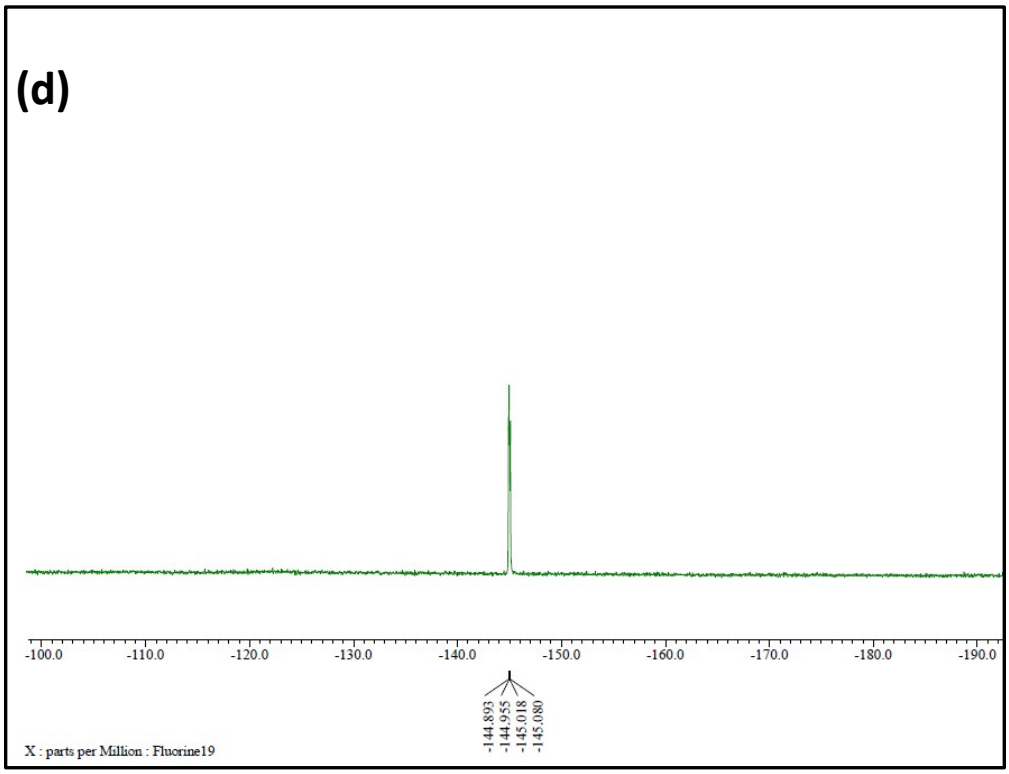

Fig. S10 ^{11}B (c) and ^{19}F (d) NMR spectra of **NPB1** in $CDCl_3$.

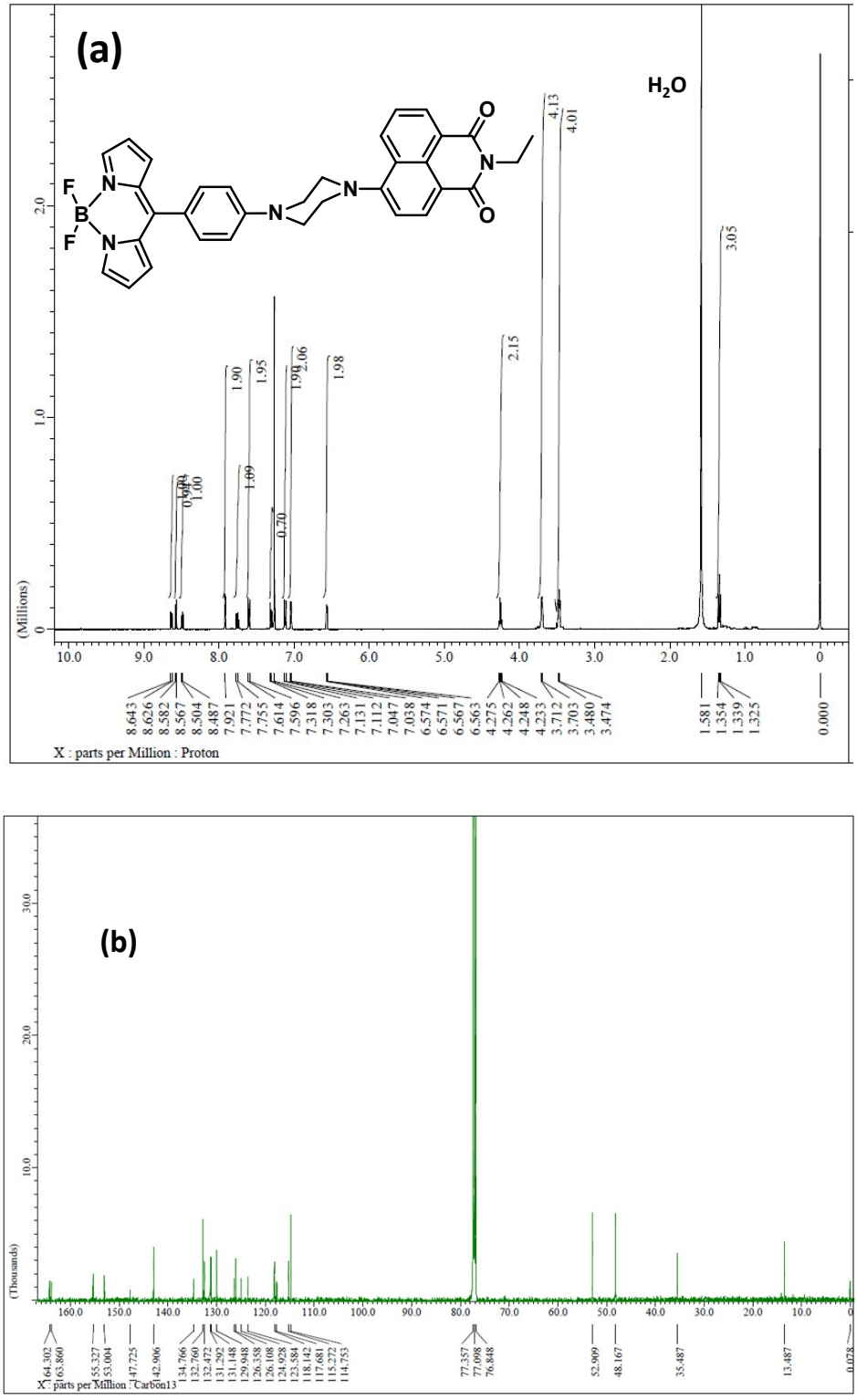

Fig. S11 ^{1}H (a) and ^{13}C (b) NMR spectra of **NPB2** in $CDCl_3$.

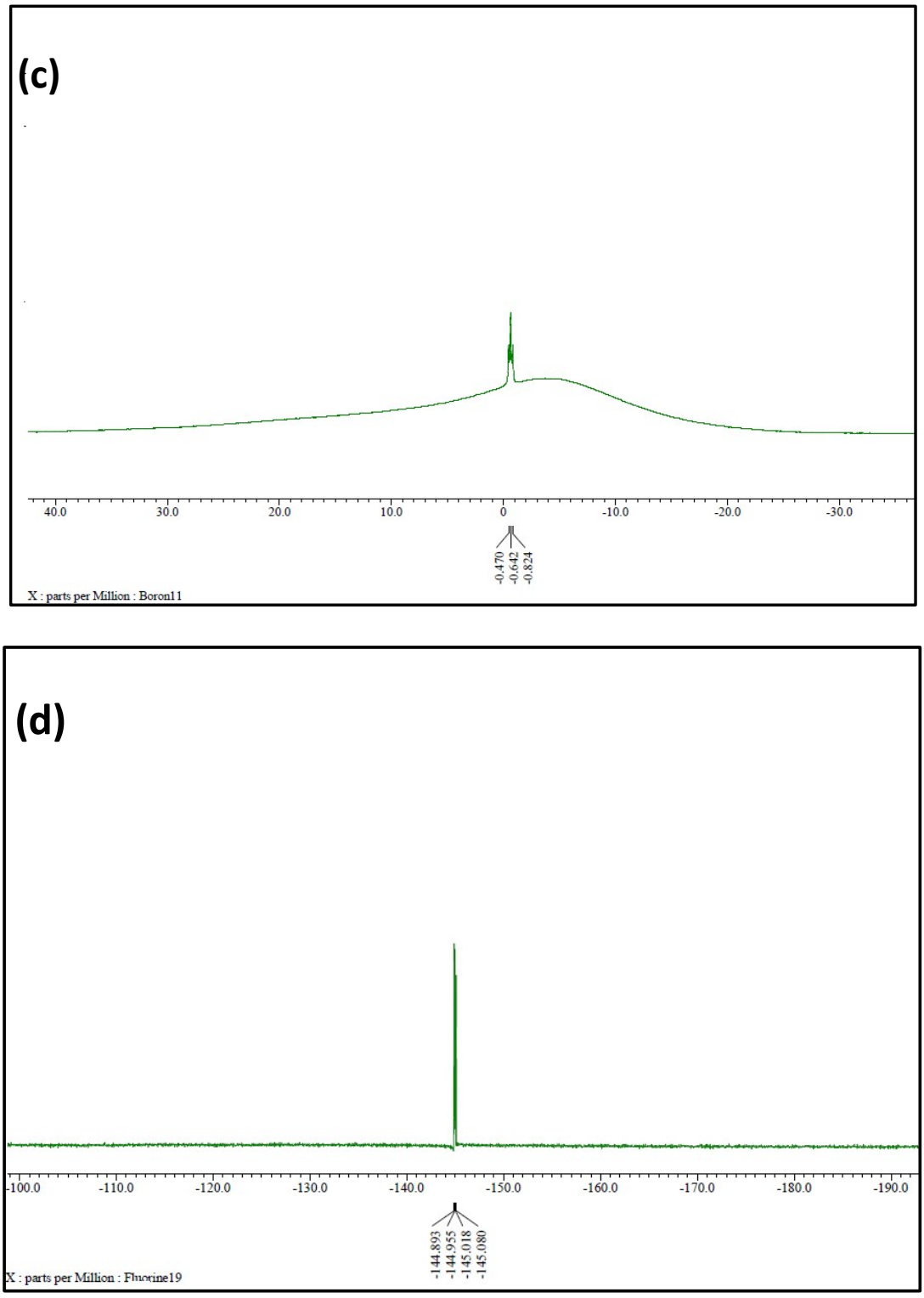

Fig. S12 ^{11}B (c) and ^{19}F (d) NMR spectra of **NPB2** in $CDCl_3$.

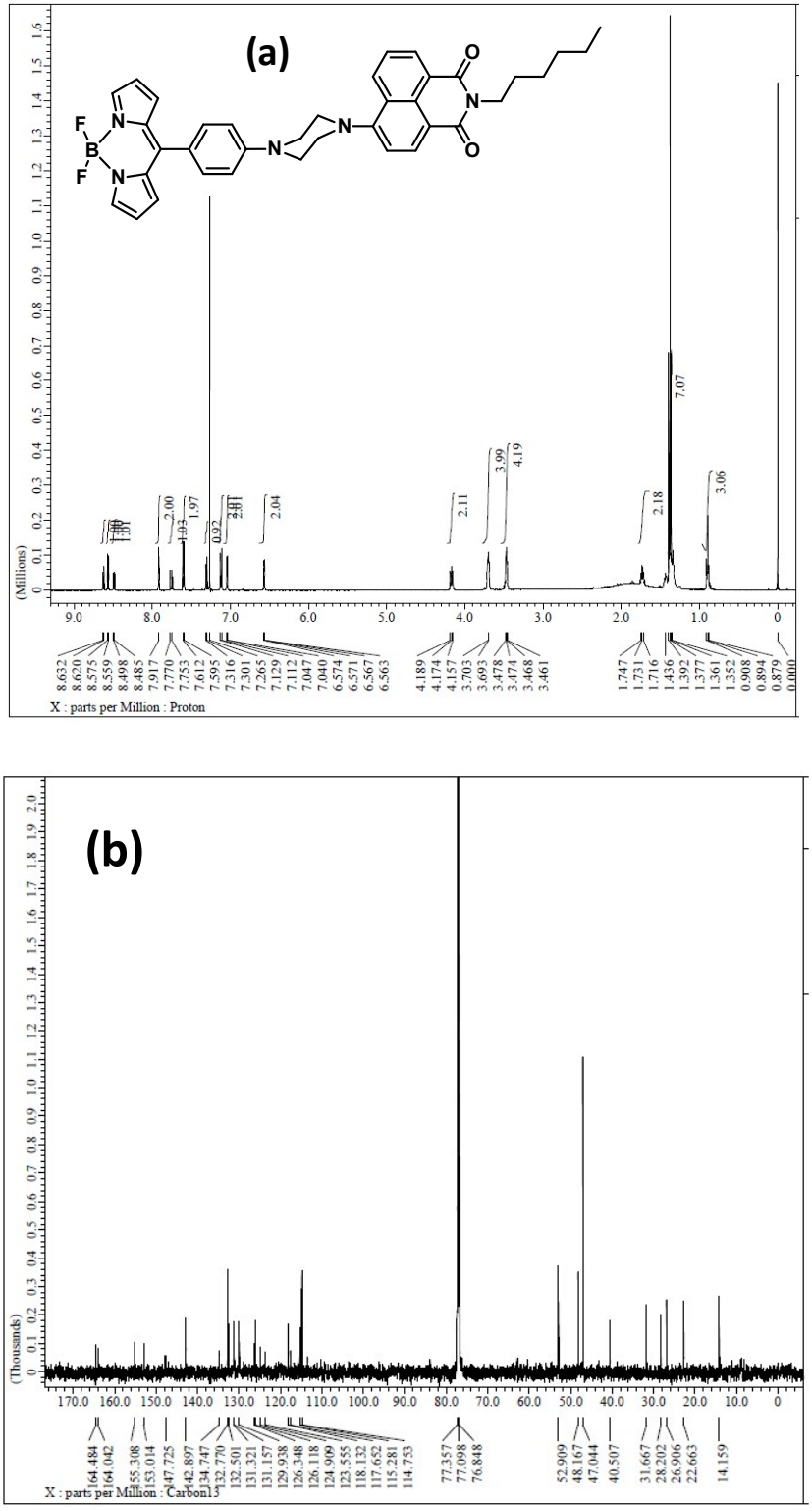

Fig. S13 ^{1}H (a) and ^{13}C (b) NMR spectra of **NPB3** in $CDCl_3$.

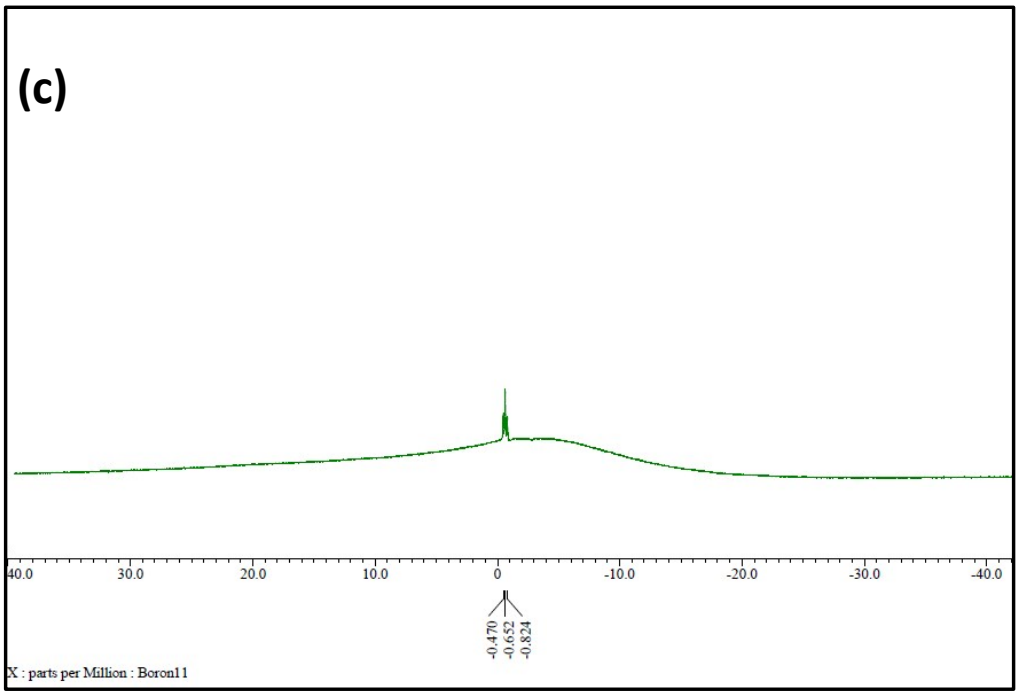

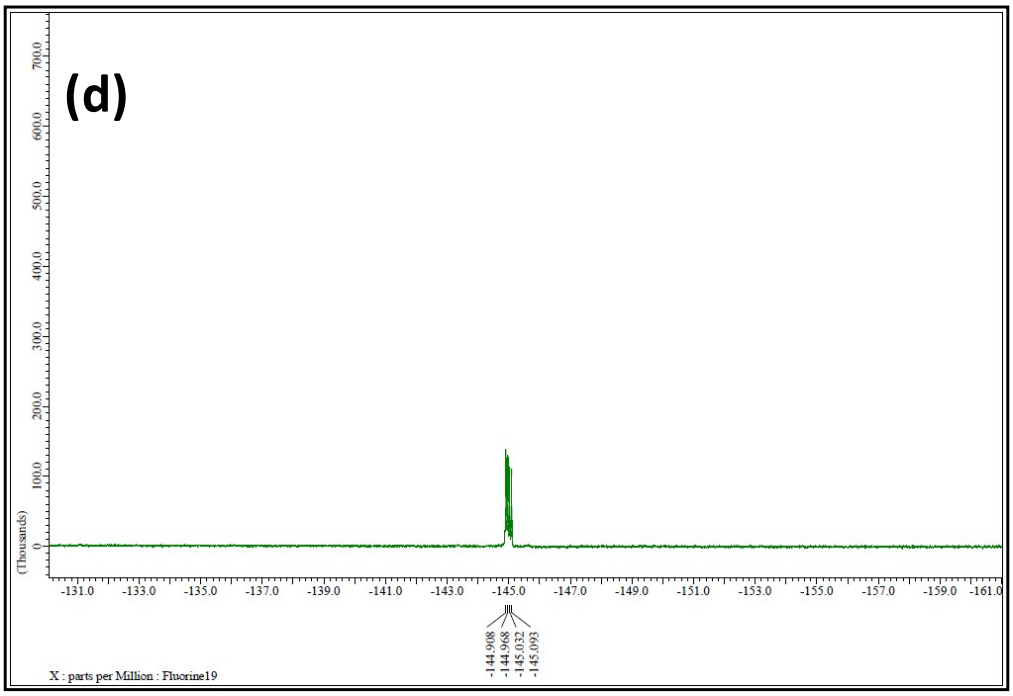

Fig. S14 ^{11}B (c) and ^{19}F (d) NMR spectra of **NPB3** in $CDCl_3$.

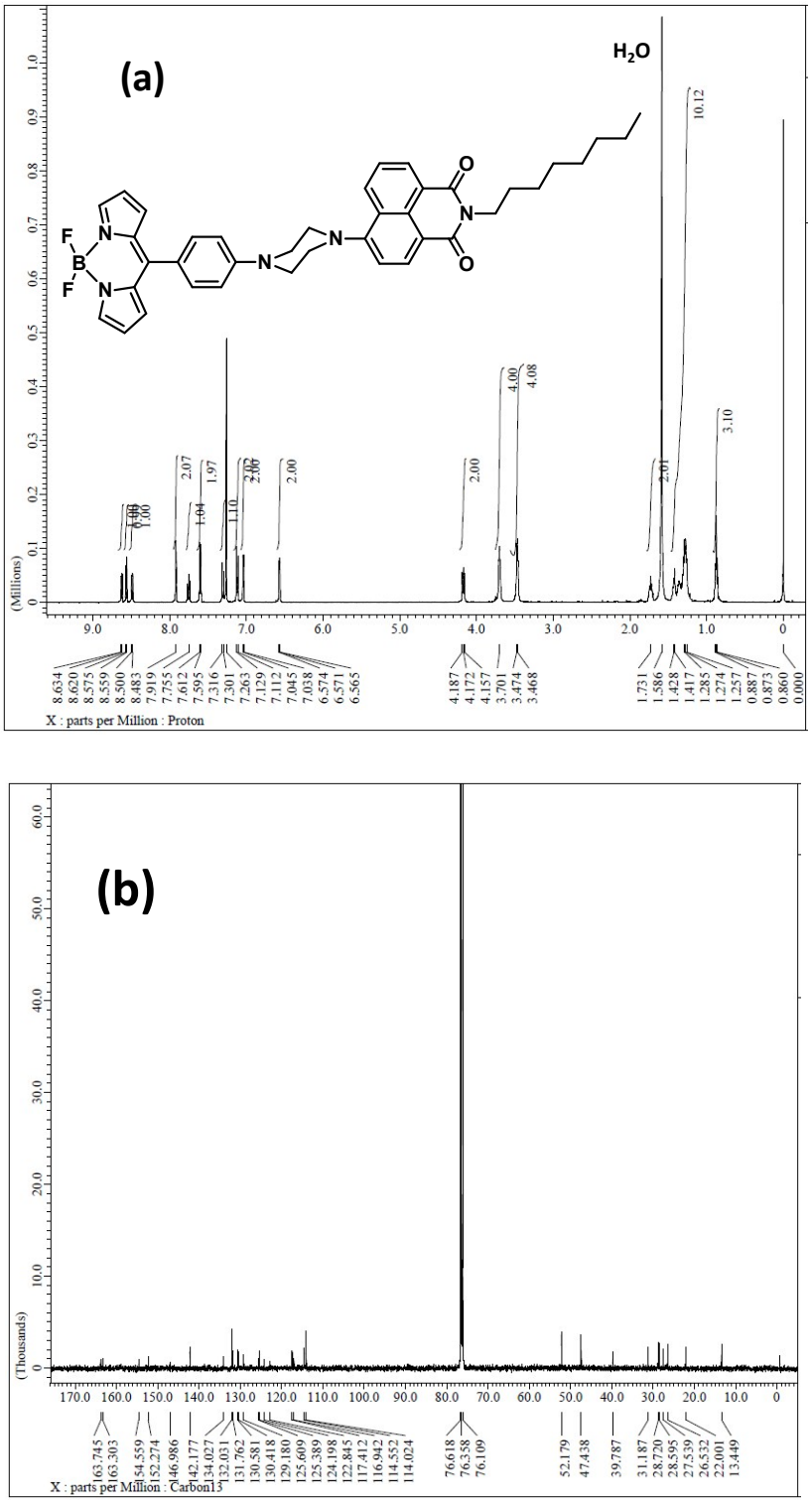

Fig. S15 ^{1}H (a) and ^{13}C (b) NMR spectra of **NPB4** in $CDCl_3$.

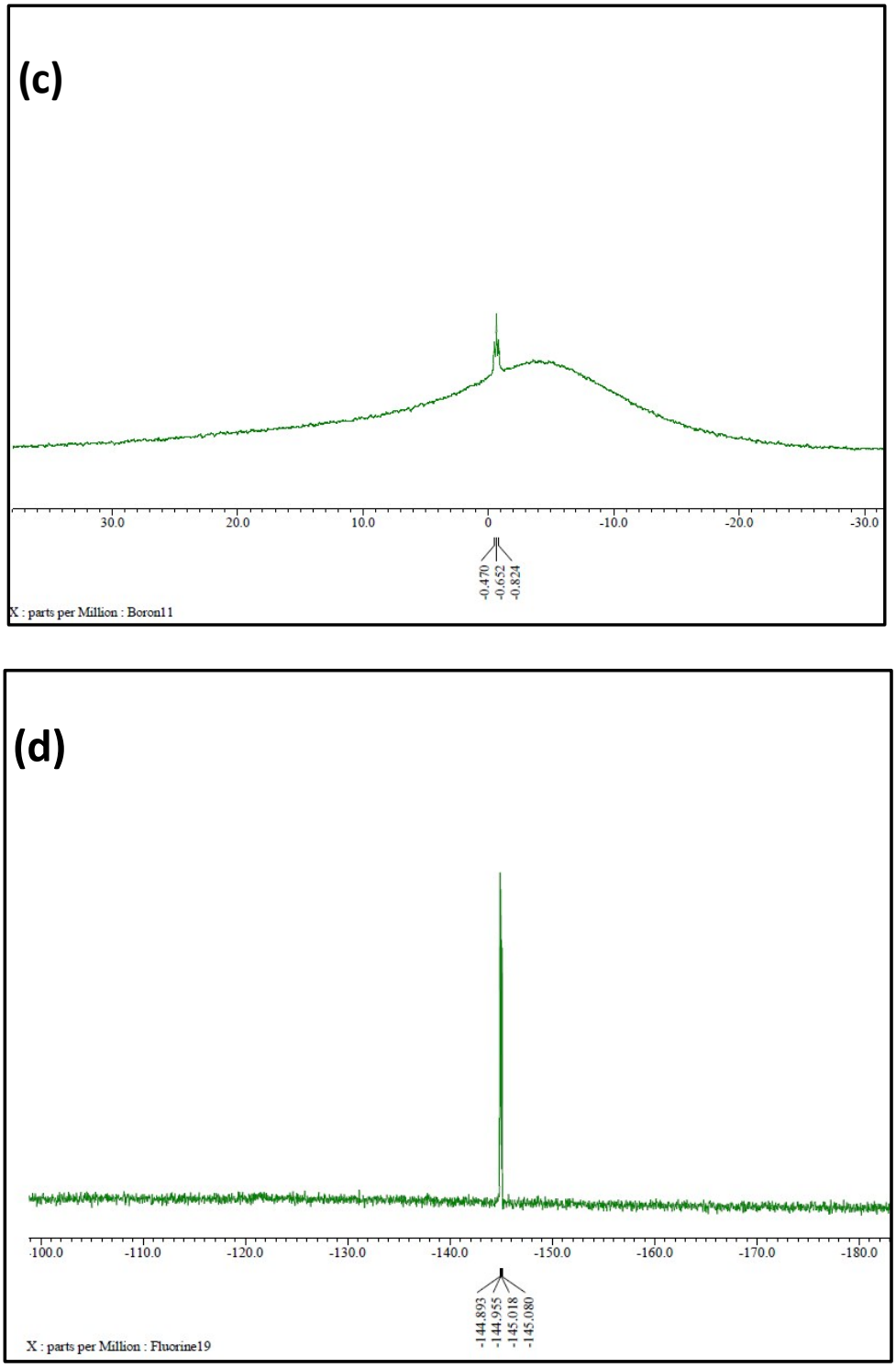

Fig. S16 ^{11}B (c) and ^{19}F (d) NMR spectra of **NPB4** in $CDCl_3$.

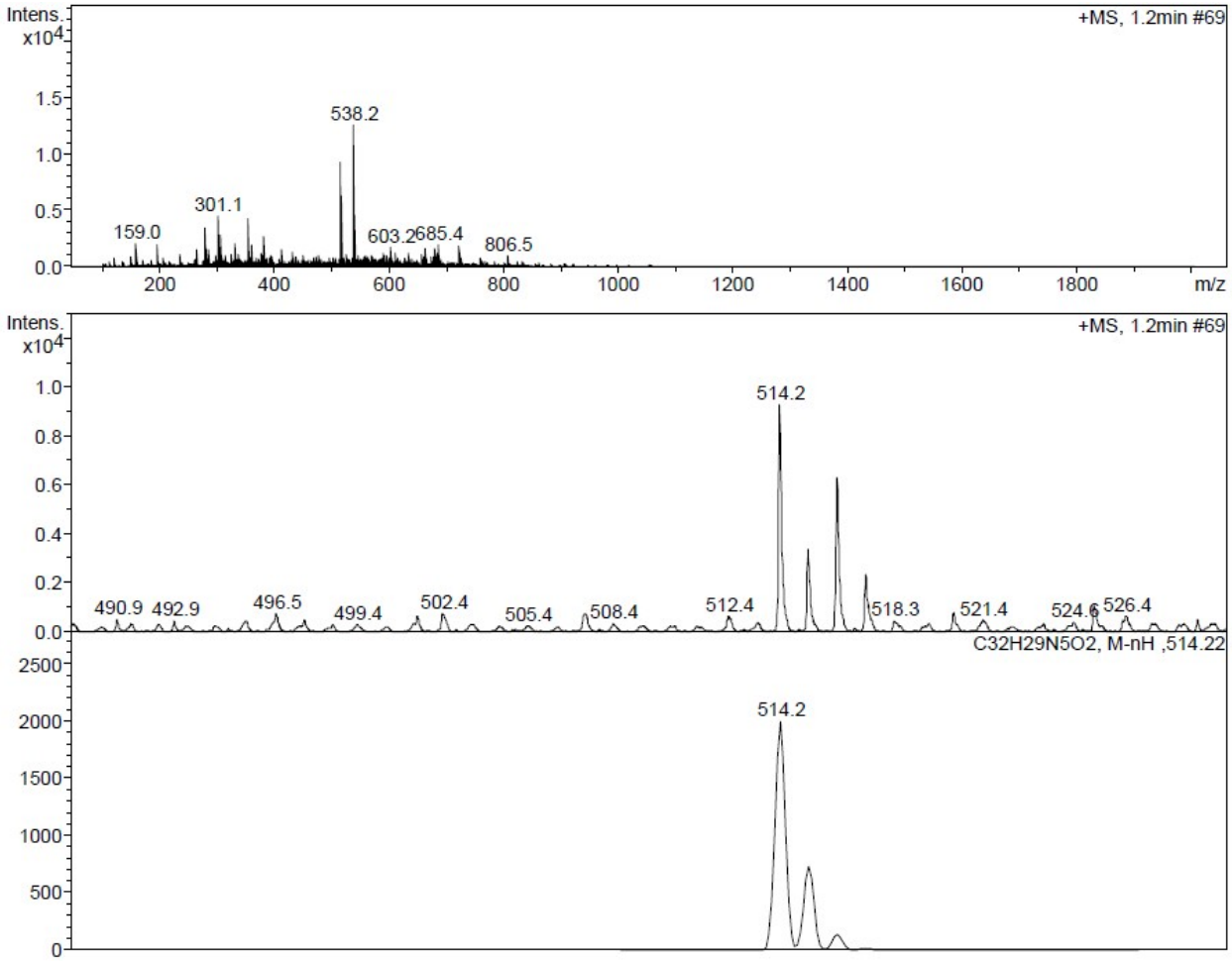

Fig. S17 ESI-MS spectra of **6A**.

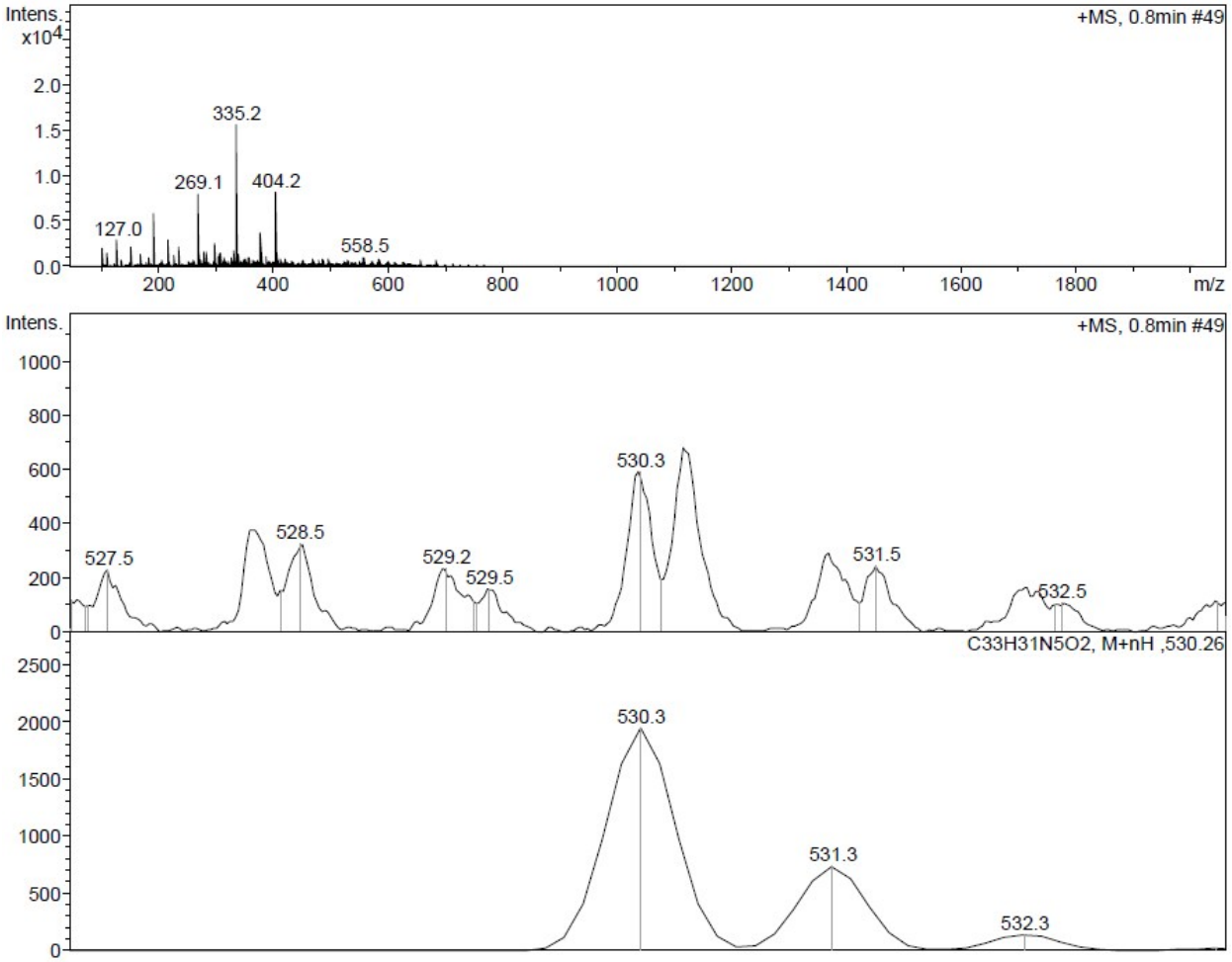

Fig. S18 ESI-MS spectra of **6B**.

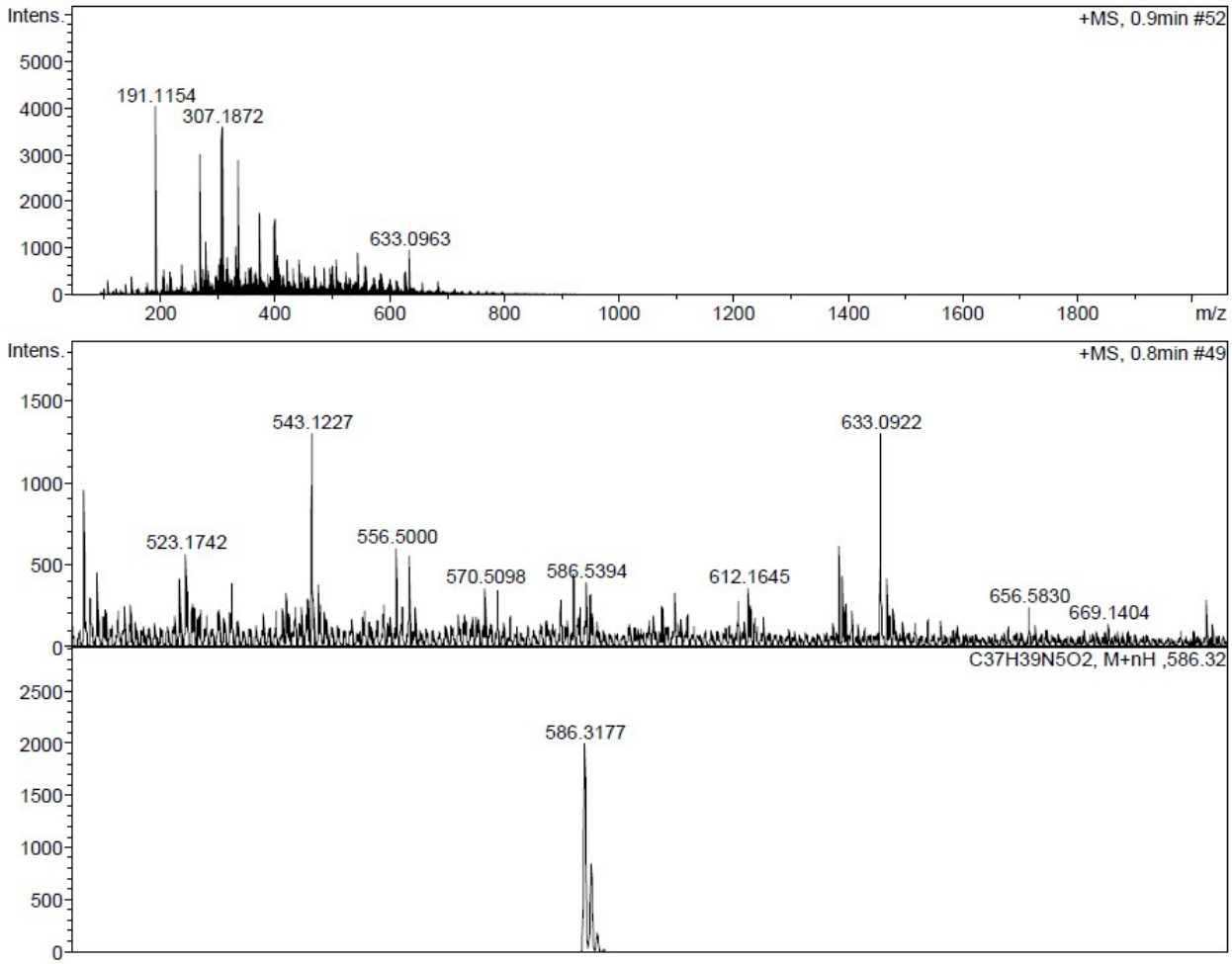

Fig. S19 HRMS spectra of **6C**.

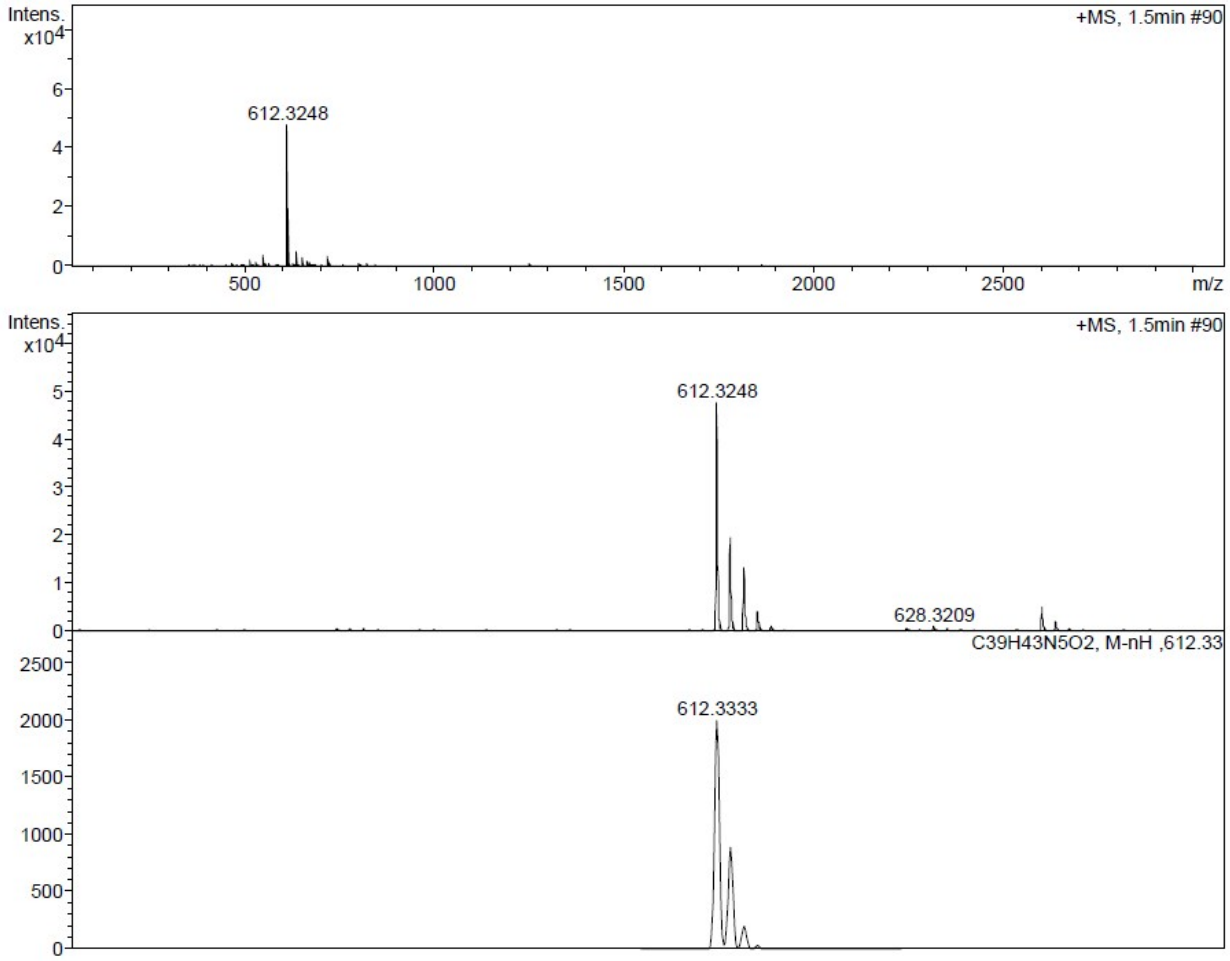

Fig. S20 HRMS spectra of **6D**.

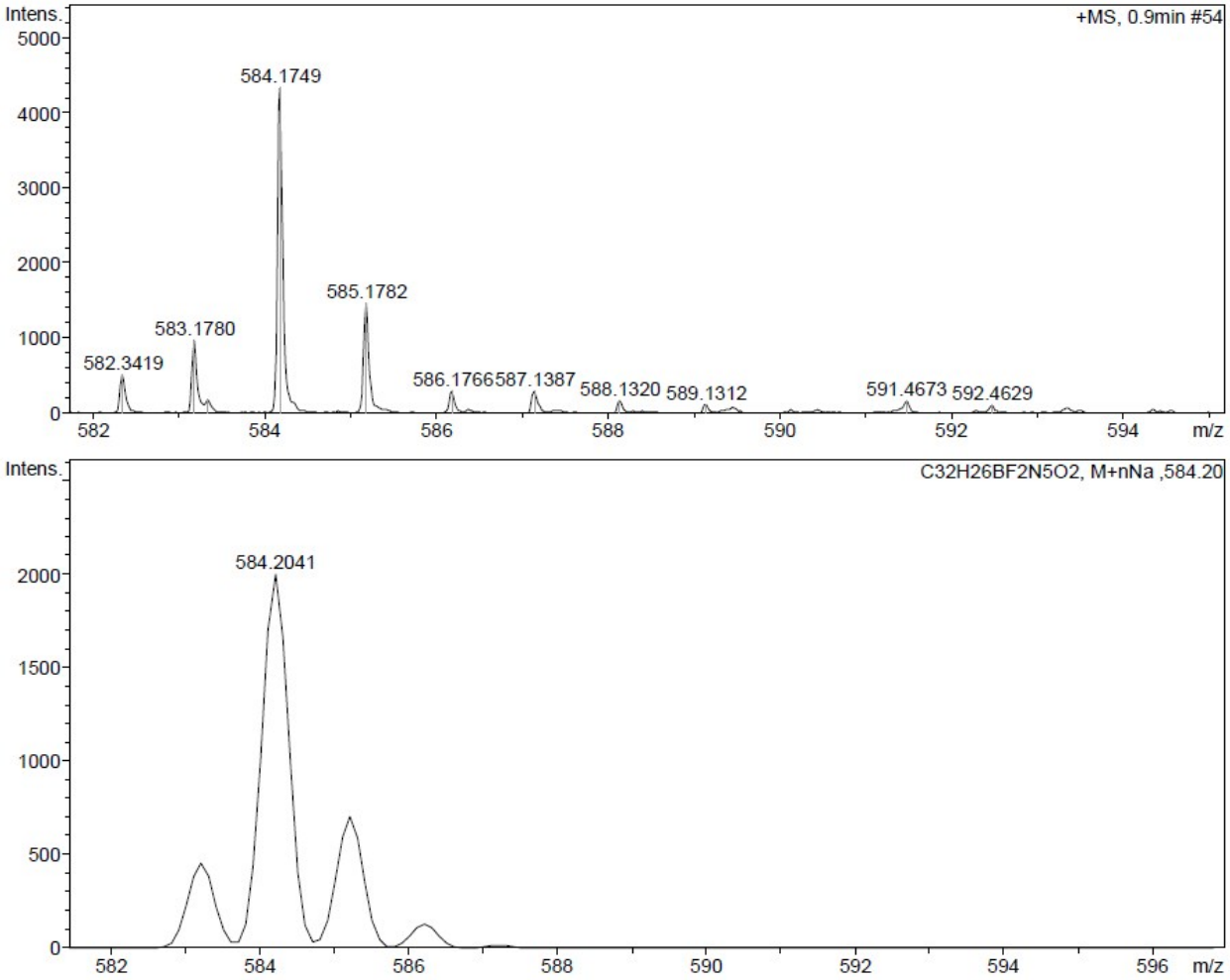

Fig. S21 HRMS spectra of **NPB1**.

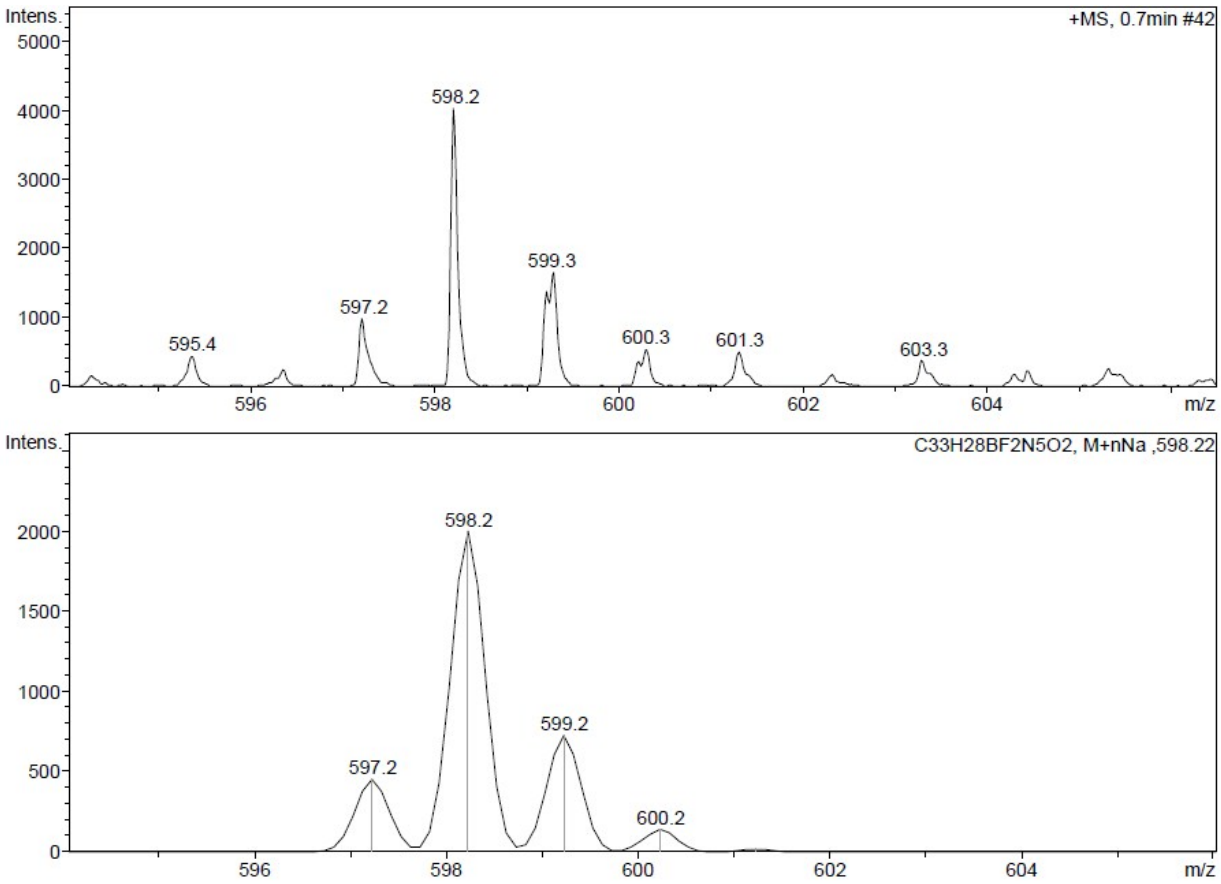

Fig. S22 ESI-MS spectra of **NPB2**.

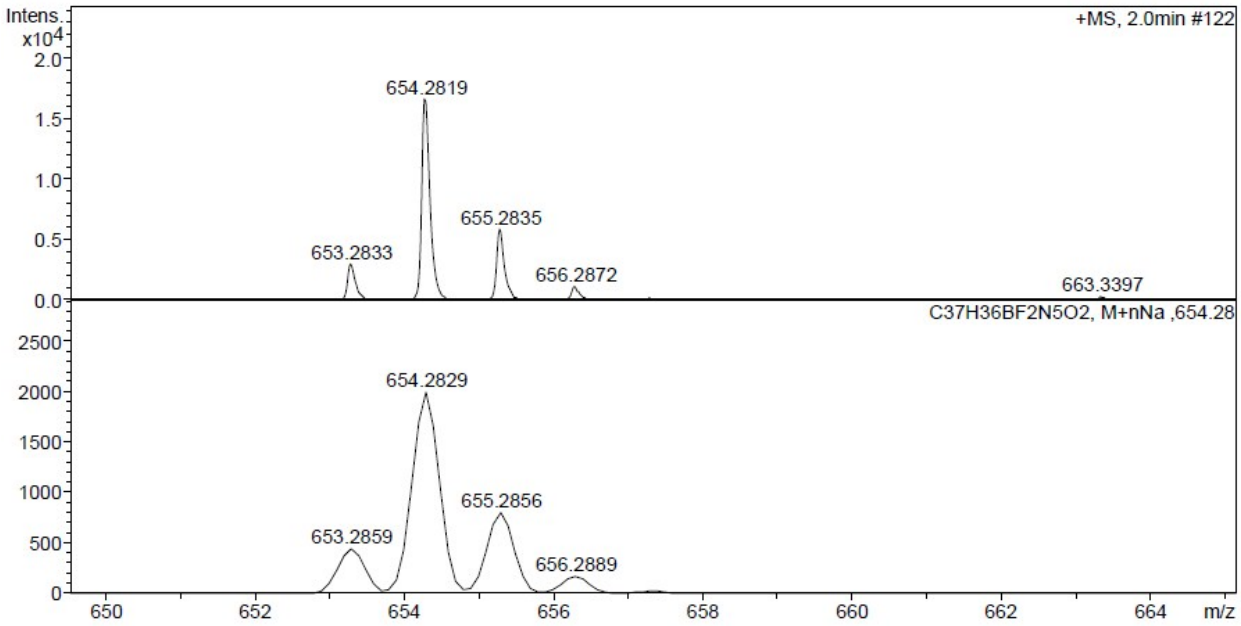

Fig. S23 HRMS spectra of **NPB3**.

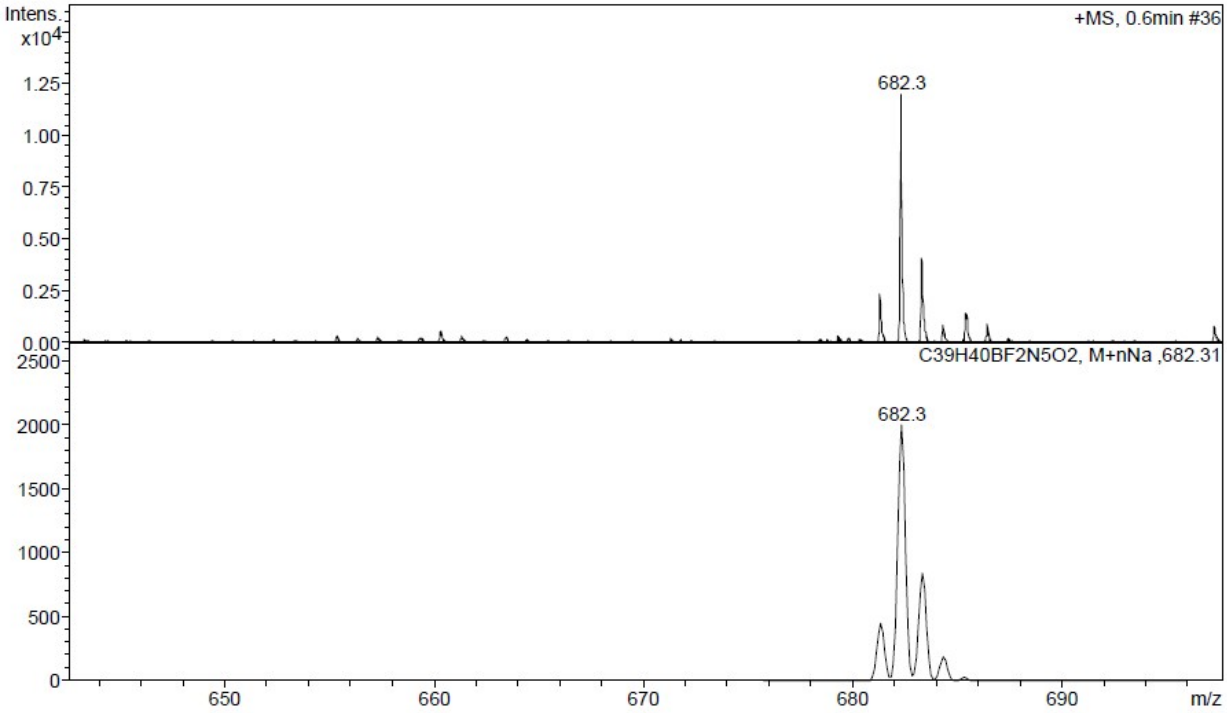

Fig. S24 ESI-MS spectra of **NPB4**.

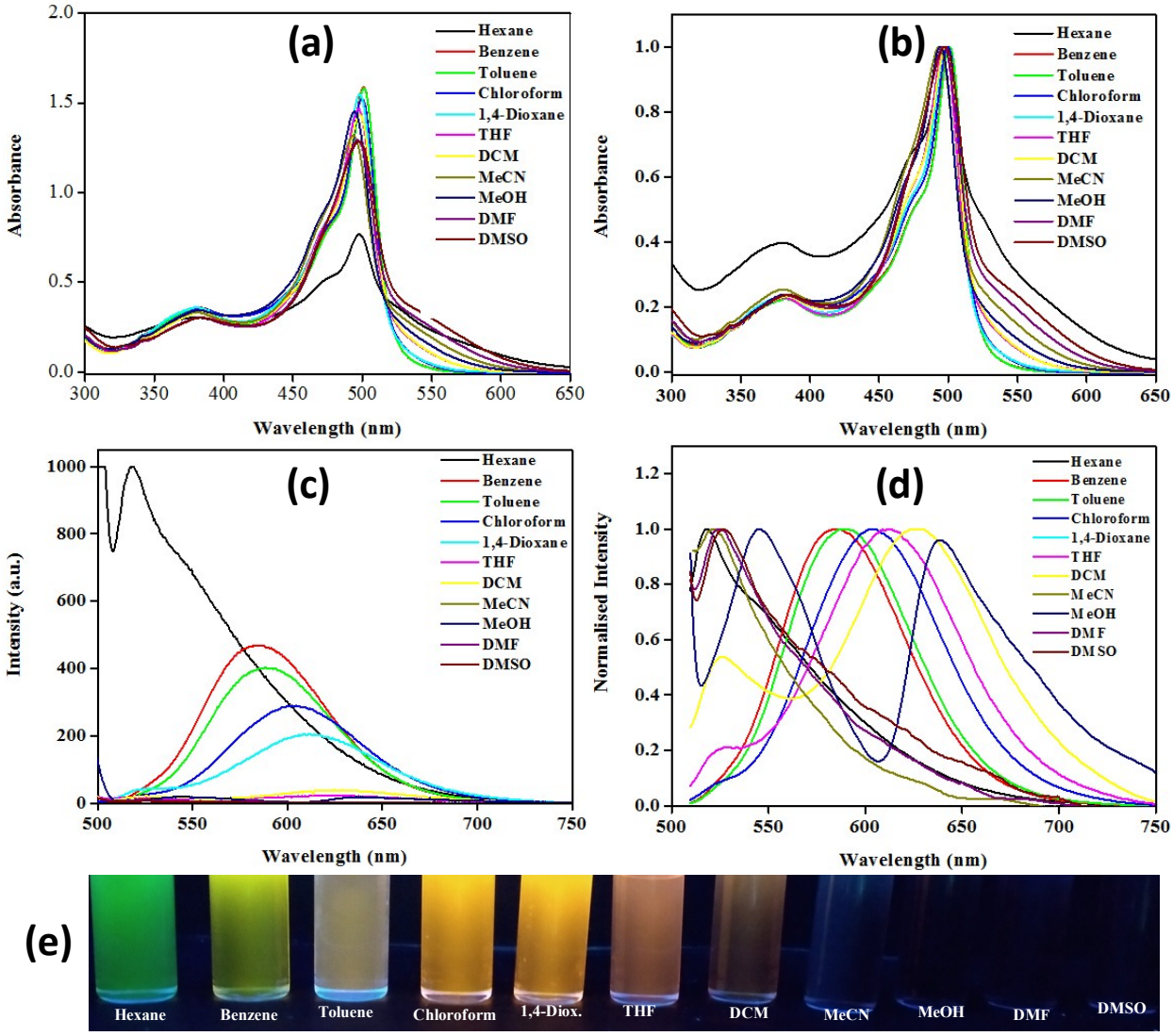

Fig. S25 Spectra in different solvents showing variation of intensity with solvent polarity: Absorption spectra (a) and its normalized representation (b), emission spectra (c) and its normalized representations (d) and photograph showing emission color change in different solvents under UV irradiation (λ_{ex}, 365 nm) (e) for **NPB1** (c, 50 μM, THF; λ_{ex}, 498 nm) [1,4-diox. = 1,4-dioxane, THF = tetrahydrofuran, DCM = dichloromethane, MeCN = acetonitrile, MeOH = methanol, DMF = N,N-methylformamide, DMSO = dimethylsulfoxide].

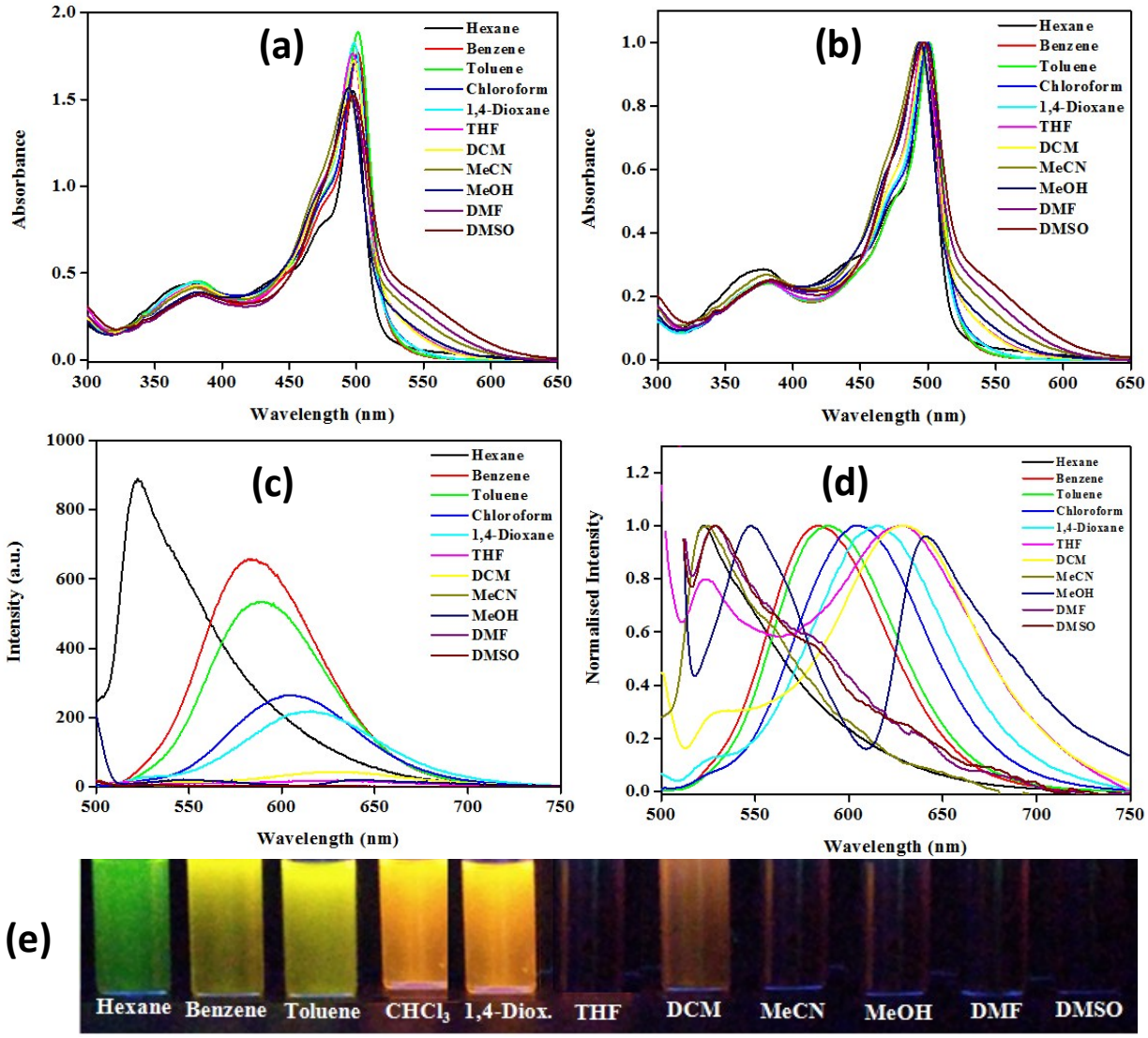

Fig. S26 Spectra in different solvents showing variation of intensity with solvent polarity: Absorption spectra (a) and its normalized representation (b), emission spectra (c) and its normalized representations (d) and photograph showing emission color change in different solvents under UV irradiation (λ_{ex}, 365 nm) (e) for **NPB2** (c, 50 μM, THF; λ_{ex}, 498 nm) [1,4-diox. = 1,4-dioxane, THF = tetrahydrofuran, DCM = dichloromethane, MeCN = acetonitrile, MeOH = methanol, DMF = N,N-methylformamide, DMSO = dimethylsulfoxide].

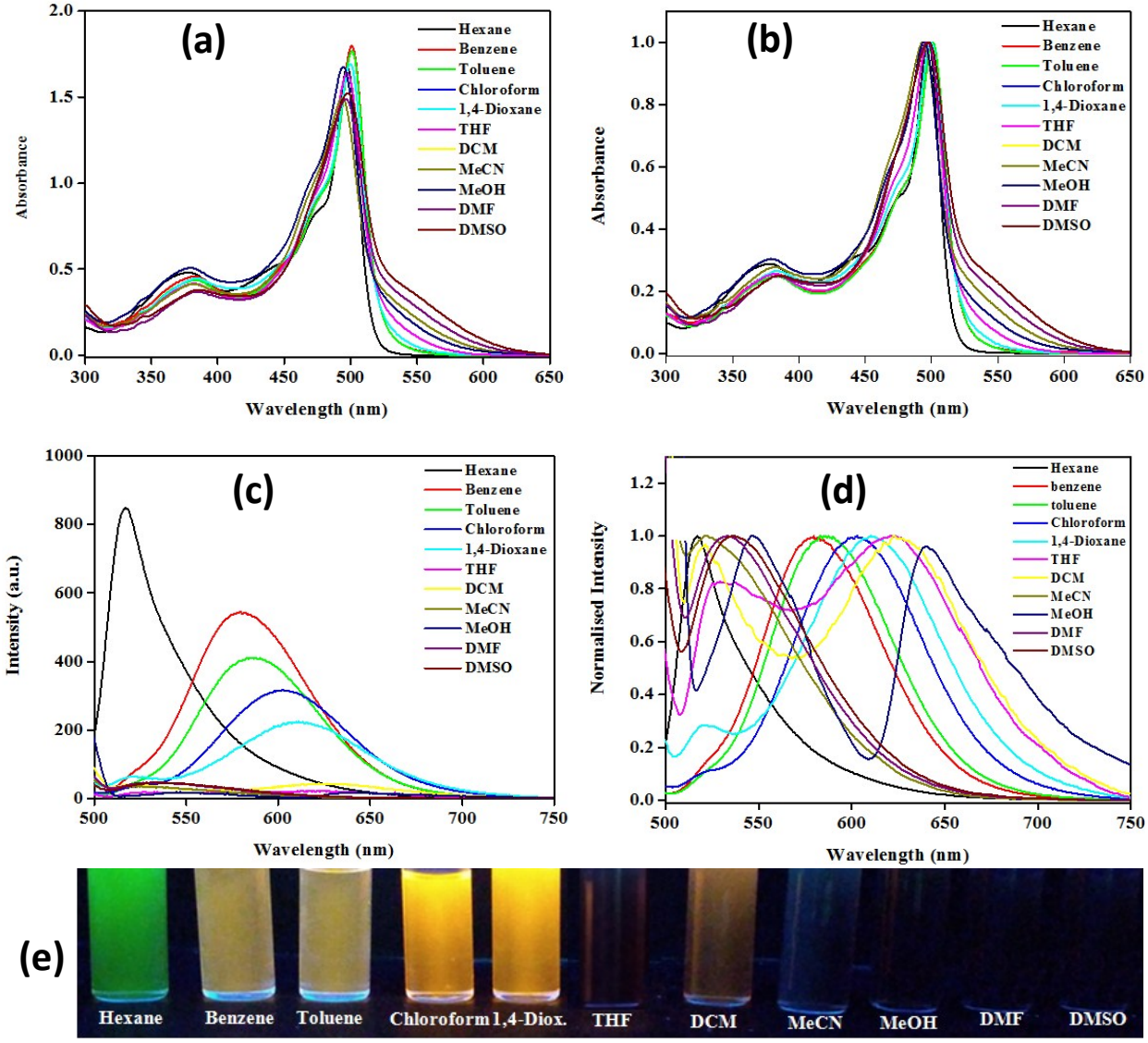

Fig. S27 Spectra in different solvents showing variation of intensity with solvent polarity: Absorption spectra (a) and its normalized representation (b), emission spectra (c) and its normalized representations (d) and photograph showing emission color change in different

solvents under UV irradiation (λ_{ex}, 365 nm) (e) for **NPB3** (c, 50 μM, THF; λ_{ex}, 498 nm) [1,4-diox. = 1,4-dioxane, THF = tetrahydrofuran, DCM = dichloromethane, MeCN = acetonitrile, MeOH = methanol, DMF = N,N-methylformamide, DMSO = dimethylsulfoxide].

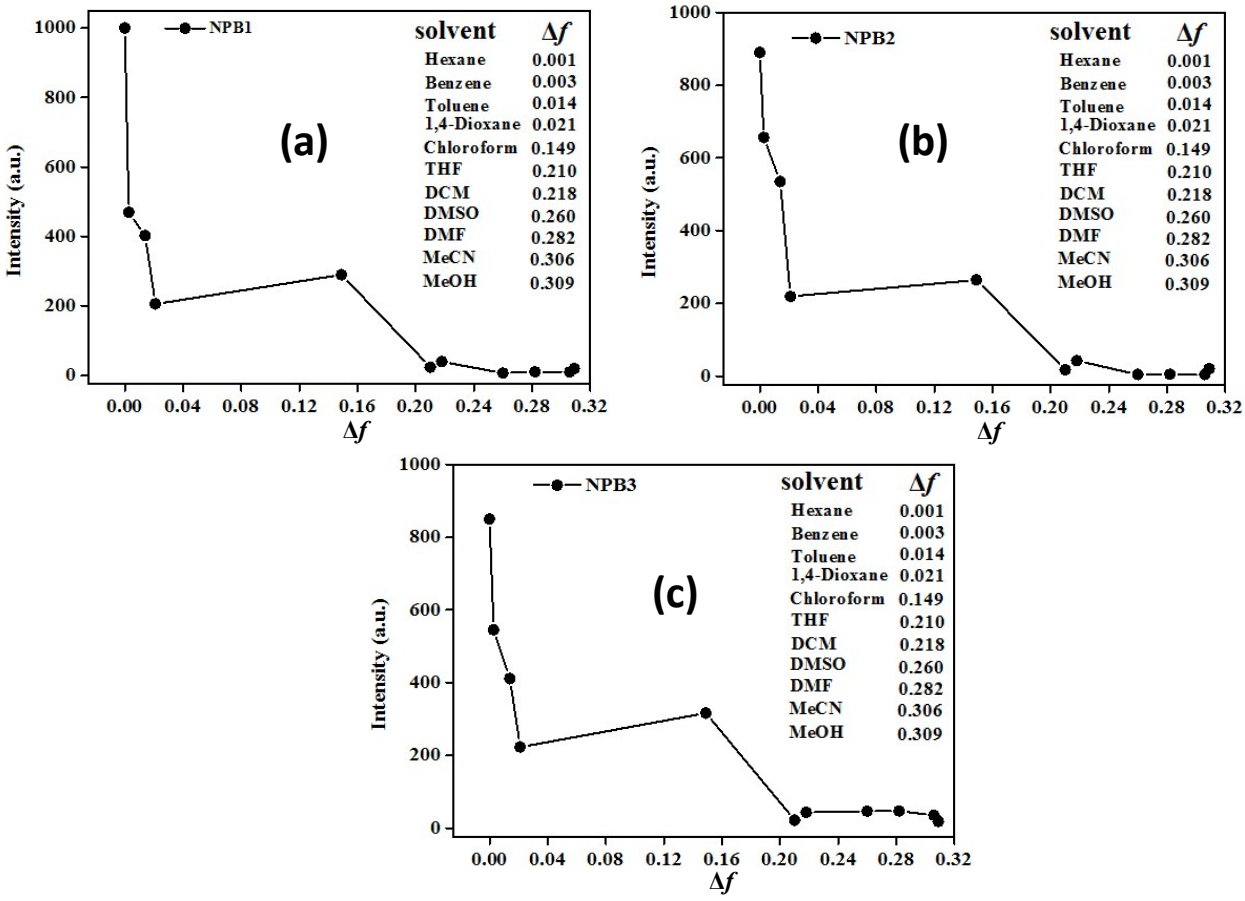

Fig. S28 Plot of emission intensity *vs* solvent polarity parameter (Δf) for **NPB1** (a), **NPB2** (b), and **NPB3** (c) (c, 50 μM in THF, λ_{ex}, 498 nm) [THF = tetrahydrofuran, DCM = dichloromethane, MeCN = acetonitrile, MeOH = methanol, DMF = N,N-methylformamide, DMSO = dimethylsulfoxide].

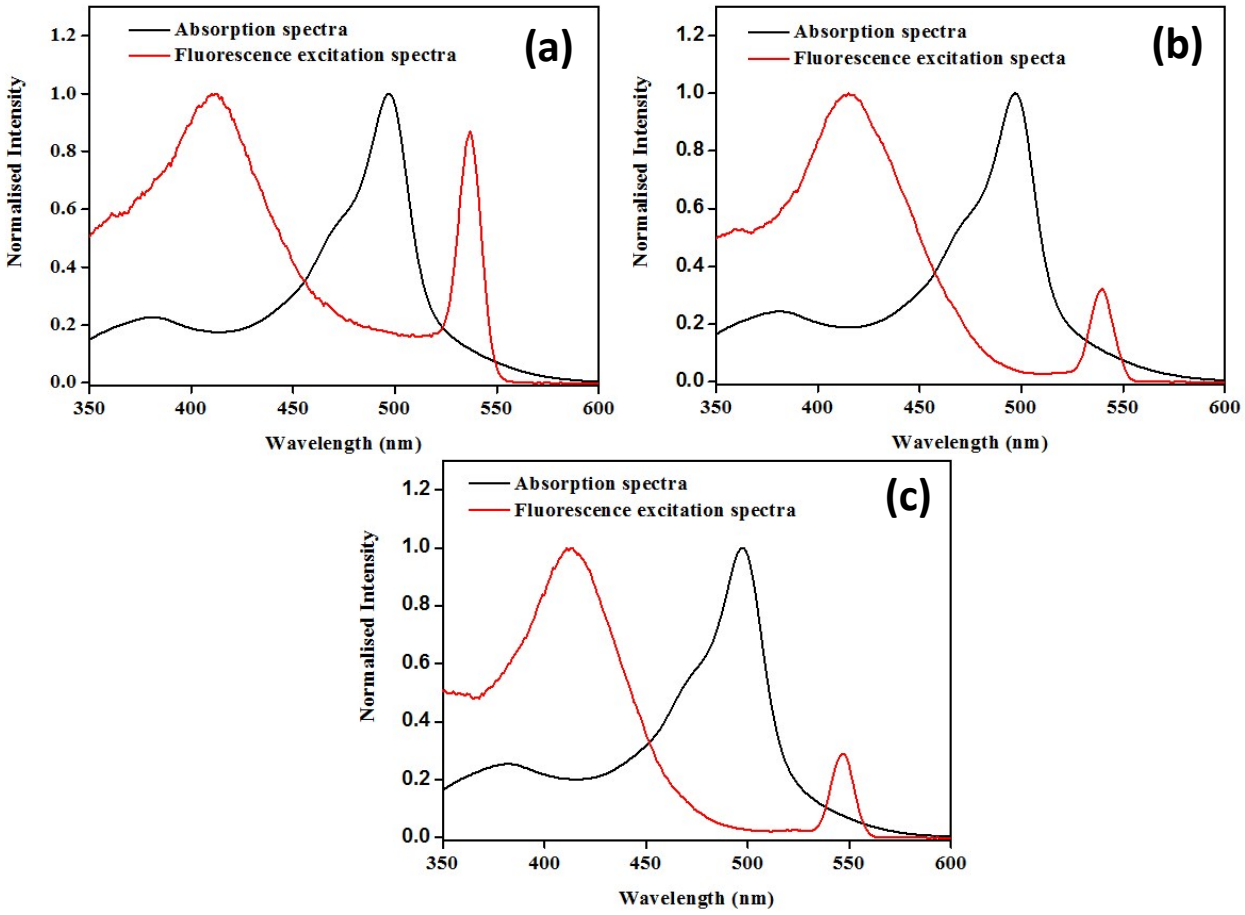

Fig. S29 Excitation spectra of **NPB1** (a), **NPB2** (b), and **NPB3** (c) at λ_{em} , 520 nm, 522 nm, and 526 nm respectively (c, 50 μM in THF).

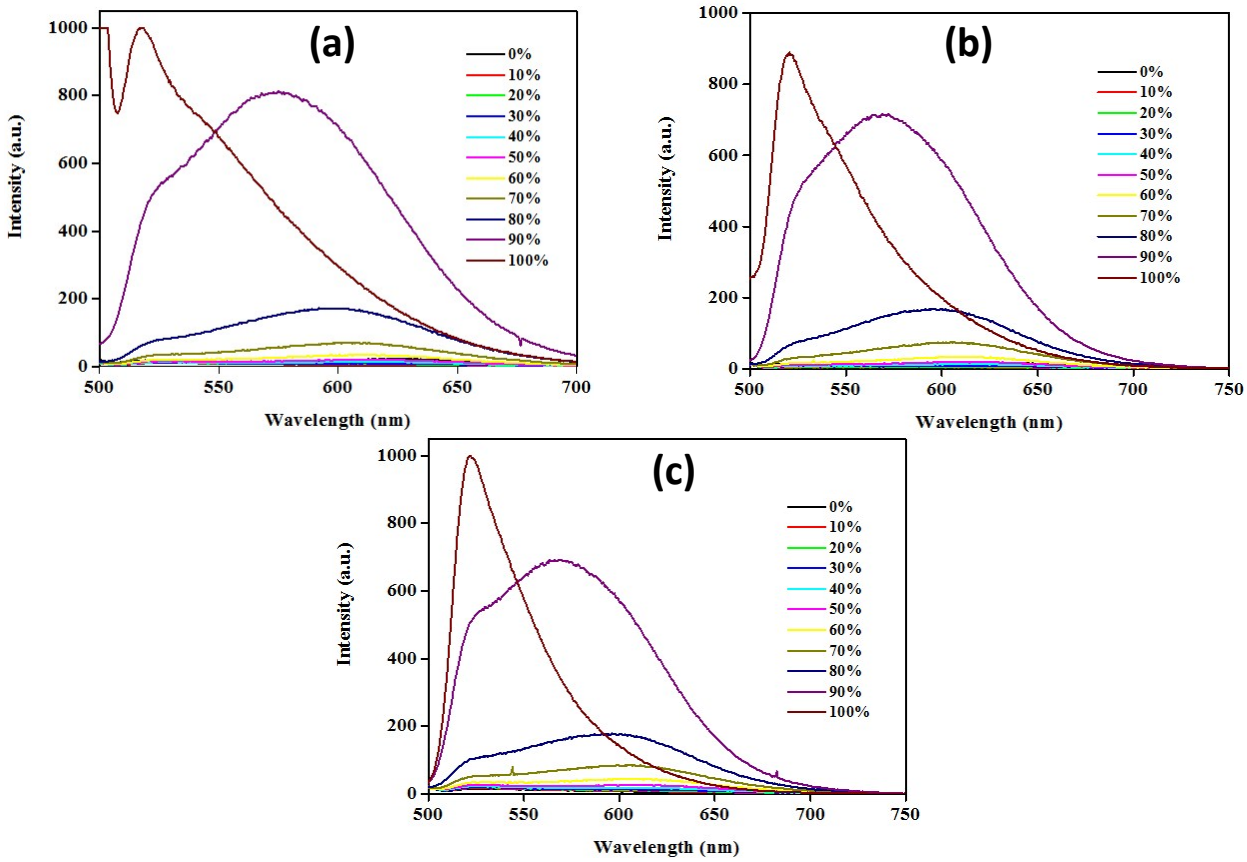

Fig. S30 Emission spectra of **NPB1** (a), **NPB2** (b)**,** and **NPB3** (c) with varying hexane volume fractions, (c, 50 μM in THF, λ_{ex}, 498 nm).

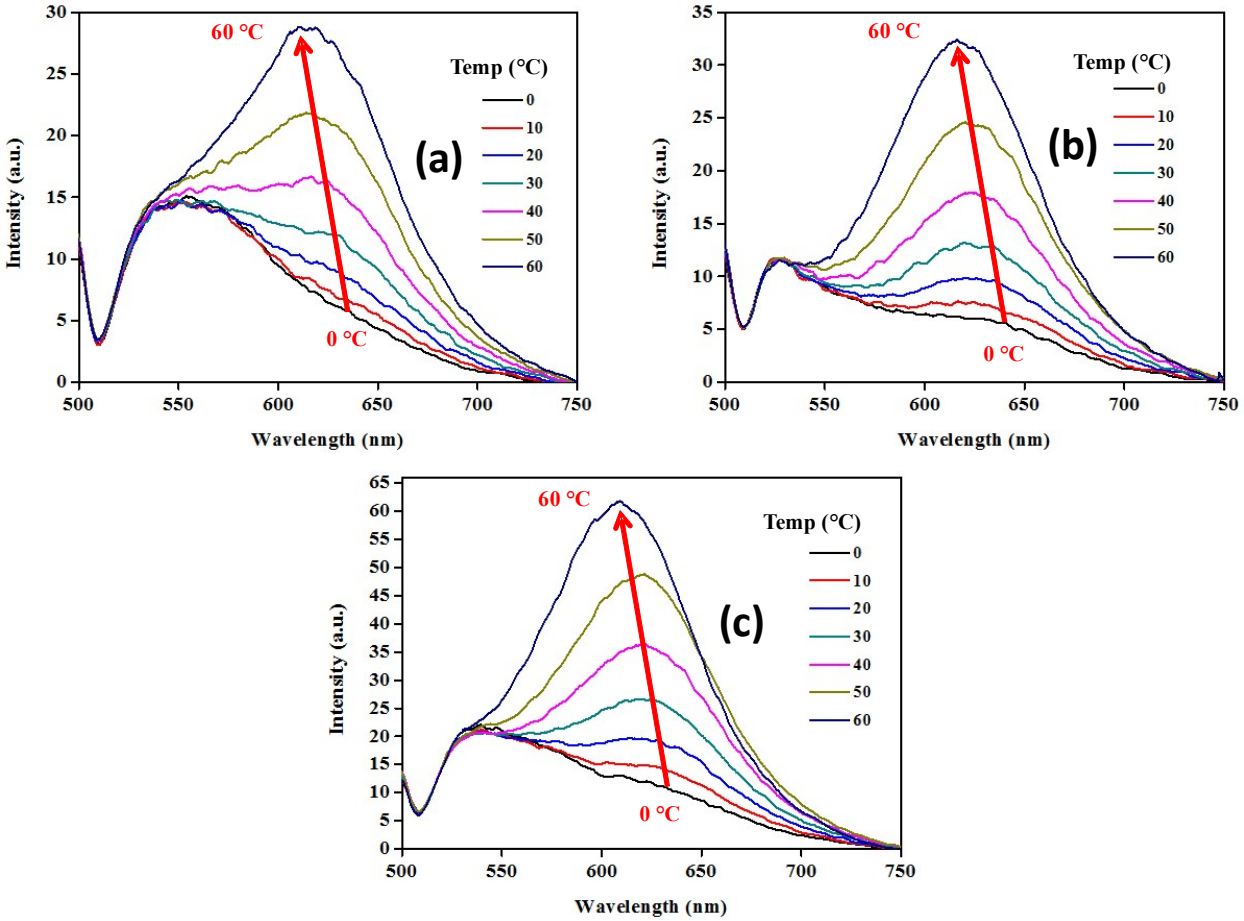

Fig. S31 Emission spectra of **NPB1** (a), **NPB2** (b)**,** and **NPB3** (c) in THF with varying temperature, (c, 50 μM in THF, λ_{ex}, 498 nm).

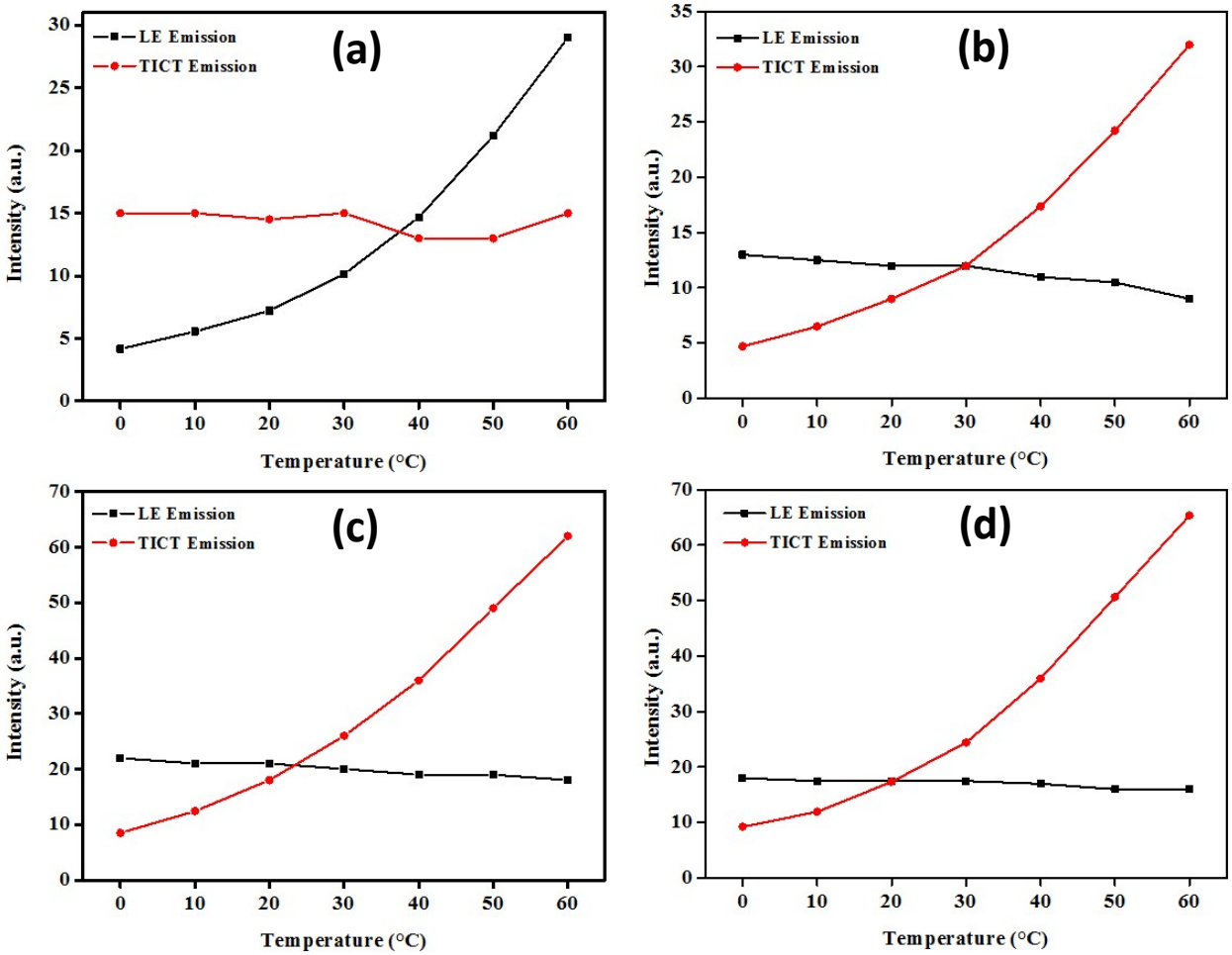

Fig. S32 Plot of emission intensity *vs* temperature (°C) for **NPB1** (a), **NPB2** (b)**, NPB3** (c), and **NPB4** (d) (c, 50 μM, THF; λ_{ex}, 498 nm).

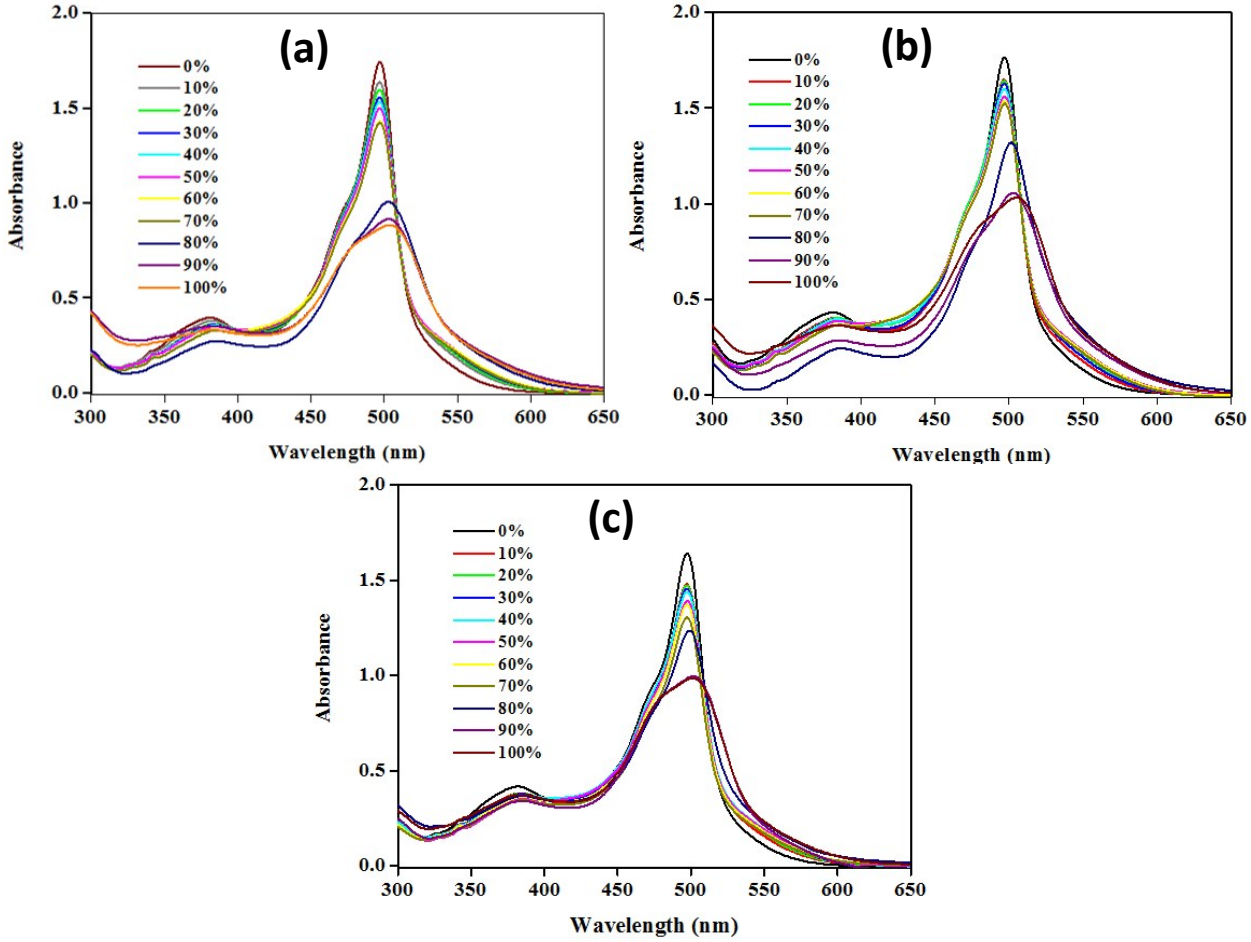

Fig. S33 Absorption spectra for **NPB1** (a), **NPB2** (b) and **NPB3** (c) in THF/water mixtures with varying water volume fractions (c, 50 μM in THF, λ_{ex}, 498 nm).

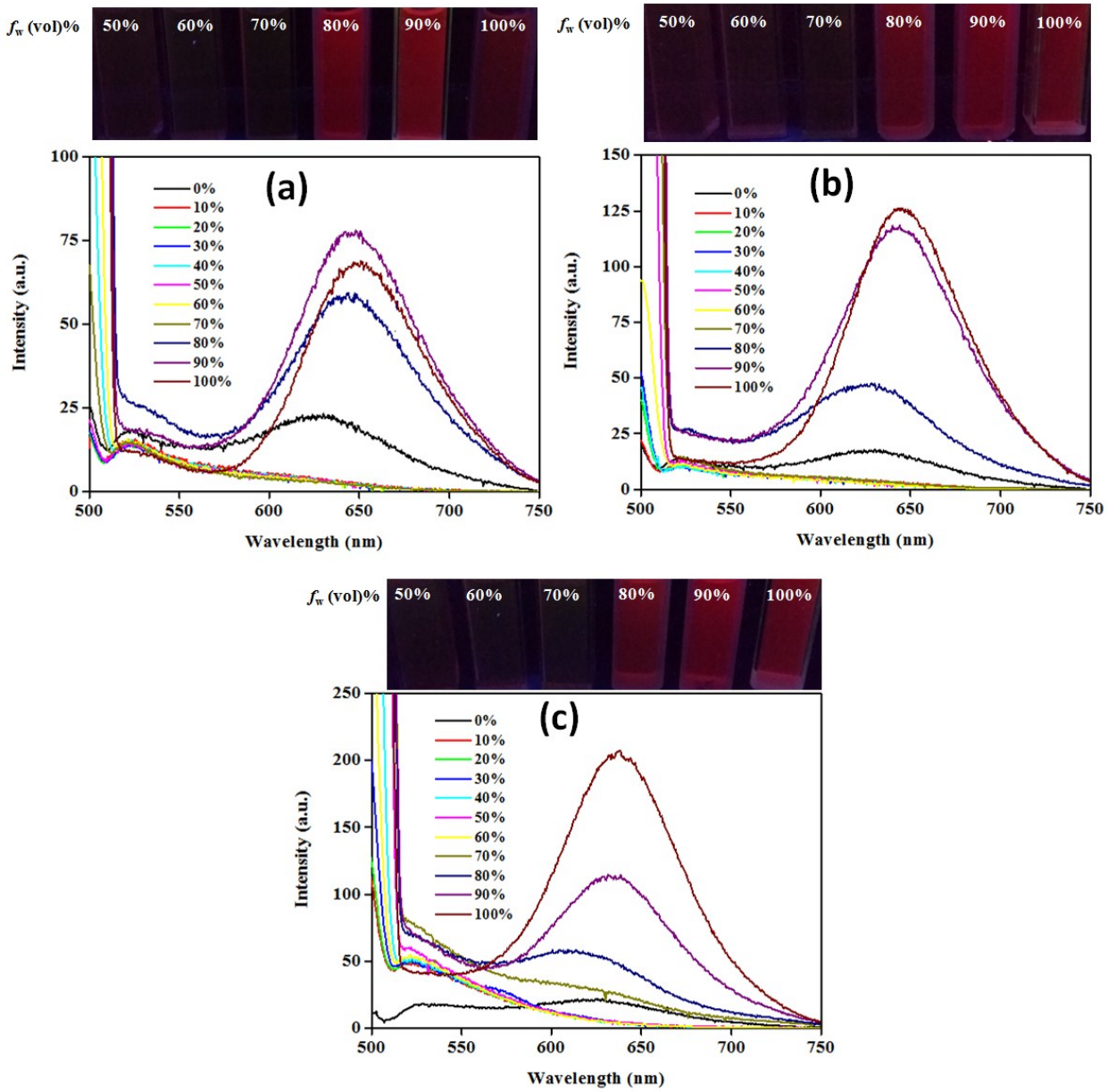

Fig. S34 Emission spectra **NPB1** (a), **NPB2** (b) and **NPB3** (c) in THF/water mixtures with varying water volume fractions (c, 50 μM in THF, λ_{ex}, 498 nm).

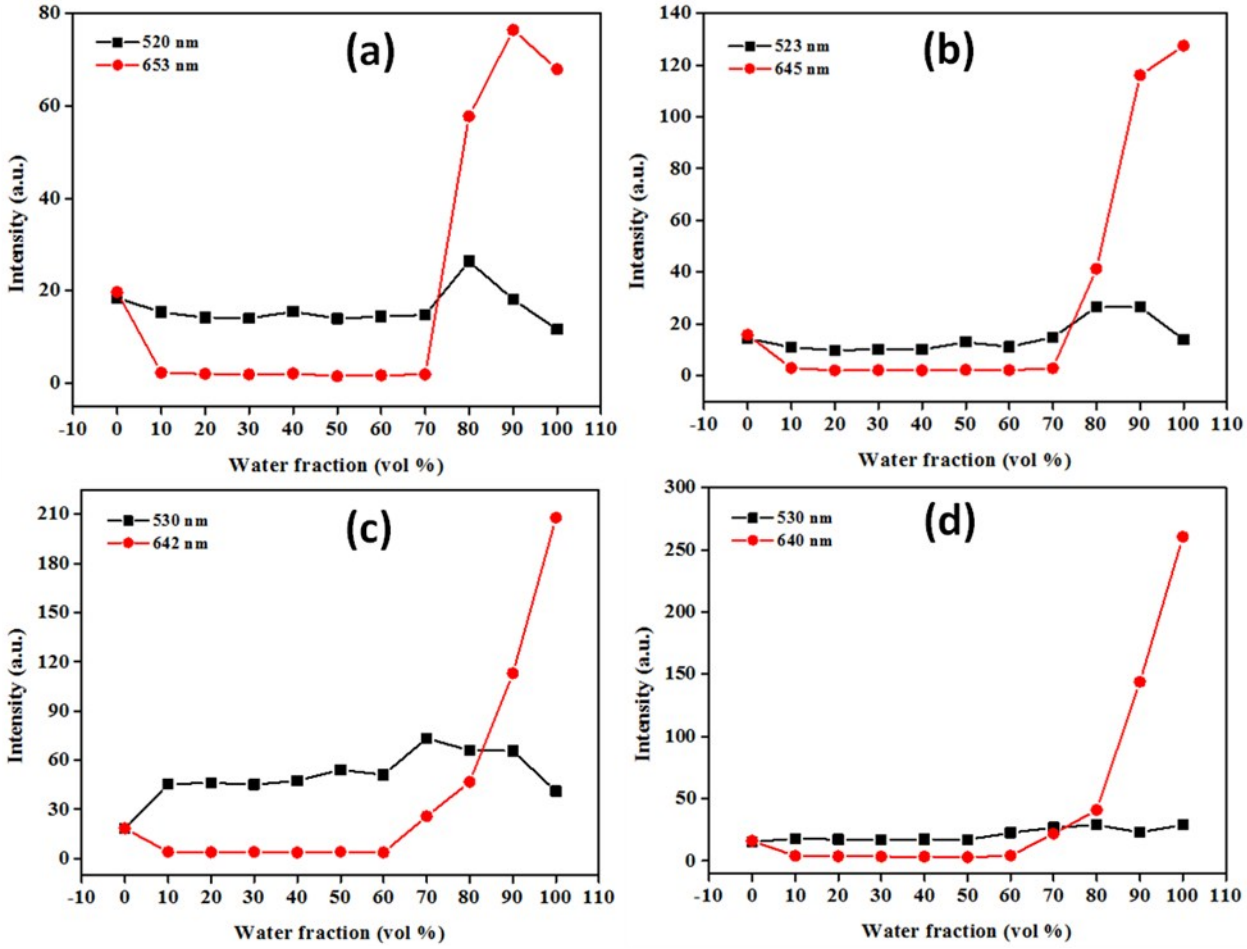

Fig. S35 Emission intensity changes for **NPB1** (a), **NPB2** (b), **NPB3** (c) and **NPB4** (d) with varying water volume fractions, (c, 50 μM in THF, λ_{ex}, 498 nm).

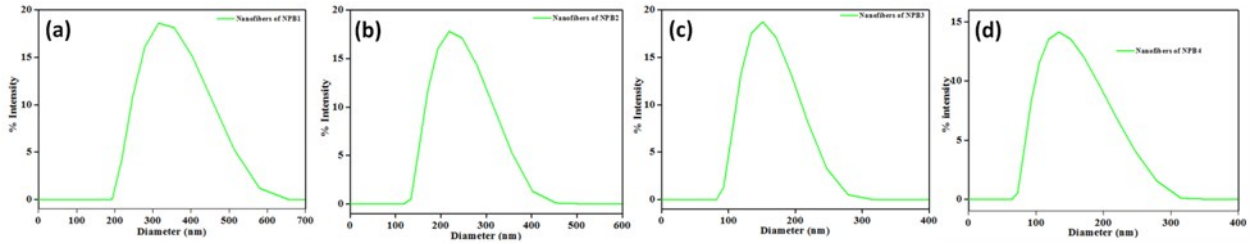

Fig. S36 DLS figures of **NPB1 (**a), **NPB2** (b) and **NPB3** (c) and **NPB4** (d) at 99% f_w. (c, 50 μM in THF, λ_{ex}, 498 nm).

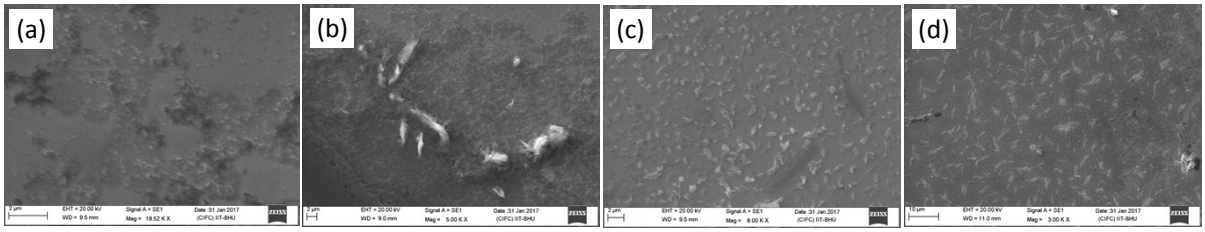

Fig. S37 SEM images of the aggregates of **NPB1** (a), **NPB2** (b), **NPB3** (c) and **NPB4** (d) formed in a mixture of THF/water (f_w 99%; c, 50 μM in THF).

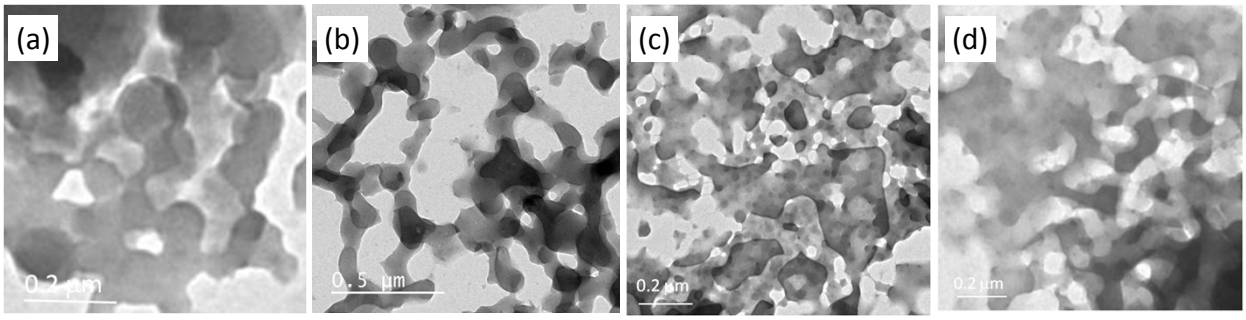

Fig. S38 TEM images of the aggregates for **NPB1** (a), **NPB2** (b), **NPB3** (c) and **NPB4** (d) formed in a mixture of THF/water (f_w 99%; c, 50 μM in THF).

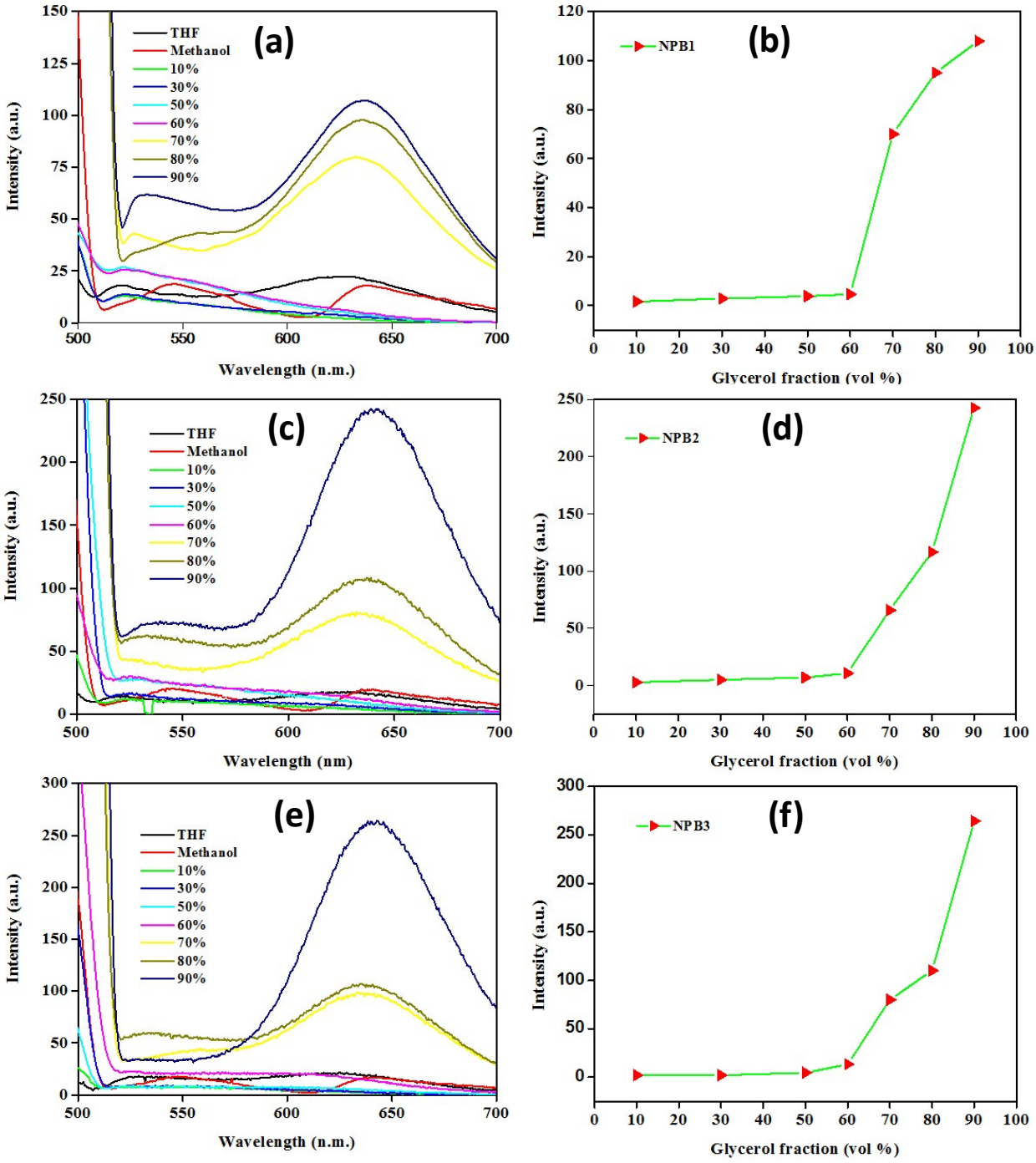

Fig. S39 Emission spectra (a), (c), and (e) and plot of maximum emission intensity *vs* glycerol fraction (b), (d) and (f) for **NPB1**, **NPB2** and **NPB3**, respectively in methanol/glycerol mixture, (c, 50 μM in THF, λ_{ex}, 498 nm).

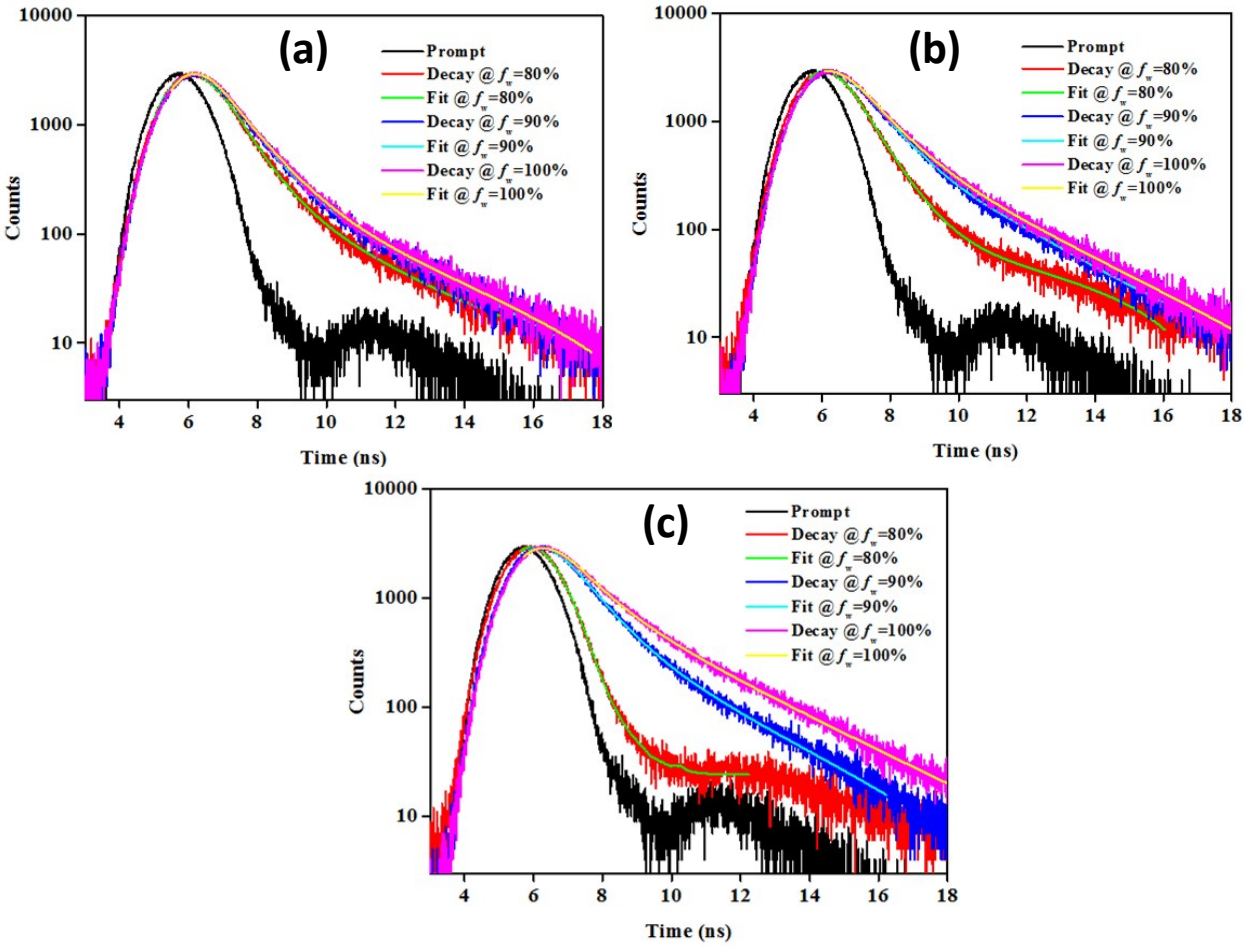

Fig. S40 Time-resolved emission decay profiles for **NPB1** (a) at 651nm, **NPB2** (b) at 645 nm, **NPB3** at 642 nm with varying $f_{w,}$ (c, 50 μM in THF, λ_{ex}, 498 nm).

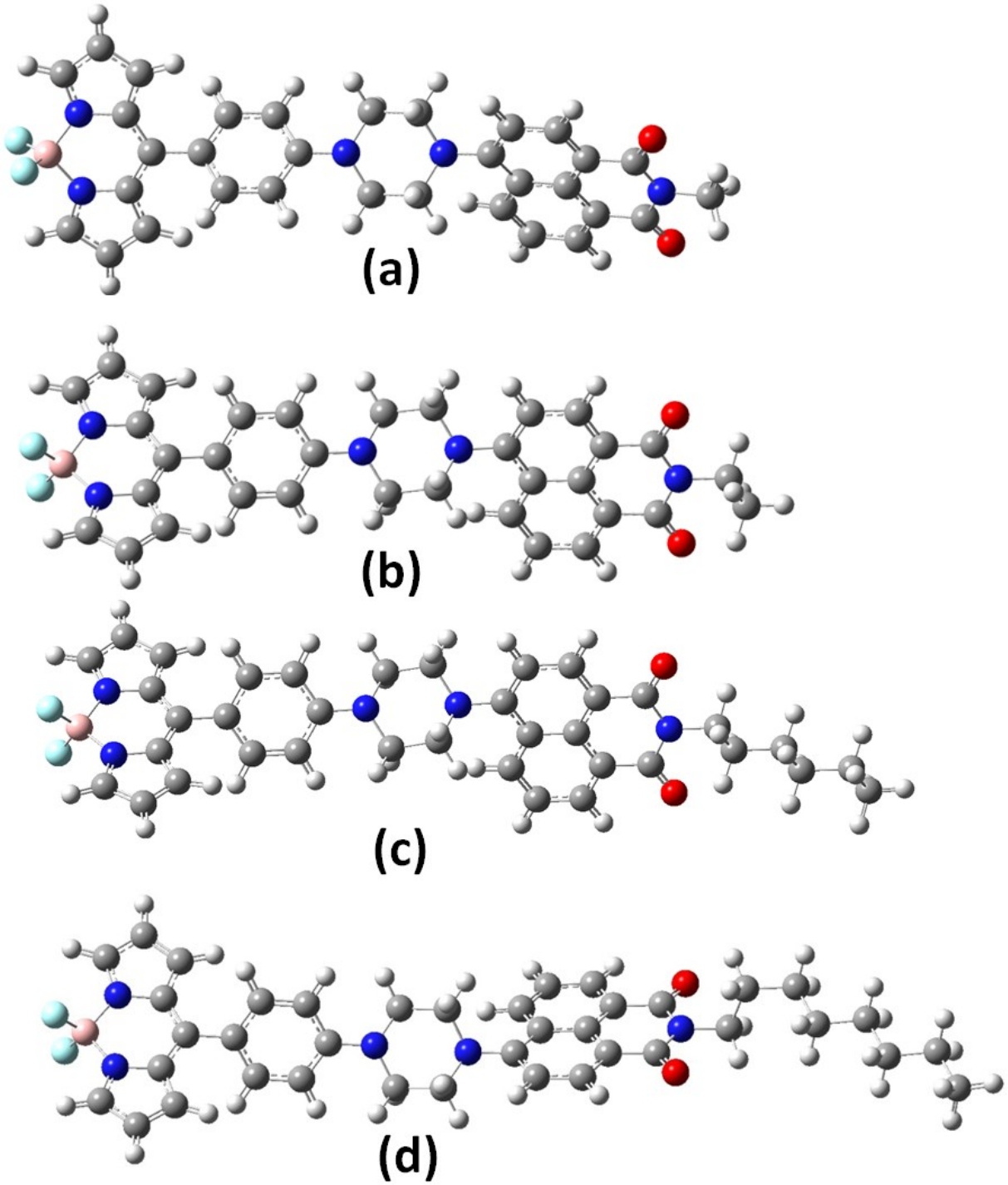

Fig. S41 DFT optimized structures of **NPB1** (a), **NPB2** (b), **NPB3** (c) and **NPB4 (d).**

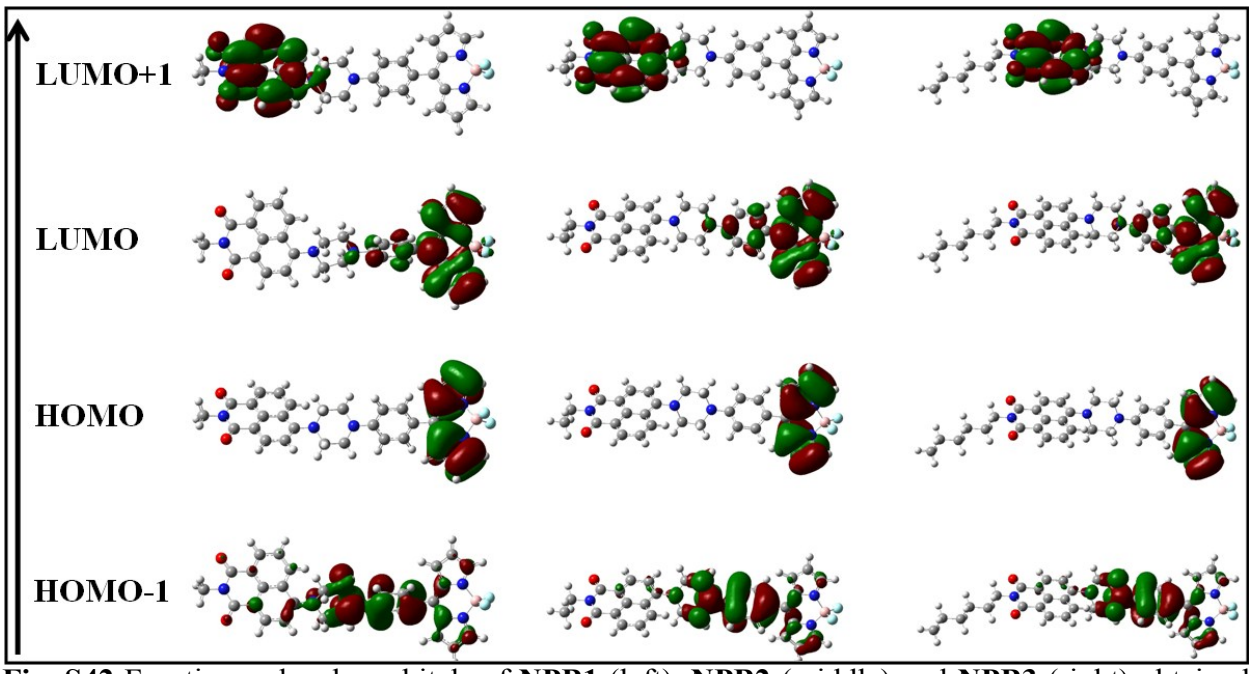

Fig. S42 Frontier molecular orbitals of **NPB1** (left), **NPB2** (middle) and **NPB3** (right) obtained from DFT calculations.

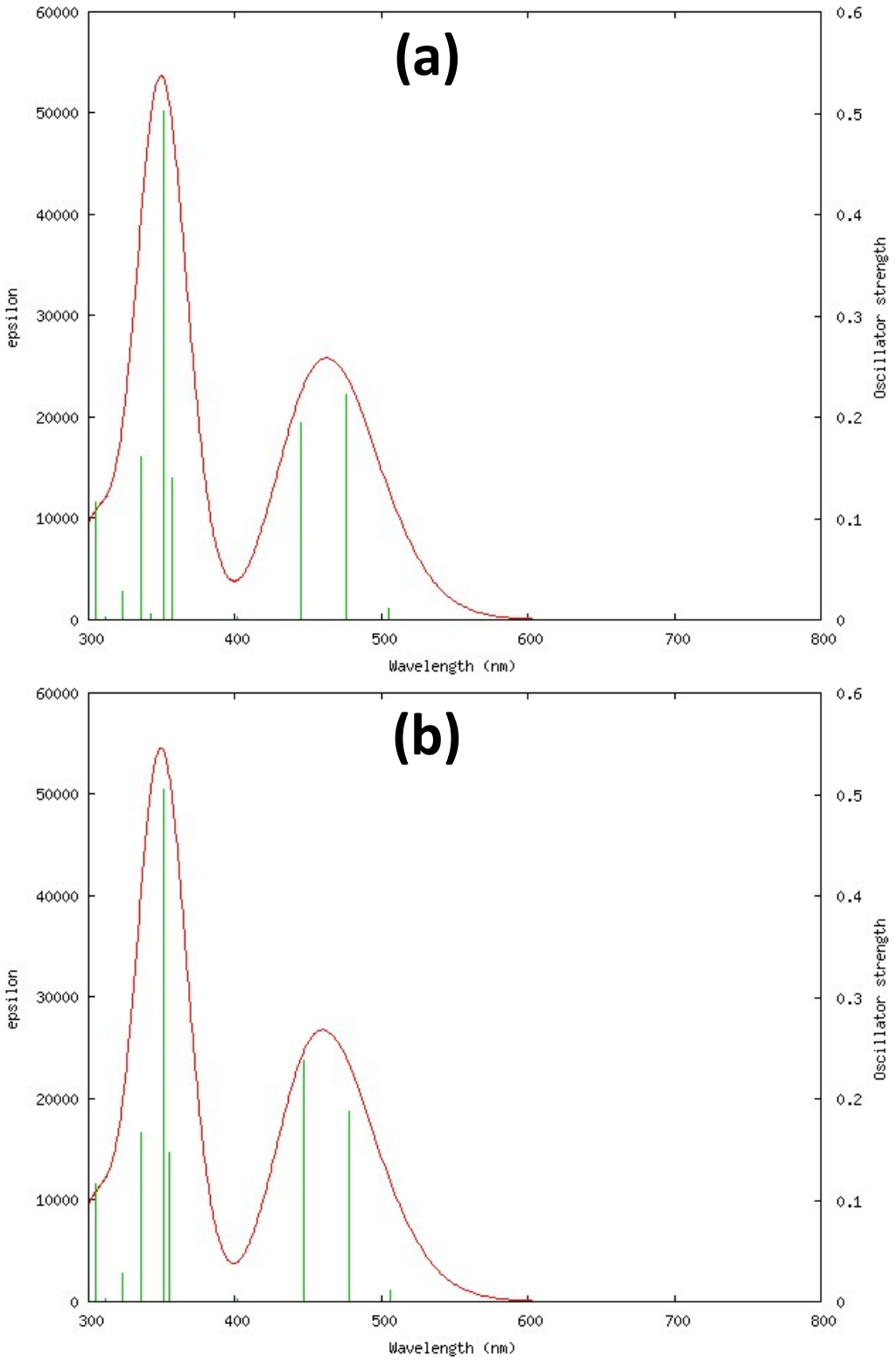

Fig. S43 UV/Vis spectra of **NPB1** (a), **NPB2** (b) from TD-DFT calculations.

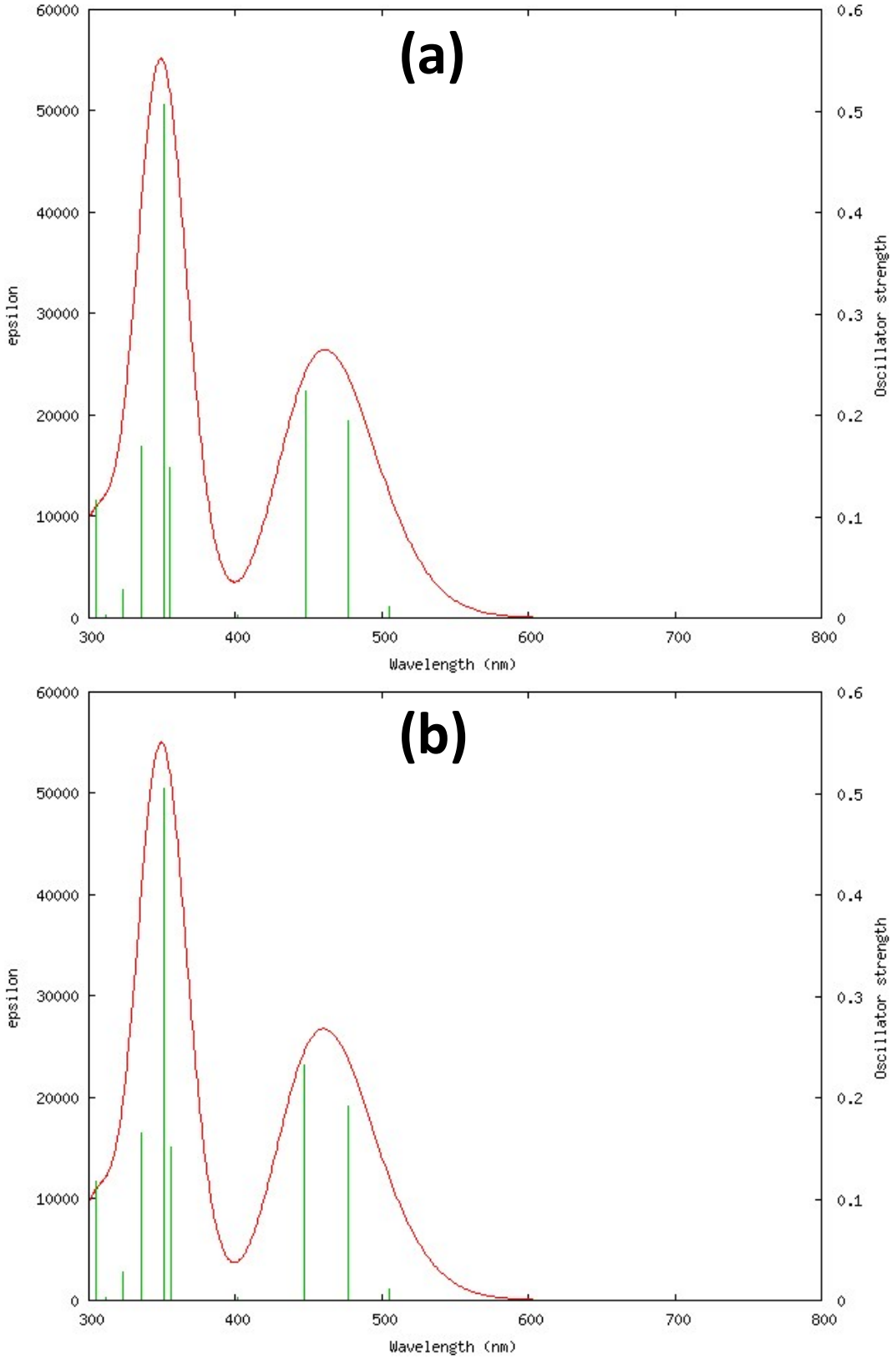

Fig. S44 UV/Vis spectra of **NPB3** (a), **NPB4** (b) from TD-DFT calculations

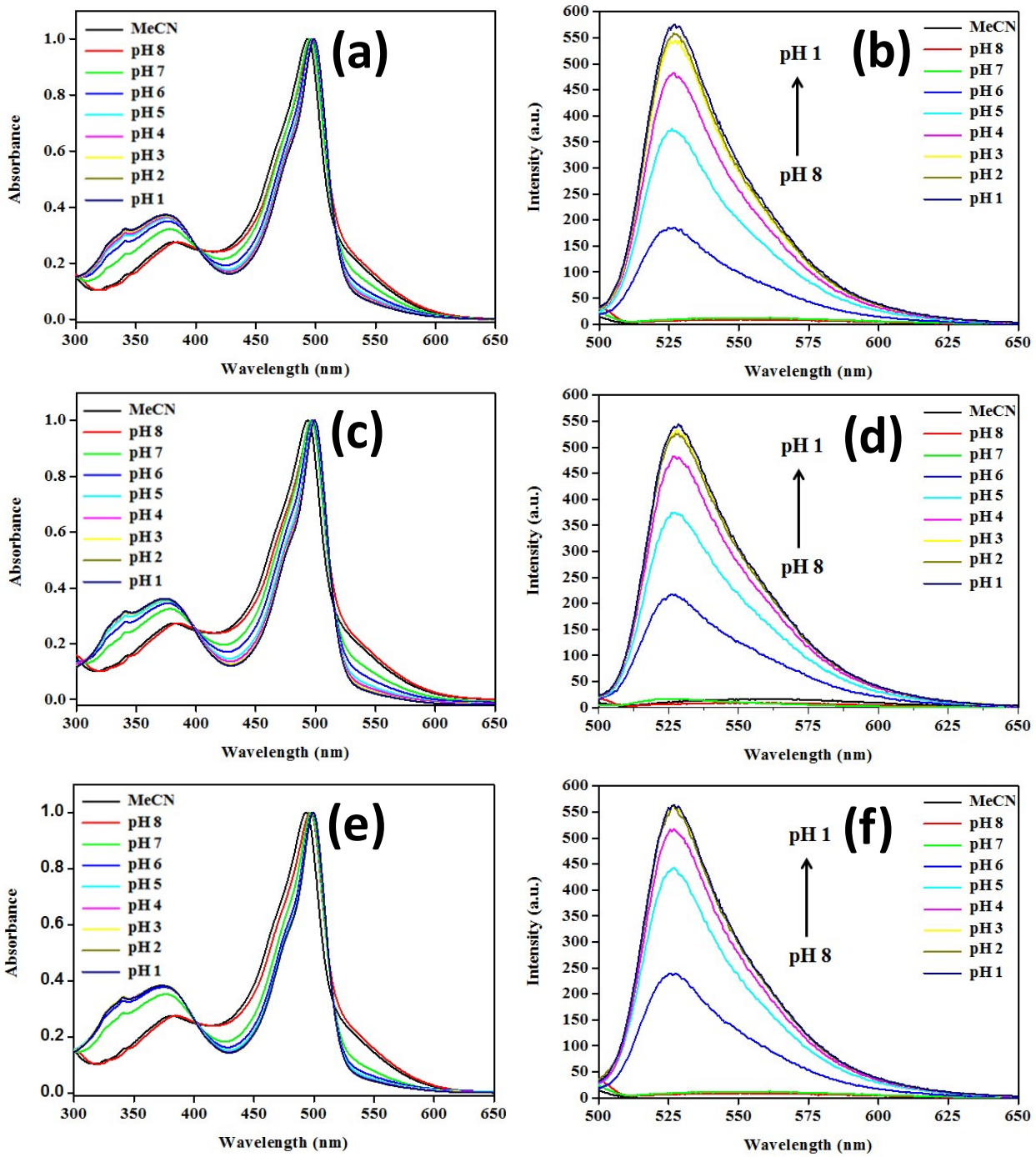

Fig. S45 Normalised representation of absorption spectra (a, c, e) and emission spectra (b, d f) for probes **NPB1**, **NPB2** and **NPB3** respectively in buffer solution at different pH.

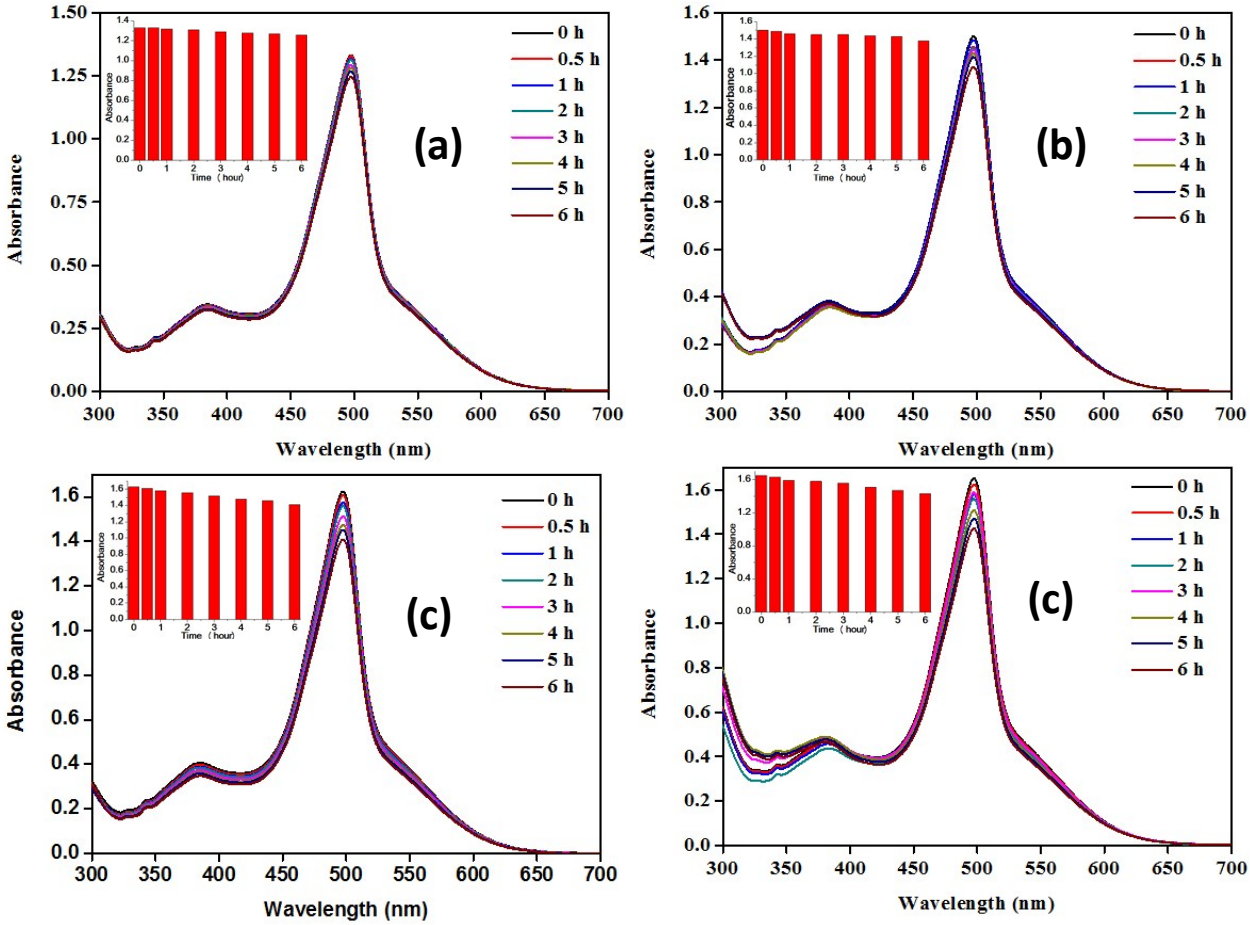

Fig. S46 Time-dependent absorption spectra for **NPB1** (a), **NPB2** (b), **NPB3** (c), and **NPB4** (d) in DMSO under the irradiation of visible light (400–700 nm).

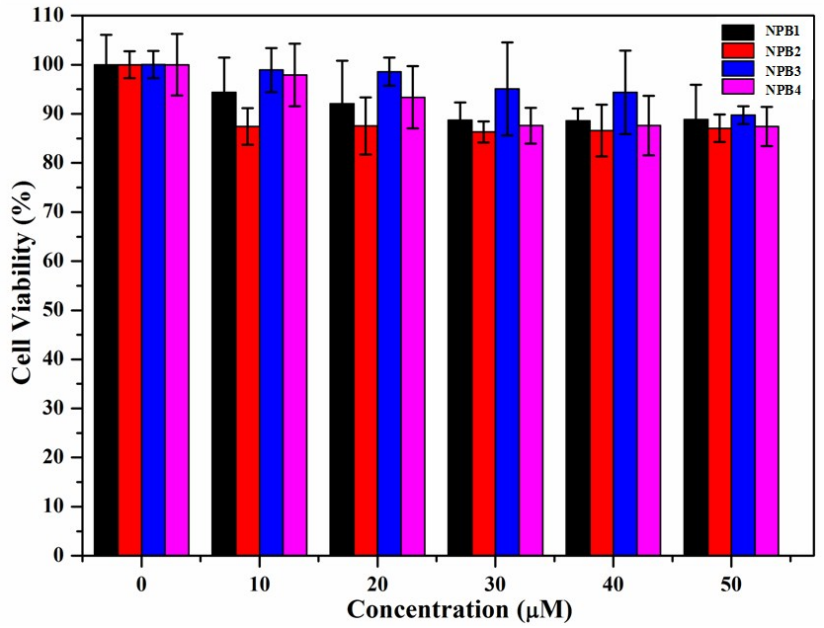

Fig. S47 Cytotoxicity profile for **NPB1**–**NPB4** against HeLa cell line for 16 h.

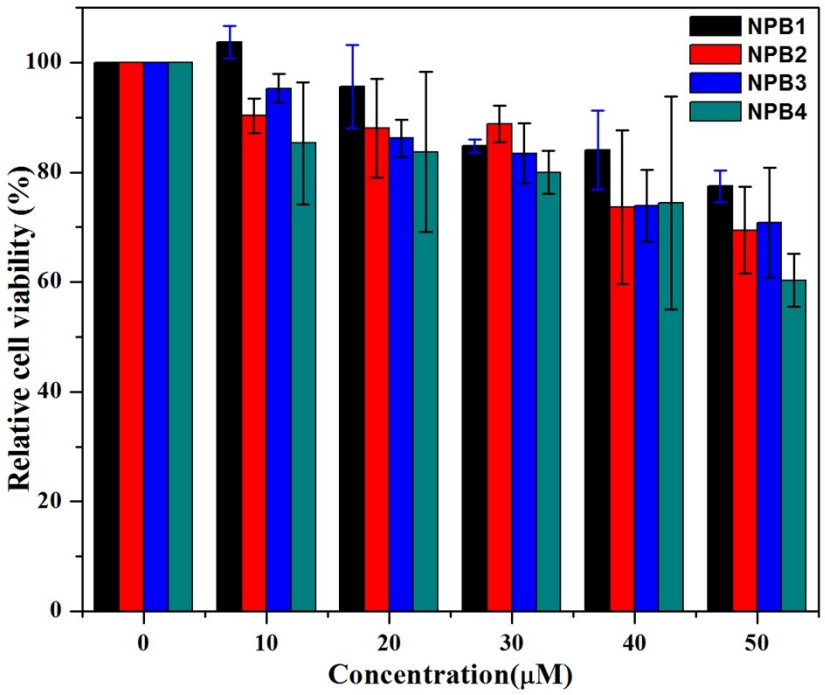

Fig. S48 Cytotoxicity profile for **NPB1**–**NPB4** against HeLa cell line for 48 h.

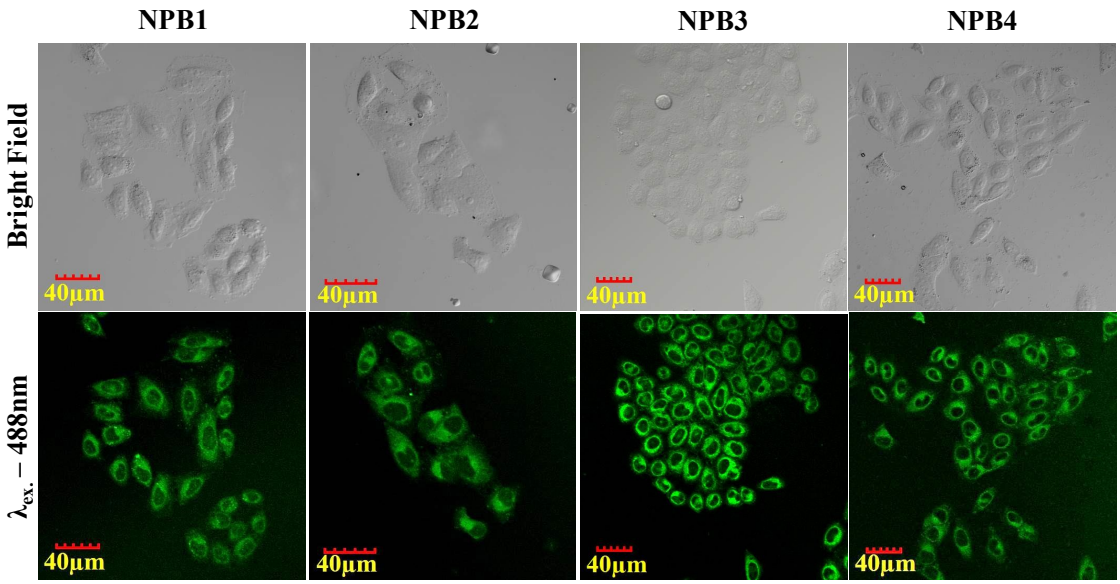

Fig. S49 Bio-imaging of HeLa cells following treatment with **NPB1**–**NPB4**.

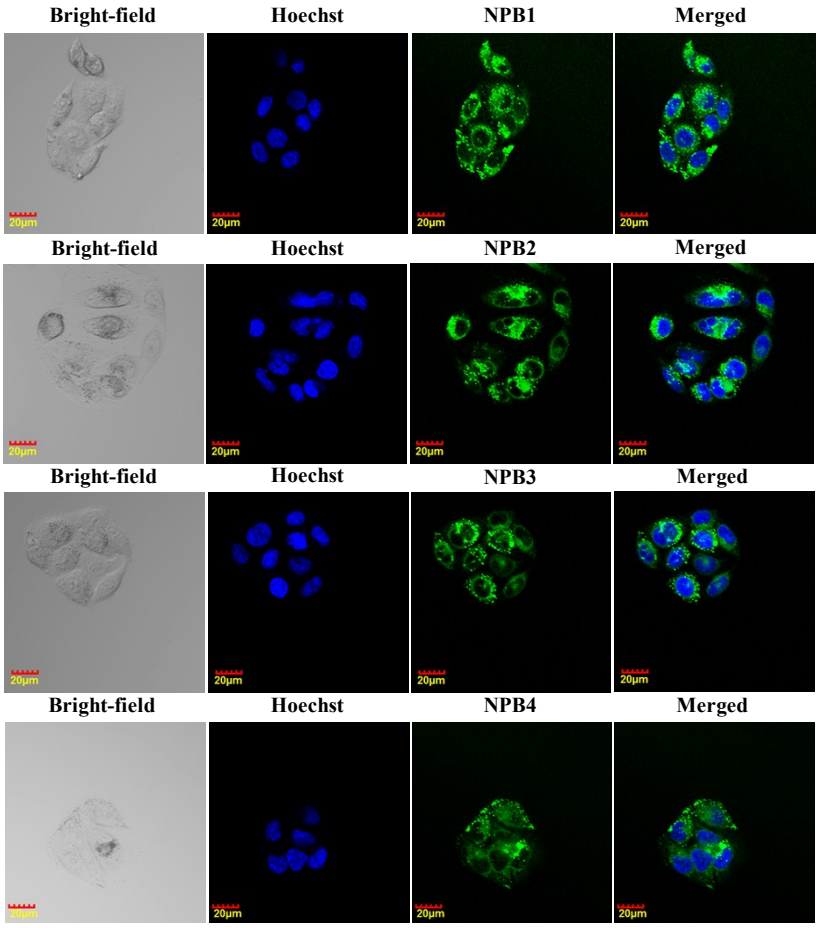

Fig. S50 Confocal images of HeLa cells following treatment with **NPB1**–**NPB4** and co-stained with Hoechst 33342.

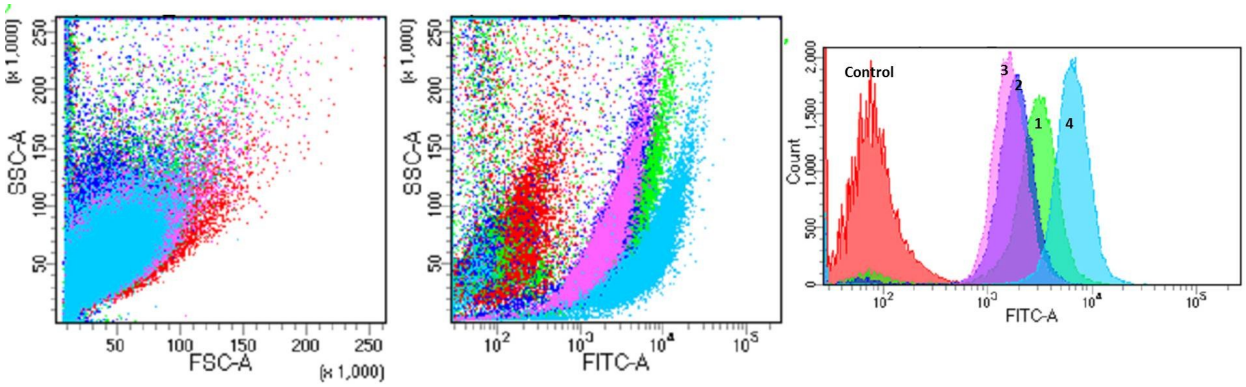

Fig. S51 Flow cytometry analysis of cell staining using **NPB1** (1), **NPB2** (2), **NPB3** (3) and **NPB4** (4).

Table S1. Photophysical data for **NPB1–NPB4** in different solvents with varying polarities

solvents	**NPB1**			**NPB2**		
	λ_{ab}/nm	λ_{em} /nm	Stokes shift/nm	λ_{ab}/nm	λ_{em}/nm	Stokes shift/nm
Hexane	498	516	18	497	522	25
Benzene	501	583	82	501	583	82
Toluene	501	589	88	501	588	89
Chloroform	498	605	107	500	603	103
1,4-dioxane	499	613	114	498	614	116
THF	497	630	133	497	629	132
DCM	498	627	129	498	630	132
MeCN	493	n.d.	-	493	n.d.	-
MeOH	494	641	147	494	641	147
DMF	496	n.d.	-	496	n.d.	-
DMSO	498	n.d.	-	497	n.d.	-
solvents	**NPB3**			**NPB4**		
	λ_{ab}/nm	λ_{em}/nm	Stokes shift/nm	λ_{ab}/nm	λ_{em}/nm	Stokes shift/nm
Hexane	497	516	19	498	521	23
Benzene	501	580	79	501	581	82
Toluene	501	585	84	502	586	84
Chloroform	500	600	100	500	603	103
1,4-dioxane	498	611	113	498	611	613
THF	497	626	129	497	626	129
DCM	495	626	131	495	630	135
MeCN	493	n.d.	-	493	n.d.	-
MeOH	494	640	146	494	640	146
DMF	497	n.d.	-	497	n.d.	-
DMSO	498	n.d.	-	498	n.d.	-

(c, 50 μM in THF, λ_{ex} = 498 nm), Abbreviations: λ_{ab} = absorption maximum, λ_{em} = emission maximum).

Table S2. Quantum yields for **NPB1**–**NPB4** in different solvents

Solvents	Φ_F for NPB1	Φ_F for NPB2	Φ_F for NPB3	Φ_F for NPB4
Hexane	0.517	0.509	0.503	0.478
Benzene	0.774	0.727	0.783	0.774
Toluene	0.579	0.521	0.571	0.577
1,4-dioxane	0.026	0.027	0.024	0.022
Chloroform	0.174	0.184	0.163	0.158
THF	0.010	0.008	0.008	0.009
DCM	0.162	0.157	0.148	0.173
MeCN	0.009	0.007	0.006	0.008
MeOH	0.010	0.011	0.010	0.012
DMF	0.013	0.012	0.013	0.018
DMSO	0.009	0.009	0.010	0.011
Water (aggregated state)	0.070	0.097	0.131	0.155
Solid state[a]	**0.0925**	**0.1021**	**0.1276**	**0.1339**

Φ_F = fluorescence quantum yield, Φ_F in solution calculated by using Rhodamine 6G dye as standard (Φ = 0.95 in water) and [a] absolute fluorescence quantum yield in solid state measured with a calibrated integrating sphere

Table S3. Fluorescence data for **NPB1–NPB4** in THF/hexane mixture at varying hexane fractions

Hexane (vol %)	Emission Wavelength (nm)			
	NPB1	**NPB2**	**NPB3**	**NPB4**
0%	520, 630	522, 629	526, 626	527, 627
10%	525, 628	522, 629	519, 626	522, 626
20%	525, 622	521, 625	519, 626	522, 624
30%	525, 622	521, 625	519, 625	522, 623
40%	525, 622	521, 625	519, 625	522, 623
50%	525, 617	521, 619	519, 620	522, 623
60%	524, 616	521, 615	519, 615	523, 618
70%	524, 613	521, 608	519, 610	522, 614
80%	524, 598	596	518, 603	521, 600
90%	575	567	520, 566	567
100%	517	520	517	522

(c, 50 μM in THF, λ_{ex}, 498 nm).

Table S4. Emission maxima (λ_{em}) of lower energy band (TICT emission) for **NPB1**–**NPB4** with varying temperature

Temperature (°C)	**NPB1 (λ_{em}/nm)**	**NPB2 (λ_{em}/nm)**	**NPB3 (λ_{em}/nm)**	**NPB4 (λ_{em}/nm)**
0	(520) n.d.	(522) n.d.	(526) n.d.	(527) n.d.
10	(520) 644	(522) 640	(526) 635	(527) 635
20	(520) 634	(522) 628	(526) 629	(527) 627
30	(520) 627	(522) 626	(526) 621	(527) 623
40	(520) 616	(522) 623	(526) 619	(527) 620
50	(520) 615	(522) 620	(526) 616	(527) 617
60	(520) 610	(522) 613	(526) 607	(527) 612

(Values in parentheses denotes LE emission values, abbreviations: λ_{em} = emission maximum, and n.d. = not detectable)

Table S5. Photophysical data for compounds **NPB1–NPB4** in THF/water mixture at varying water fractions

Water (vol %)	**NPB1**			**NPB2**		
	λ_{ab}/nm	λ_{em}/nm	Stokes shift	λ_{ab}/nm	λ_{em}/nm	Stokes shift
0	497	520, 630	-	498	522, 629	-
10 to 60	497	523, n.d.	-	497	523, n.d.	-
70	497	523, n.d.	-	497	523, n.d.	-
80	503	n.d., 645	142 nm	502	n.d., 629	127 nm
90	504	n.d., 648	144 nm	503	n.d., 643	140 nm
100	504	n.d., 651	146 nm	506	n.d., 645	139 nm
Water (vol %)	**NPB3**			**NPB4**		
	λ_{ab}/nm	λ_{em}/nm	Stokes shift	λ_{ab}/nm	λ_{em}/nm	Stokes shift
0	498	526, 626	-	498	527, 627	-
10 to 60	497	523, n.d.	-	497	521, n.d.	-
70	497	523, n.d.	-	502	n.d., 621	-
80	499	n.d., 623	124 nm	502	n.d., 625	123 nm
90	502	n.d., 634	132 nm	503	n.d., 634	131 nm
100	503	n.d., 642	139 nm	516	n.d., 640	124 nm

(c, 50 μM in THF, λ_{ex}, 498 nm), Abbreviations: λ_{ab} = absorption maximum, λ_{em} = emission maximum, and n.d. = not detectable (signal too weak to be accurately determined).

Table S6. Emission spectra of **NPB1**–**NPB4** with varying glycerol volume fractions

Glycerol (vol %)	**NPB1** (λ_{em}/nm)	**NPB2** (λ_{em}/nm)	**NPB3** (λ_{em}/nm)	**NPB4** (λ_{em}/nm)
THF	520, 630	522, 629	526, 626	527, 627
Methanol	545, 641	544, 639	546, 640	547, 640
10 to 60%	n.d.	n.d.	n.d.	n.d.
70%	638	637	639	640
80%	638	638	639	640
90%	640	639	641	641

Table S7. Time resolved fluorescence data for compounds **NPB1**–**NPB4**

Water (Vol %)	**NPB1**						**NPB2**					
	λ_{em} (nm)	**λ_{em} (nm)**	**τ_1/ τ_2 (ns)**		**A_1/A_2**		**λ_{ex} (nm)**	**λ_{em} (nm)**	**τ_1 /τ_2 (ns)**		**A_1/A_2**	
0 to 70	460	645	τ_1	n.d	A_1	n.d.	460	645	τ_1	n.d	A_1	n.d
			τ_2	n.d.	A_2	n.d.			τ_2	n.d.	A_2	n.d.
80	460	645	τ_1	0.70	A_1	0.94	460	645	τ_1	0.77	A_1	0.81
			τ_2	2.49	A_2	0.06			τ_2	2.82	A_2	0.19
90	460	645	τ_1	0.86	A_1	0.93	460	645	τ_1	0.85	A_1	0.87
			τ_2	3.06	A_2	0.07			τ_2	2.56	A_2	0.13
100	460	645	τ_1	0.96	A_1	0.94	460	645	τ_1	0.95	A_1	0.86
			τ_2	3.68	A_2	0.06			τ_2	2.85	A_2	0.14
Water (Vol %)	**NPB3**						**NPB4**					
	λ_{ex} (nm)	**λ_{em} (nm)**	**τ_1/ τ_2 (ns)**		**A_1/A_2**		**λ_{ex} (nm)**	**λ_{em} (nm)**	**τ_1/τ_2 (ns)**		**A_1/A_2**	
0 to 70	460	640	τ_1	n.d	A_1	n.d	460	640	τ_1	n.d	A_1	n.d
			τ_2	n.d.	A_2	n.d.			τ_2	n.d.	A_2	n.d.
80	460	640	τ_1	0.48	A_1	0.14	460	640	τ_1	0.50	A_1	0.15
			τ_2	0.15	A_2	0.86			τ_2	0.15	A_2	0.85
90	460	640	τ_1	0.86	A_1	0.89	460	640	τ_1	0.80	A_1	0.91
			τ_2	2.69	A_2	0.11			τ_2	2.64	A_2	0.09
100	460	640	τ_1	0.90	A_1	0.75	460	640	τ_1	0.84	A_1	0.75
			τ_2	2.73	A_2	0.25			τ_2	2.69	A_2	0.25

(c, 50 μM in THF, λ_{ex}, 498 nm), Abbreviations: λ_{ab} = absorption maximum, λ_{em} = emission maximum, and n.d. = not detectable (signal too weak to be accurately determined). Dynamic parameters determined from $I = A1 \exp(-t/\tau1) + A2 \exp(-t/\tau2)$, where $A1/A2$ and $\tau1/\tau2$ are the fractions (A) and lifetimes (τ)

Table S8. Selected crystallographic parameters for **NPB1**, **NPB3** and **NPB4**

Crystal Data	**NPB1**	**NPB3**	**NPB4**
Empirical formula	$C_{32}H_{26}BF_2N_5O_2$	$C_{37}H_{36}BF_2N_5O_2$	$C_{39}H_{40}BF_2N_5O_2$
Crystal system	triclinic	monoclinic	triclinic
Space group	'P -1'	'P 21/n'	'P -1'
a (Å)	11.8174(2)	16.786(3)	10.4139(4)
b (Å)	14.496(2)	9.3658(2)	12.2447(4)
c (Å)	16.208(2)	20.888(4)	14.2584(6)
α (°)	92.150(3)	90	94.395(3)
β (°)	105.524(3)	97.685(6)	103.037(3)
γ (°)	103.757(3)	90	103.628(3)
V (Å^3)	2583.2(6)	3254.4(1)	1705.18(1)
Z	2	4	2
F(000)	1168	1328	696
ρ_{calc} (Mg m^{-3})	1.443	1.289	1.285
T (K)	296(2)	300(2)	293(2)
μ (mm^{-1})	0.102	0.089	0.709
refln collected	5690	7029	6604
GOF on F^2	1.019	1.047	1.082
Final R1 on	0.0568	0.1254	0.0576
Final wR2 on	0.1280	0.3680	0.1723

Table S9. Selected bond distances in **NPB1– NPB4**

Bond length (Å)	**NPB1**		**NPB2**	**NPB3**		**NPB4**	
	Crystal	DFT	DFT	Crystal	DFT	Crystal	DFT
N1–B1	1.539(3)	1.568	1.568	1.53(2)	1.568	1.537(2)	1.568
N2–B1	1.533(3)	1.566	1.566	1.54(2)	1.566	1.532(3)	1.566
C5–C10	1.464(3)	1.476	1.476	1.51(3)	1.476	1.466(2)	1.476
N3–C13	1.396(3)	1.403	1.403	1.407(3)	1.403	1.397(2)	1.403
N4–C20	1.415(3)	1.415	1.414	1.40(2)	1.414	1.409(2)	1.414
N5–C30	1.391(3)	1.400	1.401	1.39(2)	1.402	1.398(3)	1.402
N5–C31	1.402(3)	1.406	1.405	1.42(2)	1.405	1.392(2)	1.405
N5–C32	1.447(3)	1.467	1.476	1.50(2)	1.475	1.472(2)	1.475
O1–C31	1.213(3)	1.224	1.225	1.21(2)	1.225	1.216(2)	1.225
O2–C30	1.217(3)	1.224	1.225	1.24(2)	1.225	1.218(2)	1.225

Table S10. Selected bond angles in **NPB1– NPB4**

Bond Angle (°)	**NPB1**		**NPB2** DFT	**NPB3**		**NPB4**	
	Crystal	DFT		Crystal	DFT	Crystal	DFT
F1–B1–F2	108.82(2)	111.56	111.52	109.0(2)	111.53	109.82(2)	111.56
N2–B1–N1	106.26(2)	104.85	104.87	106.6(2)	104.89	106.26(2)	104.85
C4–C5–C10	120.59(2)	120.36	120.40	118(2)	120.36	121.03(2)	120.40
C10–C5–C6	119.96(2)	119.98	119.96	120.5(2)	119.98	119.76(2)	119.95
C11–C10–C5	122.0(2)	121.56	121.54	123.5(2)	121.49	122.38(1)	121.61
C15–C10–C5	121.14(2)	121.10	121.14	118.4(2)	121.16	120.82(1)	121.09
C13–N3–C16	116.44(2)	118.74	118.51	117.8(1)	118.45	117.85(1)	118.36
C13–N3–C19	117.02(2)	118.43	118.86	116.5(1)	118.73	115.90(1)	118.64
C20–N4–C17	115.89(2)	117.39	117.55	118.4(2)	117.50	117.38(1)	117.59
C20–N4–C18	116.17(2)	155.88	116.05	117.0(1)	115.88	114.99(1)	116.08
C31–N5–C32	117.3(2)	118.59	117.53	117.7(2)	117.42	118.47(1)	117.53
C32–N5–30	117.7(2)	116.25	117.46	118.3(2)	117.59	117.13(1)	117.49
C30–N5–C31	124.9(2)	126.16	24.98	123.9(2)	124.96	124.40(1)	124.96

Table S11. Selected dihedral angles from Crystal structure

	NPB1 (°)	**NPB3 (°)**	**NPB4 (°)**
Between BODIPY and Benzene ring	40.12 (A), 45.49 (B)	50.66	44.43
Between Benzene and	49.52 (A), 70.52(B)	14.36	82.95
BetweenBODIPY and	9.70 (A), 25.62 (B)	61.80	38.52

Table S12. Selected dihedral angles from DFT calculations

	NPB1 (°)	**NPB2 (°)**	**NPB3 (°)**	**NPB4 (°)**
Between BODIPY and Benzene ring	50.92	50.30	50.96	50.90
Between Benzene and	44.42	22.77	23.60	75.40
BetweenBODIPY and	13.42	71.93	73.43	24.66

Table S13. Summary of the dominant electronic transitions observed in UV/Vis spectra of compounds (**NPB1**–**NPB4**) obtained from TD-DFT calculations

Compounds	**E/ev**	**E/nm**	**Oscillator strength**	**Major contributions**
NPB1	2.6022	476.46 (**497**)	0.2224	HOMO → LUMO (97%)
	2.7865	444.94	0.1947	HOMO-1 → LUMO (96%)
	3.4723	357.07 (**380**)	0.1394	HOMO → LUMO+1 (94%)
	3.5314	351.09	0.5021	HOMO-5 → LUMO (77%)
NPB2	2.5965	477.50 (**498**)	0.1877	HOMO → LUMO (97%)
	2.7723	447.23	0.2382	HOMO-1 → LUMO (93%)
	3.4878	355.48(**381**)	0.1468	HOMO → LUMO+1 (92%)
	3.5291	351.32	0.5047	HOMO-5 → LUMO (77%)
NPB3	2.5989	477.06 (**497**)	0.1941	HOMO → LUMO (97%)
	2.7697	447.65	0.2236	HOMO-1 → LUMO (93%)
	3.4885	355.41(**381**)	0.1484	HOMO → LUMO+1 (93%)
	3.5322	351.01	0.5061	HOMO-5 → LUMO (77%)
NPB4	2.6004	476.78 (**497**)	0.1915	HOMO → LUMO (97%)
	2.7723	447.23	0.2319	HOMO-1 → LUMO (93%)
	3.4862	355.64 (**380**)	0.1514	HOMO → LUMO+1 (93%)
	3.5307	351.16	0.5047	HOMO-5 → LUMO (77%)

(E=energy, values in parentheses denote the experimental value, observed in UV/Vis spectra)

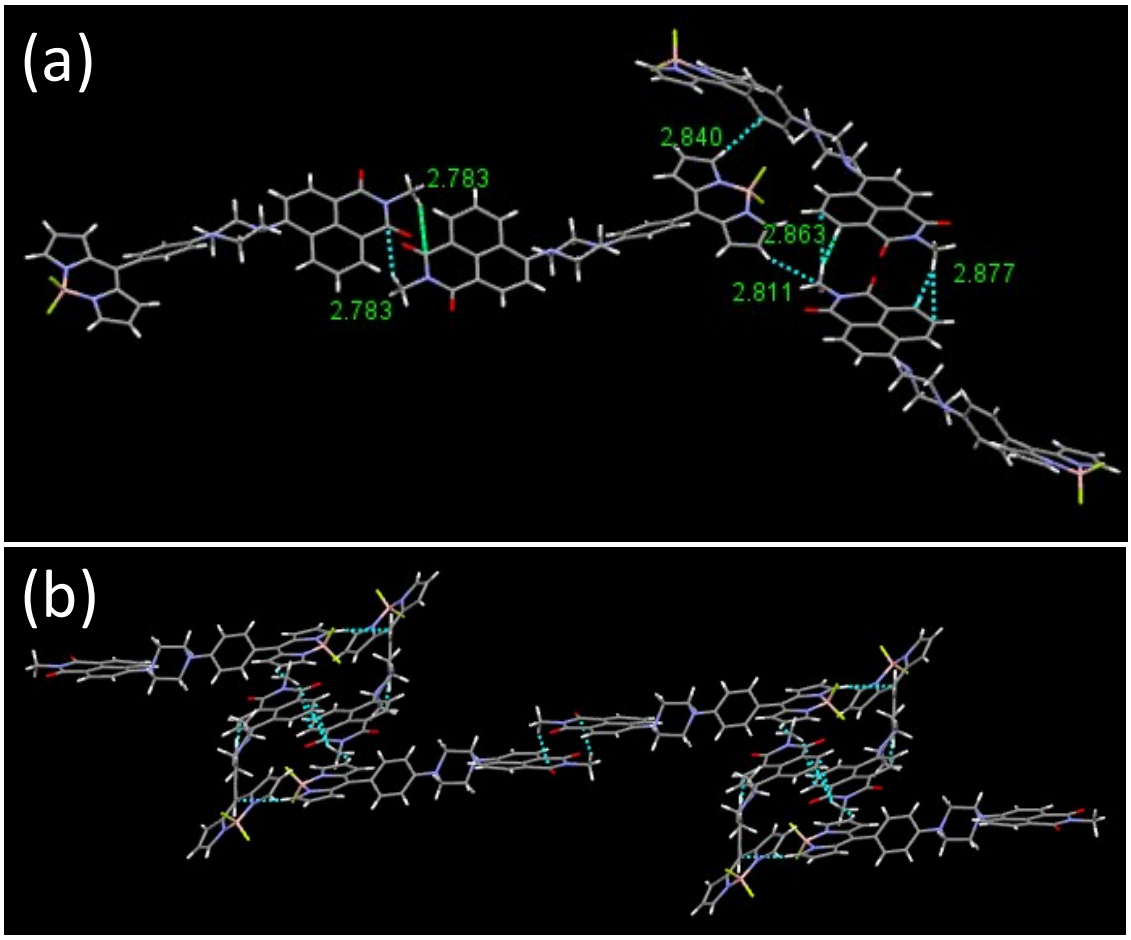

Fig. S52 Perspective view of some different C–H···π interactions (a) and crystal packing through C–H···π interactions (b) in **NPB1**.

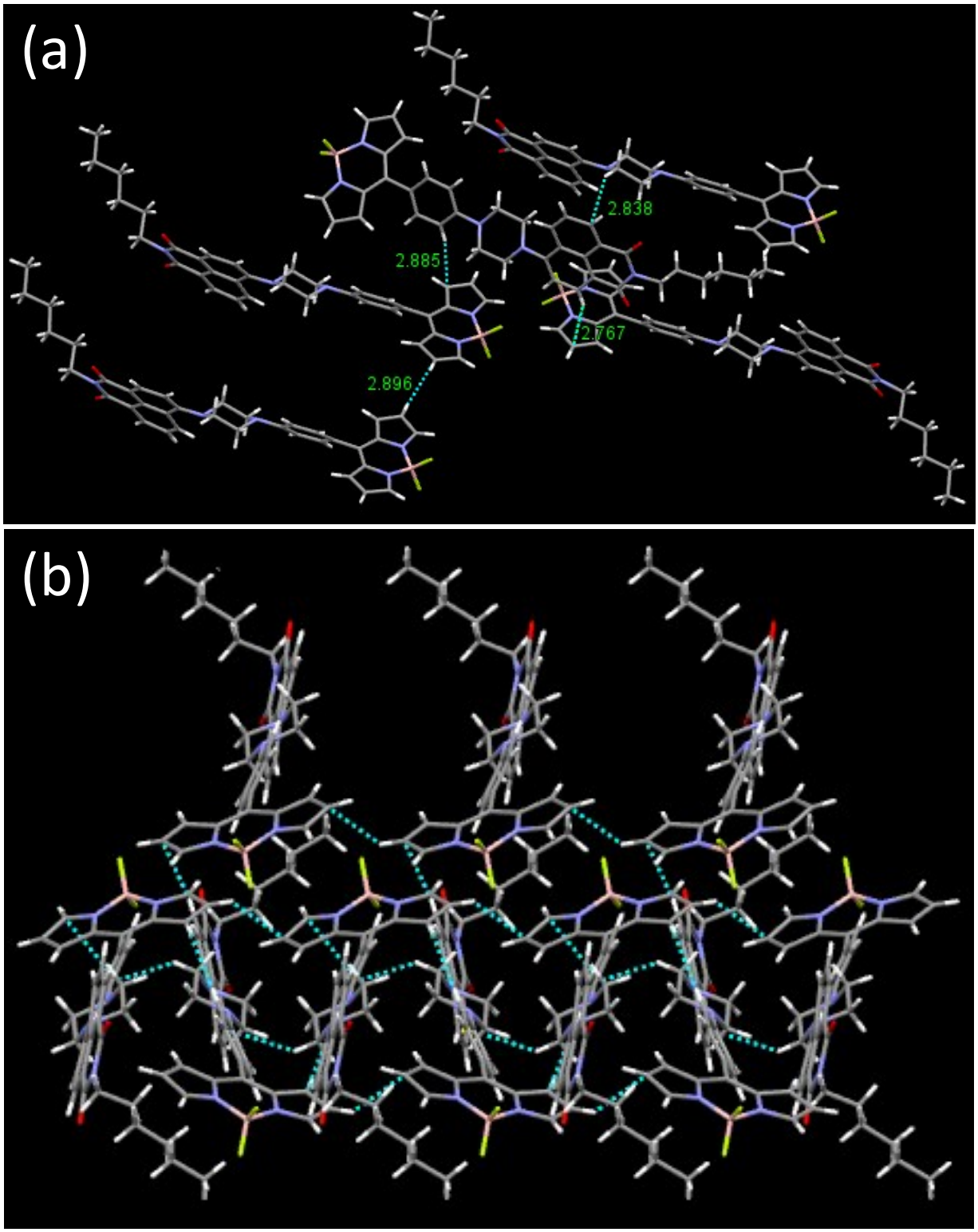

Fig. S53 Perspective view of some different C–H···π interactions (a) and crystal packing through C–H···π interactions (b) in **NPB3**.

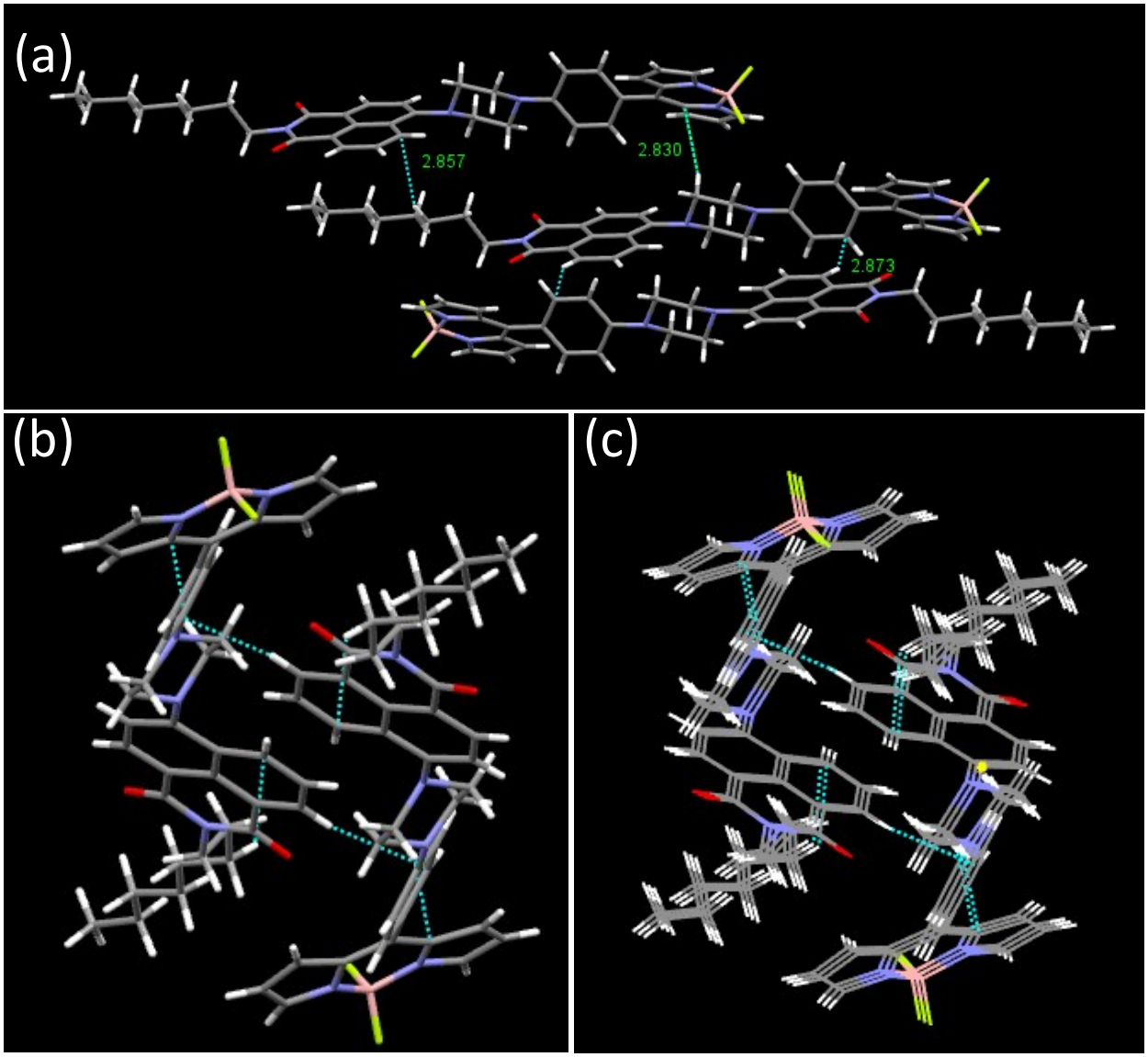

Fig. S54 Perspective view of some different C–H···π interactions (a) and crystal packing through C–H···π interactions (b) and (c) in **NPB4**.

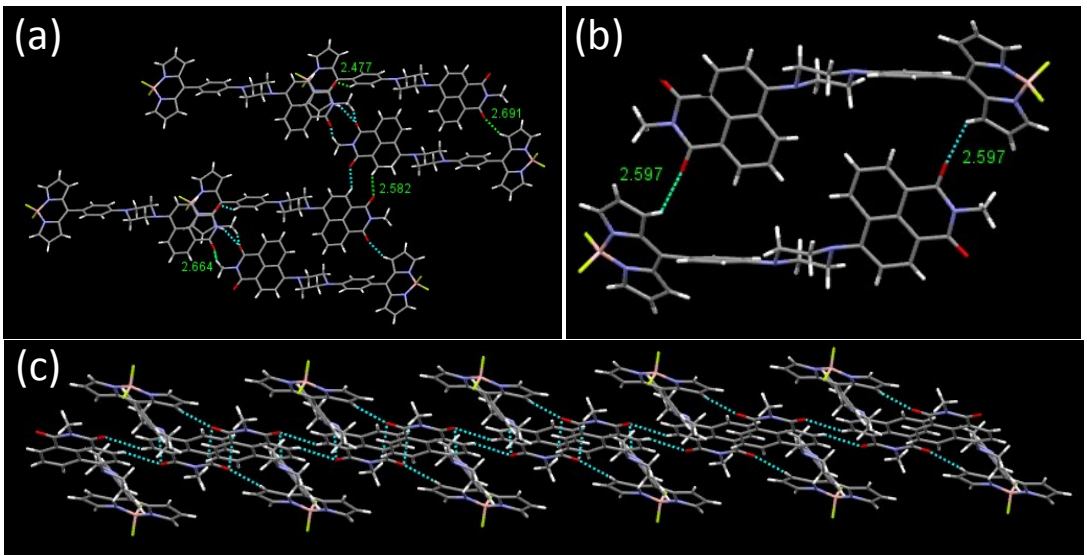

Fig. S55 Perspective view of different C–O···H–C interactions in structure A (a) and structure B (b) and crystal packing through C–O···H–C interactions (c) in **NPB1**.

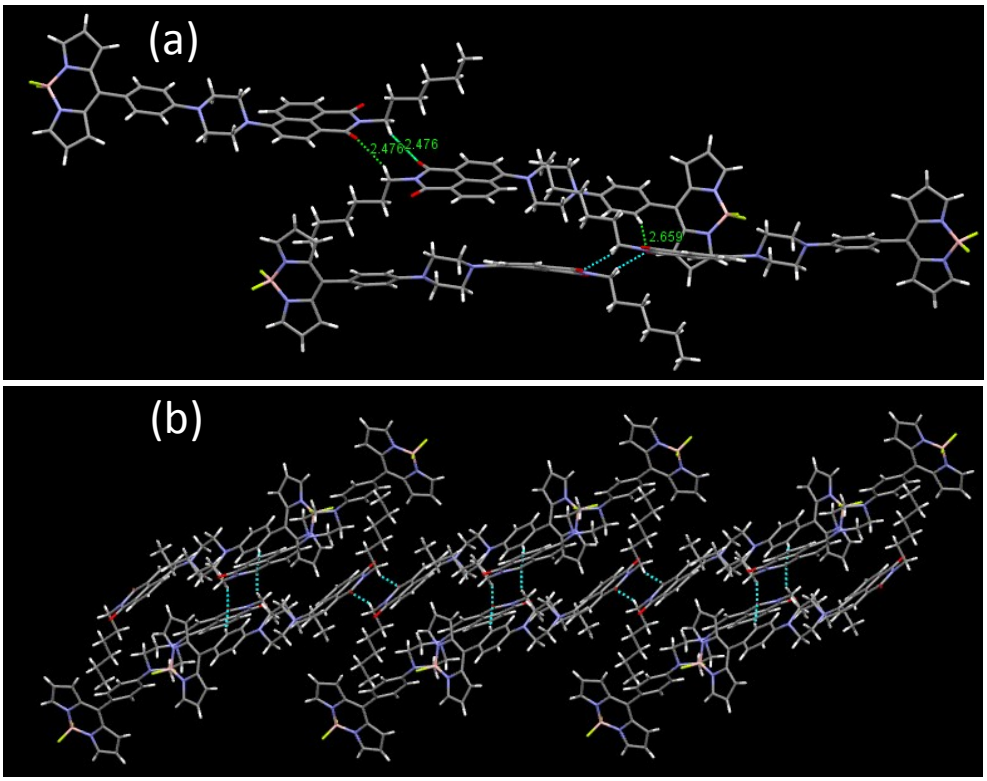

Fig. S56 Perspective view of some different C–O···H–C interaction (a) and crystal packing through C–O···H–C interaction (b) in **NPB3**.

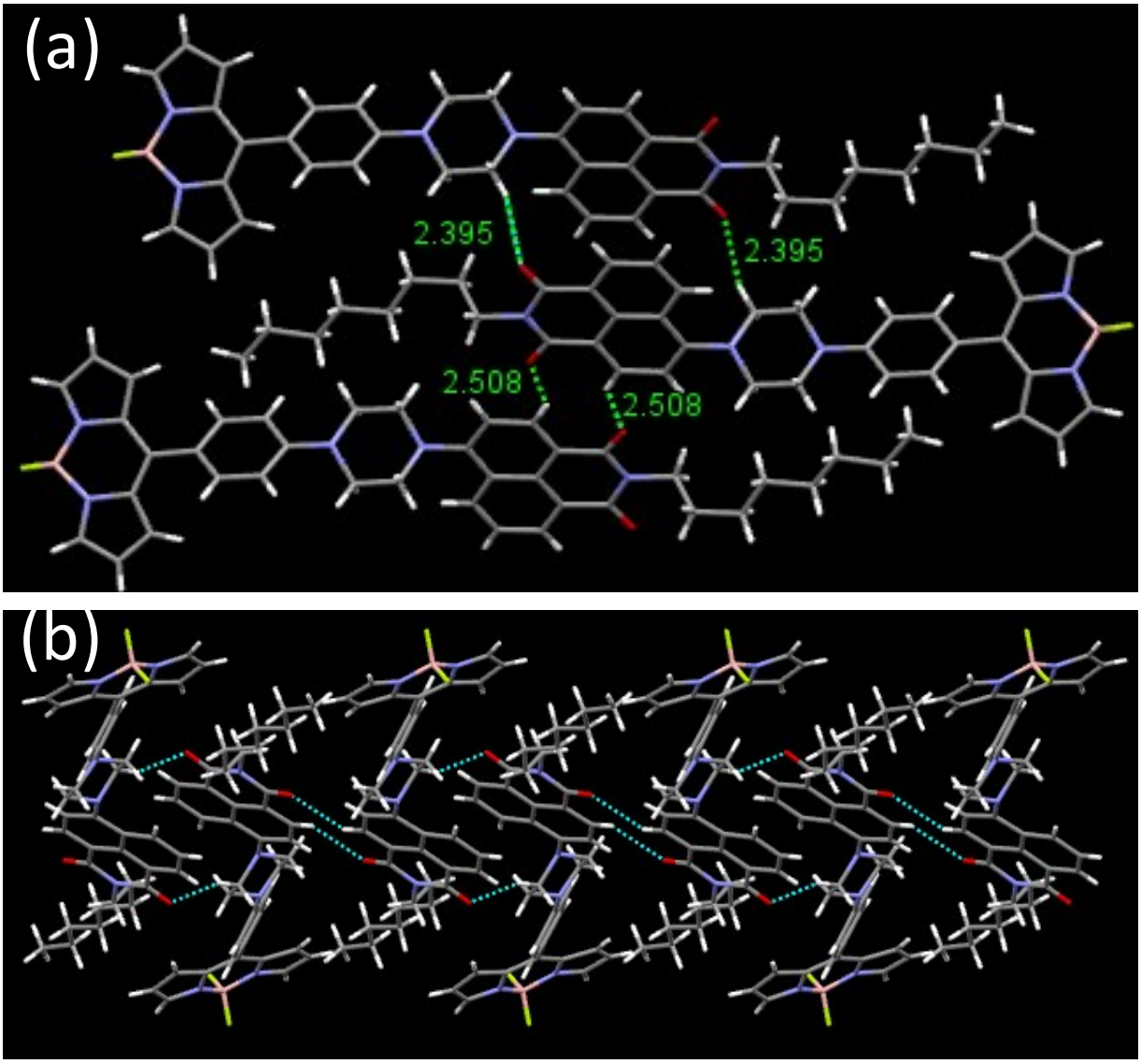

Fig. S57 Perspective view of some different C–O···H–C interaction (a) and crystal packing involving C–O···H–C interaction (b) in **NPB4**.

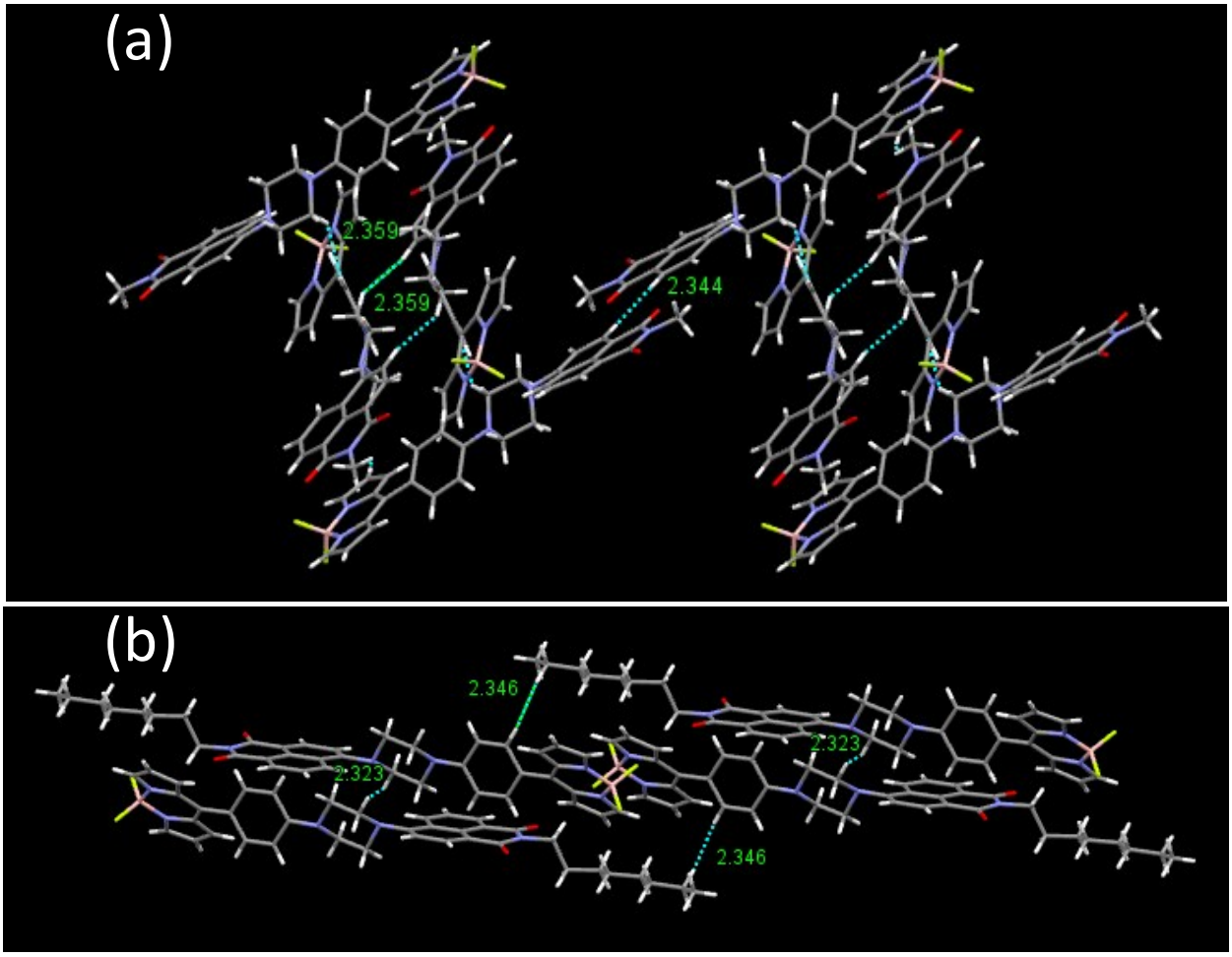

Fig. S58 Perspective view of intermolecular C–H···H–C interactions in **NPB1** (a) and **NPB3** (b). (absent in **NPB4**)

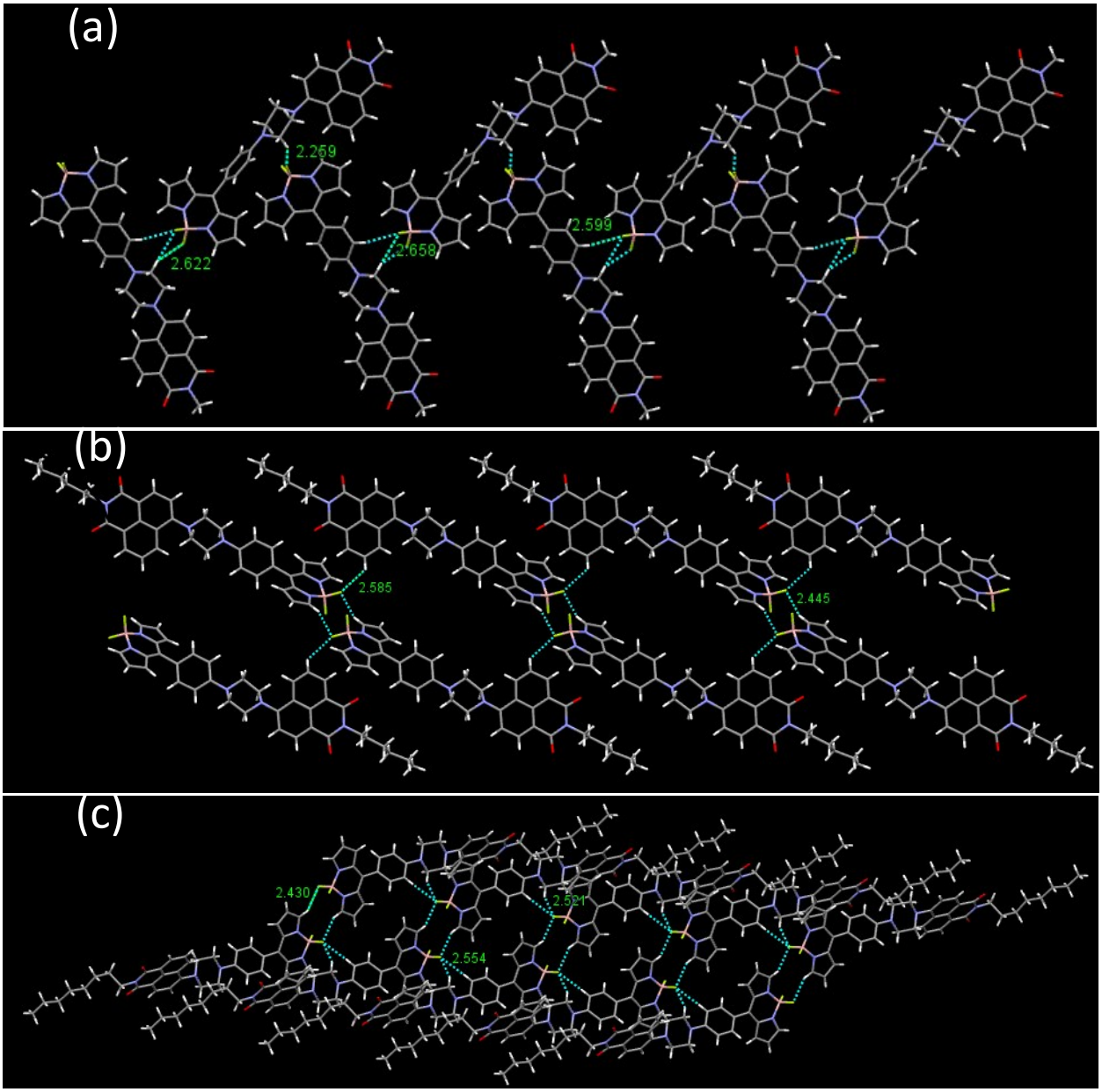

Fig. S59 Comparion of Intermolecular B–F···H–C interactions in **NPB1** (a), **NPB3** (b) and **NPB4** (c).

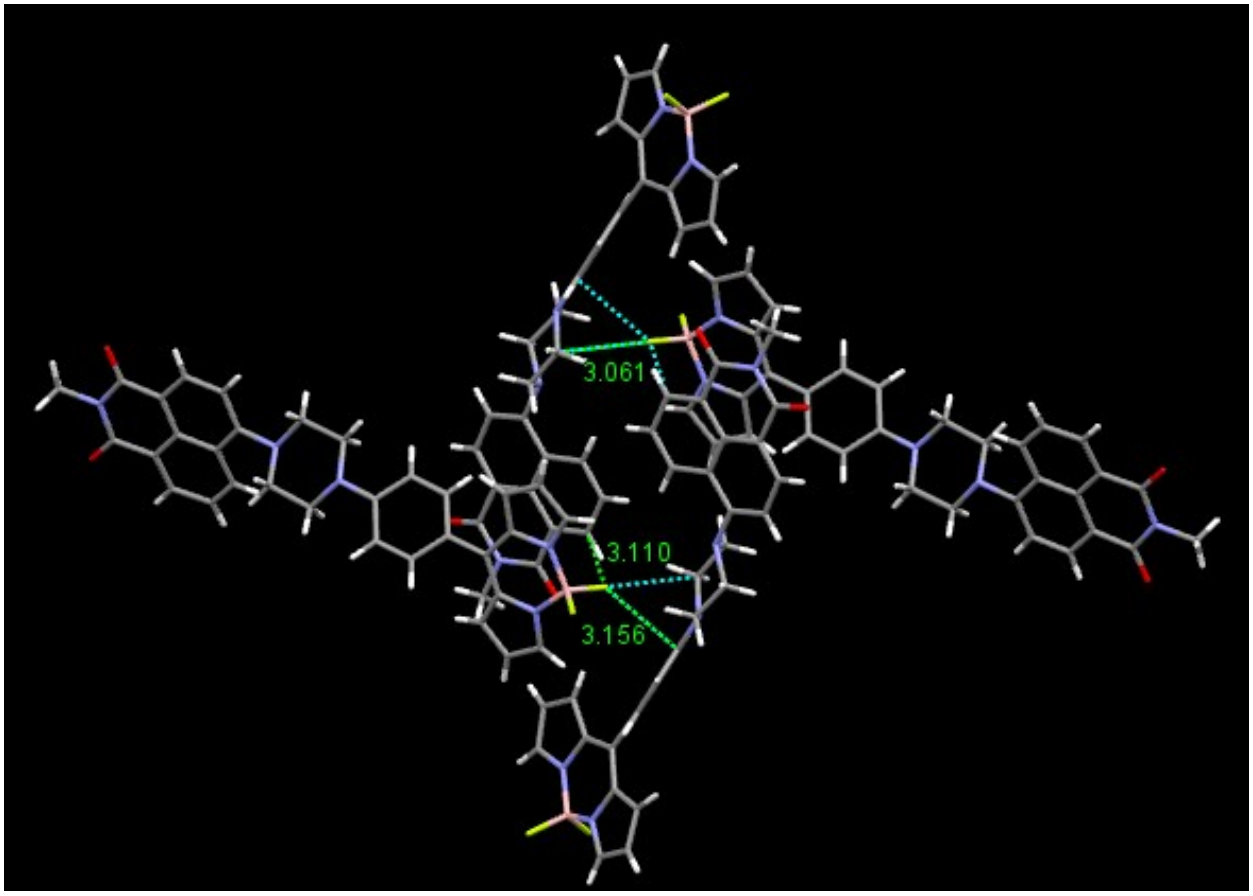

Fig. S60 Intermolecular B–F···C interactions in **NPB1** (absent in **NPB2** and **NPB3**).

References:

1. Sheldrick, G. M. SHELXL-97, Program for X-ray Crystal Structure Refinement; Gottingen University: Gottingen, Germany, **1997**. (b) G. M. Sheldrick, SHELXS-97, Program for X-ray Crystal Structure Solution; Gottingen University: Gottingen, Germany, 1997.
2. (a) A. L. Spek, PLATON, Multipurpose Crystallographic Tools Utrecht University, Utrecht, The Netherlands, 2000. (b) A. L. Spek, *Acta Crystallogr*. A, 1990, **46**, C31.
3. (a) W. R. Wadt and P. Hay, *J. Chem. Phys.,* 1985, **82**, 284–298; (b) A. D. J. Becke, *Chem. Phys.,* 1993, **98**, 5648–5652.
4. M. J. Frisch, G. W. Trucks, H. B. Schlegel, G. E. Scuseria, M. A. Robb, J. R. Cheeseman, G. Scalmani, V. Barone, B. Mennucci, G. A. Petersson, H. Nakatsuji, M. Caricato, X. Li, H. P. Hratchian, A. F. Izmaylov, J. Bloino, G. Zheng, J. L. Sonnenberg, M. Hada, M. Ehara, K. Toyota, R. Fukuda, J. Hasegawa, M. Ishida, T. Nakajima, Y. Honda, O. Kitao, H. Nakai, T. Vreven, J. A. Montgomery, Jr. J. E. Peralta, F. Ogliaro, M. Bearpark, J. J. Heyd, E. Brothers, K. N. Kudin, V. N. Staroverov, R. Kobayashi, J. Normand, K. Raghavachari, A. Rendell, J. C. Burant, S. S. Iyengar, J. Tomasi, M. Cossi, N. Rega, J. M. Millam, M. Klene, J. E. Knox, J. B. Cross, V. Bakken, C. Adamo, J. Jaramillo, R. Gomperts, R. E. Stratmann, O. Yazyev, A. J. Austin, R. Cammi, C. Pomelli, J. W. Ochterski, R. L. Martin, K. Morokuma, V. G. Zakrzewski, G. A. Voth, P. Salvador, J. J. Dannenberg, S. Dapprich, A. D. Daniels, Ö. Farkas, J. B. Foresman, J. V. Ortiz, J. Cioslowski, D. J. Fox, Gaussian 09, revision A.1, Gaussian, Inc., Wallingford, CT, 2009.
5. D. D. Perrin, W. L. F. Armango, D. R. Perrin, Purification of laboratory Chemicals, Pergamon: Oxford, U.K. 1986.
6. C. Zhang, Z. Liu, Y. Li, W. He, X. Gao and Z. Guo, *Chem. Commun*. 2013, **49**, 11430–11432.
7. C. Peebles, P. M. Alvey, V. Lynch and B. L. Iverson, *Crystal Growth & Design,* 2014, **14**, 290–299.
8. T. Gunnlaugsson, P. E. Kruger, P. Jensen, J. Tierney, H. D. P. Ali and G. M. Hussey, *J. Org. Chem*., 2005, **70**, 10875–10878.

9. X. Wang, Z. Chen, L. Tong, S. Tan, W. Zhou, T. Peng, K. Han, J. Ding, H. Xie and Y. Xu, *Eur. J. Med. Chem.,* 2013, **65**, 477–486.
10. X. Feng, T. Zhang, J. -T. Liu, J. -Y. Miao and B. -X. Zhao, *Chem. Commun.*, 2016, **52**, 3131–3134.
11. Q. -C. Wang, D. Qu, J. Ren, L. Xu, M. Liu and H. Tian, *Dyes and Pigments*, 2003, **59**, 163–172.
12. Y. Bao, H. D. Keersmaecker, S. Corneillie, F. Yu, H. Mizuno, G. Zhang, J. Hofkens, B. Mendrek, A. Kowalczuk and M. Smet, *Chem. Mater.*, 2015, **27**, 3450–3455.